Design and Optimization of Carbon Nano Tubes production in Chemical Vapor Deposition Reactor

BY

Nasser H. Al Hammad

A Thesis Presented to the

DEANSHIP OF GRADUATE STUDIES

KING FAHD UNIVERSITY OF PETROLEUM & MINERALS

DHAHRAN, SAUDI ARABIA

In Partial Fulfillment of the
Requirements for the Degree of

MASTER OF SCIENCE

In

CHEMICAL ENGINEERING

December 23, 2013

DHAHRAN, SAUDI ARABIA

DEANSHIP OF GRADUATE STUDIES

This thesis, written by Nasser H. Al Hammad under the direction of his thesis advisor and approved by his thesis committee, has been presented to and accepted by the Dean of Graduate Studies, in partial fulfilment of the requirements for the degree of MASTER OF SCIENCE in Chemical Engineering.

Thesis Committee

Thesis Advisor
Dr. Eid M. Al Mutairi

Co Advisor
Dr. Muataz A. Atieh

Department Chairman
Dr. Usamah A. Al-Mubaiyedh

Member
Dr. Abdul-Hadi A. Al-Juhani

Dean Of Graduate Studies
Dr. Salam A. Zummo

Member
Dr. Tahar Laoui

20/3/14
Date:

Member
Dr. Abdallah A. Al-Shammari

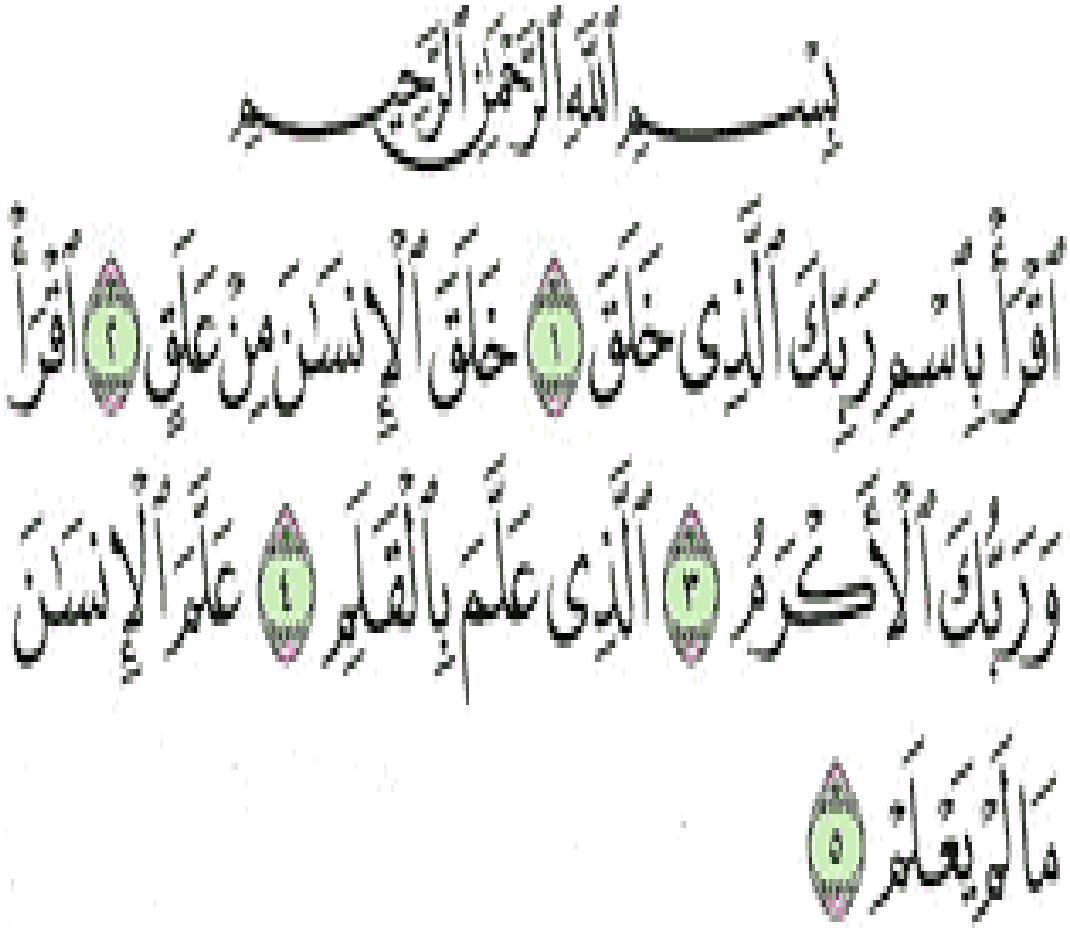
بِسْمِ اللَّهِ الرَّحْمَٰنِ الرَّحِيمِ

اقْرَأْ بِاسْمِ رَبِّكَ الَّذِي خَلَقَ ﴿١﴾ خَلَقَ الْإِنسَانَ مِنْ عَلَقٍ ﴿٢﴾ اقْرَأْ

وَرَبُّكَ الْأَكْرَمُ ﴿٣﴾ الَّذِي عَلَّمَ بِالْقَلَمِ ﴿٤﴾ عَلَّمَ الْإِنسَانَ

مَا لَمْ يَعْلَمْ ﴿٥﴾

Dedicated to my Parents, Spouse and my Family

ACKNOWLEDGMENT

Acknowledgment is due to the King Fahd University of Petroleum & Minerals for supporting this research.

I wish to express my appreciation to ***Dr. Eid Al Mutairi*** who served as my major advisor for his great support, encouragements, and ideas which really enriched this research from all aspects. I wish also to thank ***Dr. Mut'z Atieh*** who served as co-advisor of this research for his extended support, technical assistance with his great knowledge in CNT's and help with his great experience during the experimentations stage. I also wish to thank the other members of my thesis/dissertation committee, ***Dr. Abdulhadi Al Juhani, Dr. Abdullah Al Shamari*** and ***Dr. Tahar Laui.***

In addition, I would like to express my appreciation to the Chemical Engineering Department and King Fahad of Petroleum and Minerals University for giving me this opportunity and the unlimited resources that were given during all the stages of the research progress.

Finally, I wish to express my appreciation to my Parents, family and my Sons and Daughters for their support, encouragement and patient during the development of the research.

Table of Contents

List of Tables

List of Figures

Nomenclature

n	level of the factorial design
k	number of factors
Y	response for given levels (Yield), (g)
Ycal	calculated yield, (g)
Yobs	observed yield, (g)
βo	response of Y when both main effects are 0
βn	coefficients considering interactions
X_1	First Factor
X_2	second Factor
X_3	Third Factor
(X^TX)	data matrix
$(X^TX)^{-1}$	inverse matrix
X^TY	multiplication of data and inverse matrices
T	Temperature, (C^o)
I	P-xylene injection rate, (Ml/hr)
F	Hydrogen flow rate, (Ml/mint)
R^2	coefficient of determination

Q^2	estimate of the predictive ability of the model
$\propto$	alpha level
P value	calculated probability
F test	test group variance against a null hypothesis

Thesis Abstract

NAME: Nasser H. Al Hammad

TITLE: Design & Optimization of CNT's prod. in CVD Reactor

MAJOR: Chemical Engineering

DATE OF DEGREE: December 23, 2013

The Chemical Vapor Deposition (CVD) parameters were studied to selectively synthesize Carbon Nano Tubes (CNT's). Experimental runs using Vertical Chemical Vapor Deposition (CVD) reactor were performed at a fixed reaction time of one hour and different operating temperatures (700-1000 C^o), hydrogen flow rates (100-3000 mL/mint) and P-xylene flow rates (5-40 mL/hr). Ferrocene [$Fe(C_5H_5)_2$] catalyst was used in the process in the form of powder which is mixed and dissolved with P-xylene (C_8H_{10}) at a ratio of 1% of Fe (50 mL solvent, 1.6 g Ferrocene) to the hydrocarbon. The P-xylene as the source of the hydrocarbon was cracked by hydrogen while argon gas was used to flush the CVD reactor to prevent oxidation of the catalytic metal at the reaction temperatures. Effects of the various operating parameters on the yield and quality of CNT's such as temperature and the flow rates of hydrocarbon and hydrogen are presented in this study. The effects of the different reaction conditions on the CNT's yield and various dimensions of the CNTs formed were also investigated. A design of experiment

package was used for the generation and evaluation of statistical experimental designs. A 3^k statistical factorial design approach was adopted to develop the mathematical models in order to study and optimize the operating conditions. Multiple Linear Regression (MLR) was used to fit the mathematical models. The morphologies of the CNTs were characterized and examined by Scanning Electron Microscopy (SEM) at different growth temperatures for the surface morphology of the samples and Thermal Gravity Analyzer (TGA) was used to analyze purity of CNT's. A design of experiment optimizer was used to find the optimum conditions for the yield and quality of CNT's where optimum yield was found to be at a temperature of 892 C^o and H_2 flow rate of 1497 mL/mint with P-xylene rate of 5 mL/hr. However, to control quality, higher H_2 flow rate (3000 mL/mint) need to be considered to improve average diameters and aspect ratios of the produced CNT's.

ملخص بحث الرسالة

درجة الماجستير في الهندسة الكيميائية

الاسم: **ناصر حماد الحماد**

عنوان الرسالة: **التصميم الأمثل لأنابيب الكربون متناهية الصغر باستخدام مفاعل يعمل بترسيب البخار الكيميائي**

التخصص: **الهندسة الكيميائية**

تأريخ التخّرج: **ديسمبر 2013**

تم دراسة عوامل التشغيل بمفاعل مستمر يعمل بترسيب البخار الكيميائي من أجل إنتاج انتقائي لأنابيب الكربون متناهية الصغر. التجارب المعملية تمت باستخدام مفاعل عمودي لترسيب الأبخرة الكيميائية حيث ثبت وقت التفاعل لمدة ساعة واحدة وتحت درجات حرارة تشغيل مختلفة (700-1000 C^{O})، و معدلات تدفق الهيدروجين (100-3000 مل / دقيقة) ومعدلات تدفق للبرازايلين (5 -40 مل / ساعة). أستخدم محفز الفيروسين [$Fe(C_5H_5)_2$] في العملية على شكل مسحوق مخلوط ومذاب مع البرازايلين (C_8H_{10}) بنسبة 1 ٪ من الحديد (50 مل مذيب ، 1.6 غرام الفيروسين) إلى الهيدروكاربون. البرازايلين كمصدر هيدروكاربوني تم تكسيره بالهيدروجين في حين أستخدم غاز الأرجون لمنع الأكسدة بالمفاعل للمعادن المحفزة تحت درجات حرارة التفاعل. الآثار المترتبة على مختلف معايير التشغيل لإنتاجية الأنابيب متناهية الصغر مثل درجة الحرارة ، ومعدلات تدفق النفط والهيدروجين تم عرضها في هذه الدراسة. تم التحقق من تأثير ظروف التفاعل المختلفة على إنتاج وأبعاد الأنابيب النانوية الكربونية. برنامج لتوليد وتقييم التصاميم التجريبية الإحصائية تم استخدامه لتصميم التجارب وتطوير النموذج الرياضي بحيث أعتمد منهج تصميم

مضروب الإحصائية لتصميم العمليات التجريبية لدراسة وتحسين ظروف التشغيل من خلال نموذج تحسيني لإكتشاف مستويات التشغيل المثلى. أستخدمت متعددة الانحدار الخطي لتناسب النموذج الرياضي بواسطة برنامج تصميم التجارب. تم فحص الأشكال التضاريسية من الأنابيب النانوية الكربونية بواسطة المجهر الإلكتروني في درجات حرارة النمو المختلفة لتضاريس سطح العينات وأستخدم محلل الجاذبية لتحليل نقاوة العينات. تم استخدام تصميم محسن التجربة لإيجاد الظروف المثلى لإنتاج الأنابيب متناهية الصغر حيث وجد أن العائد الأمثل يكون عند درجة حرارة من 892 س^0 ومعدل تدفق الهيدروجين 1497 مل / الدقيقة والبرازايلين 5 مل/ الساعة. وبالمقابل للتحكم بجودة الإنتاج، فإن علينا النظر لتدفق أعلى ل H_2 (3000 مل /الدقيقة) لتحسين متوسط الأقطار ونسبة الطول للقطر للأنابيب المتناهية الصغر المنتجة.

CHAPTER 1

Introduction and Background

Developments are being made to improve the properties of the materials and to find alternatives that can give desirable properties. As such, materials technology is attracting the attention of researchers where Nanotechnology is one of the new material technologies that are used in this regards. By definition, the development of devices, structures, and systems whose size is in the nano scales is classified under the Nanotechnology. It has seen advancement in all aspects such as: nanoparticles and powders; Nano layers and coatings; electrical, optic and mechanical Nano devices; and nanostructured biological materials. Particular interests in the carbon nanotubes are laying in the wide varieties of properties and features that carbon nanotubes attain. Nanotechnology is expected to considerably improve environmental quality and tolerance through pollution prevention, treatment, and remediation.

1.1 Background

The superior mechanical properties of carbon nanotubes (CNTs) substantiate them to be considered a potential material to revolutionize technologies and enable many advanced development to achieve the state of art technology that we see nowadays. The tensile strength and modulus of CNT's are in the range of 150 GPa and 1 TPa, respectively which is exceptionally high. In addition, CNT's have large aspect ratio, good chemical and environmental stability, low density, and high electrical and thermal conductivity. Therefore, CNTs are very attractive because of these unique properties for many structural applications such as aerospace structures, body shields, sporting and many other significant commercial importance's. CNTs

with a tensile strength greater than steel position them as possibly the hardest substances that ever exist with only one sixth of its weight compared to the steel.

Recently, breakthrough developments have been achieved in the nanostructures carbon materials. There have been several methods used to form carbon nanotubes (CNTs) such as arc discharge, laser vaporization and catalytic chemical vapor deposition (CVD) of hydrocarbons . However, the CVD method has a number of potential advantages over the arc discharge and laser vaporization methods. CVD is more suitable to scale-up than arc discharge or laser vaporization, and in fact a successful large-scale catalytic synthesis of both Single Wall Nano Tubes (SWCNTs) and Multi Wall Nano Tubes (MWCNTs) have been developed using the CVD method. Moreover, Nanotube synthesis can be achieved under relatively moderate conditions by catalytic techniques giving more control over the growth process . They are good adsorption materials for wastewater treatment, as they exhibit extremely large specific surface area.

There are many methods for characterization of CNT's needed to understand CNT's properties. The SEM method is one of the methods that used for this objective. Other method used also is Transmission Electron Microscopy (TEM) which is very useful tools for imaging and structure analysis. However, among all electrons beam instruments, SEM is the most commonly used to obtain Nano scale information from various Nano materials. High-quality images are obtained with an image resolution of 0.5 nm.

In general, there are many books, articles; papers were found in the open media that describes CNT's from structures, properties, and production point of view. However, only few literatures were found attempting to optimize CNT's adopting

statistical approach or Design Of Experiments (DOE) to achieve this objective. As the field of CNT's production is a growing field, those literatures to optimize CNT's are trying to understand the nature of the reactions that take place, catalysts and the operating parameters to identify optimum conditions.

1.2 Scope of the work

In this proposal, the CVD method was adopted and experimental runs were performed to measure CNTs yield at various operating conditions of the CVD to study the parameters that affect the yield of CNTs and optimize the process parameters with respect to high purity and yield. In this regard, Design Of Experiment (DOE) was used where we have adopted a 3^k statistical factorial design with interaction between the various parameters to develop a mathematical model to optimize yields based on the obtained experimental runs.

The Optimization procedure involving DOE or factorial designs and analysis of response variables is powerful, efficient and also a systematic tool in knowing the parameters that are effecting CNT's yield in both quantitative and qualitative aspects. In order to optimize the operating parameters in the CVD system, mathematical models were developed that imitate the experimental where regression was used to fit those models. In statistical, regression is an attempt to determine the strength of the relationship between one dependent variable and a series of other changing variables known as independent variables. In this research, we have used Multiple Linear Regression (MLR) method which to describe the experimental data.

To understand properties of CNTs, it is quite necessary to characterize their structure at an atomic level. In this study, we have used for characterization Scanning Electron Microscope (SEM) to understand the morphologies of CNT's, and determine the length and diameter of every yield obtained and then made comparison and analysis to find optimum operating conditions to produce the best yield. The purity was determined using Thermal Gravity Analyzer (TGA).

1.3 Thesis Organization

The thesis organization starts with a literature survey addressing history of Carbon Nano Tubes, types and classification of CNT's, properties and production methods of CNT's. The research method is described in chapter 3 where we have presented the experimental system model; catalyst used for characterization of CNT's and explain in details the DOE technique presented and theory of Factorial Design in specifics. The results of experimental runs, reproducibility of the experimental runs, and characterization of CNT's using Scanning Electron Microscopy (SEM) are presented in chapter 4. Then, we have discussed regression methods in chapter 5 that we have used to describe the experimental runs adopting Least Square and Multiple Linear Regression Methods. Optimization is discussed in chapter 6 sowing the model prediction and ANOVA analysis, response contour and 3 D plots are presented and finding the optimum conditions in terms of quantity and quality to run the CVD. Finally, the effects of P-xylene flow rate, temperature and hydrogen flow rate on the yield and quality of CNT's are presented in the last chapter.

1.4 Objectives

The objectives of this project are:

- To conduct experimental runs to produce CNT's at different operating conditions.

- To characterize the produced CNT's using Scanning Electron Microscopy (SEM) and analyze purity by Thermal Gravity Analyzer (TGA).

- To develop a mathematical model (empirical equation) that describes the CNT yields by adopting a statistical factorial design based on experimental runs using a Chemical Vapor Disposition (CVD) reactor.

- To optimize operating parameters such as temperature and flow rates of hydrocarbon and hydrogen to produce optimum yield and quality of CNT's from length and diameter of CNT perspectives.

- To help researchers in this field based on the results and optimum conditions to more understand the CVD process and those parameters that are affecting the CNT's yields.

CHAPTER 2

Literature Review

In this section, we will cover the Nano tubes since discovery as a recent technology that starts to show in many aspects of the latest technology which is attracting the attention of sciences and researchers. The more understanding of the Carbon Nano Tubes could lead to breakthrough in the development of many tools in the field of biomedical, pharmaceutical and many other applications. A thorough review of the open literature in the optimization of CNT's is illustrated here with a summary of the efforts that was made and main outcome from their attempts.

2.1 Carbon Nanotube (CNT's); Historical Overview

The CNTs are constructed by the hexagonal arrangement of sp2-hybridized carbon atoms in a shape like hollow cylinders that are composed of rolled sheets of graphene in Nano scale dimensions and they were first introduced by Iijima in 1991. They have showed exceptional structures and outstanding thermal, chemical, mechanical, electrical, magnetic, optical, and surface properties where the combination of these features provides wide pharmaceutical and biomedical applications. The mechanism of formation of the CNTs is assumed to be similar to that explained by Chen et al. (2006), Das et al. (2006), Fan et al. (2006) and Huang et al. (2007) in which the catalyst was responsible for the nucleation and growth of the CNTs. The particle size of the catalyst determines to a large extent the diameter of the nanotubes formed . In 1991, Iijima discovered thin and long carbon straw having the form of nanotubes during the Transmission Electron Microscope (TEM) analysis of carbonaceous groups synthesized by an arc discharge method. This

carbon nanotube (CNT) varied in length from several nanometers to several micrometers, and had an external diameter approximately from 2.5 nm up to 30 nm. In 1992, Ebbesen and Ajayan observed that the increment of pressure in the chambers of an arc exceptionally improved the carbon nanotube yield at the cathode of the graphite [10]. In 1993, Bethune has synthesized carbon nanotubes with diameters about one nm, using methods of arc discharge. In 1996, Smalley and his group reported a method of preparation of the only single walled nanotubes with unusually homogeneous diameters by laser vaporizing of graphite. These tubes had a tendency to form aligned bundles, and they drove Smalley to baptize the bundles ' rope '. Using chemical vapor deposition (CVD), Yacamán et al., (1993) have made large achievement in synthesis and the application of carbon nanotubes. Since then, the investigations in synthesis and application have been energetically led in the entire world. Figure 1 shows the structures and carbon arrangement of the different materials related to carbon in comparison with carbon nano tubes.

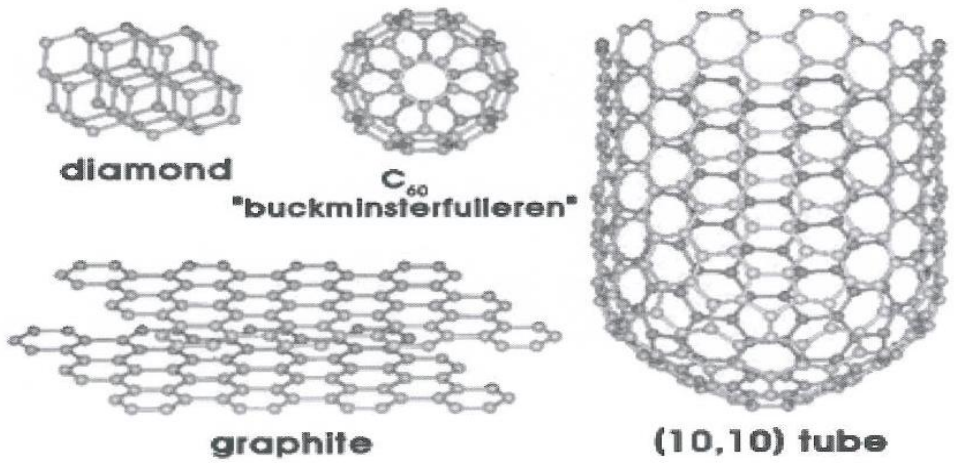

Figure 1: Carbon related materials in comparison with CNTs

In 1997, the Nano materials characterization team at the NASA Johnson Space Center started fully characterizing the Nano materials used for applications related to spaceflight and exploration. This team has been focusing on characterizing unique features and properties of single-wall carbon nanotubes (SWCNTs). In 2003, the team developed a characterization protocol to help setting standards for the assessment of the purity and dispersion of SWCNTs. The focus was to explore new and novel techniques and to modify existing analytical techniques to characterize the raw, purified, and processed SWCNT materials. This is to provide vital feedback to the production, processing, and applications teams of the space shuttles. In 2004, the NASA team observed through characterization that the properties of SWCNT material produced by the laser method vary according to the region of the production oven from which the material is harvested. Moreover, characterization has shown that the consistency of material produced from production run to production run shows both similarities and differences in its properties. In 2005, NASA team worked with Rice University to evaluate continued growth of Nanotubes for use in Quantum Conductors for the objective of making highly conducting nanotube cables using one particular type of nanotubes known as "arm-chair" nanotubes. Through the use of techniques such as Nano-area electron beam diffraction, Raman spectroscopy, UV-Vis-NIR absorption spectroscopy, and NIR fluorescence, it was possible to monitor and select these "arm-chair" nanotubes from the bulk of SWCNT material.

2.2 Carbon Nanotubes Classification; Layers

Type of carbon nanotube is determined by the number of the concentric graphene layers. Carbon nanotubes are classified as single wall carbon nanotubes and multi wall carbon nanotubes. If carbon nanotube contains one graphene layer, it is

named single wall nanotube (SWNT); whereas if it contains two or more concentric layer, it is named multi wall carbon nanotube (MWNT).

2.2.1 Single Wall Carbon Nanotube

A single wall nanotubes (SWNT) is occurred by a graphene sheet rolled into a cylinder with a diameter of about 0.4-10 nm and lengths from microns to cm. The shape of a SWNT is shown in Figure 2. If we ignore two ends of carbon nanotube and focus on the large aspect ratio of the tube, carbon nanotubes can be considered as one-dimensional nanostructures with axial symmetry and they have excellent properties because of this symmetry. A single wall carbon nanotube can be metallic or semiconductor.

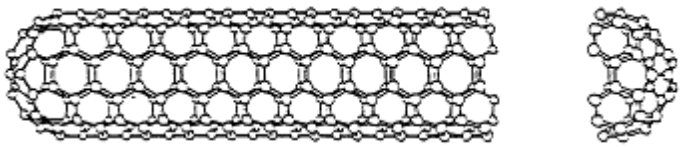

Figure 2: An illustration of a SWNT

2.2.2 Multi-Walled Carbon Nanotubes

CNTs with more than one concentric graphene cylinders coaxially arranged around a central hollow with a constant interlayer distance which is nearly equal to 0.34 nm is called multi-wall carbon nanotube. MWNTs are stronger than SWNTs although they have more defects than SWNTs. Graphite layers of SWNTs are easily separated from each other due to weak Vander Waals forces between planes, but separation of cylinders of MWNT from each other is difficult. The investigation of physical properties of MWNTs is more difficult because of the

difficulty of making measurements on the individual shells of the nanotube. The shape of a MWNT is shown in Figure 3.

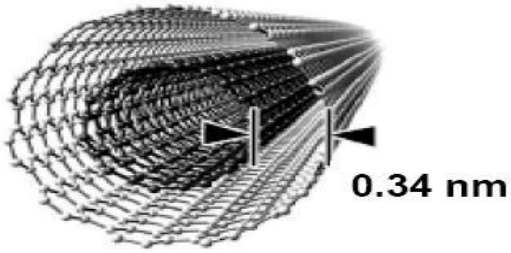

Figure 3: An illustration of a MWNT

2.3 Classification of Carbon Nanotubes; Shape

According to the direction of the hexagons which are the six membered carbon rings, the structure of CNTs can be classified in three different configurations such as armchair, zigzag and chiral carbon nanotube. In Figure 4 the formations of the three different nanotubes are shown.

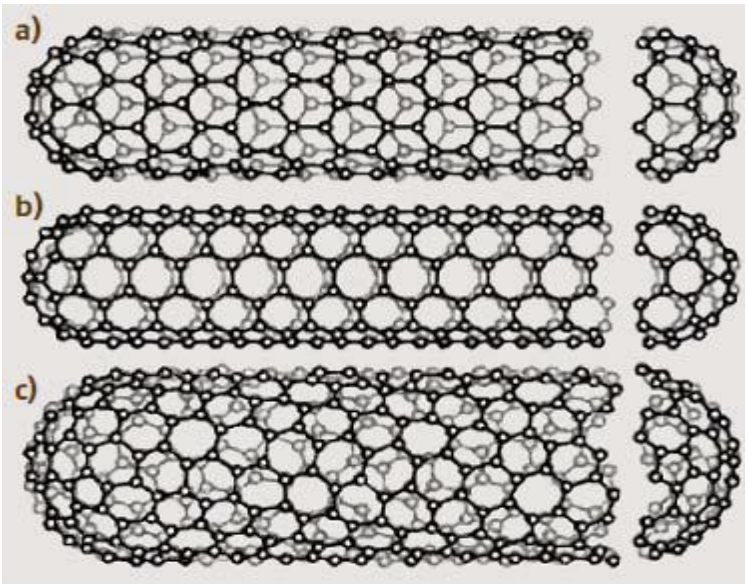

Figure 4: Classification of CNTs, a) Arm-chair, b) Zig-zag, c) Chiral CNTs

2.4 Properties of Carbon Nanotubes

Single and multi-wall nanotubes have very good elasto-mechanical properties. Possible use in making future generation of exceptionally lightweight with greatly elastic and very strong composite materials can be achieved by the nanotubes with their structural and materials features. Good electrical and mechanical properties along with high aspect-ratio have really distinguishes the nanotubes from other materials. Therefore, the applications of nanotubes have started to materialize in the commercial sector in the field of emission displays and scanning probe microscopic guidelines for metrology.

CNTs are the strongest fibers that are currently known mainly because the carbon atoms form a collection of hexagonal cells matrix in which each atom is connected via a robust chemical bond to three adjacent atoms. Thus, these compounds are possibly appropriate for applications in composite materials that require anisotropic properties.

CNT's are characterized with their very large Young Modulus in their axial direction which could reach up to 1TPa for SWCNT that is 5 times greater than steel (230 GPa) while the density is only 1.3 g/cm3. At large deflection angles of as high as 108 for length of only 1 mm, it was found that nanotube buckle elastically. For example, the strain energy storage in nanotubes for a 30 nm diameter is estimated to be 100 keV, which is an order of magnitude larger than that in SiC nanorods. Hence, the capacity of nanotubes to elastically withstand loads at large deflection angles allows them to absorb significant energy.

2.5 Production Methods of Carbon Nanotubes

Different ways can be used to produce various types of carbon nanotubes, carbon nano fibers, and other types of carbon nanostructure materials. Arc Discharge, Laser Ablation, and Chemical Vapor Deposition are the most common techniques used nowadays to produce carbon nano tubes. However, economically feasible and purification techniques for large-scale production still have to be developed. In this regard, we will limit the discussion and description to the Chemical Vapor Disposition (CVD) technique as the adopted method for nanotube synthesis.

In principle, to understand chemical vapor deposition, it can be described as a chemical process where volatile precursors are used to provide a carbon feed source at high temperatures (350–1000 C^{o}) to a catalyst particle. The heterogeneous reactions where the volatile products and solids are shaped from a volatile precursor through chemical reactions in which the solid products are deposited on a substrate are termed as a Chemical Vapor Deposition (CVD). Metals are used to catalyze CNT growth. Usually, transition metals, in particular iron, cobalt and nickel are used as catalysts because of their high carbon solubility into these metals. The advantage of the CVD method is that it allows control over the morphology and structure of the CNTs produced. Both MWNT and SWCNT syntheses have been well developed. The CVD method can be applied to the industrial production of CNTs in the form of powder and forests.

2.6 Chemical Vapor Deposition (CVD)

The deposition of a solid on a heated surface from a chemical reaction in the vapor phase is called Chemical Vapor Deposition. Since it involves the deposition of atoms or molecules species or a combination of them, it is classified as part of vapor-transfer processes. In the CVD-method, different hydrocarbons can be

decomposed over different metals (Fe, Co, Ni) at temperatures between 500 and 1200°C. The CVD method before it's use for the CNT's synthesis was used for a long time for the synthesis of carbon fibers and there were no signs that it could also be used for the synthesis of carbon nanotubes until Yacamán et al., (1993) where he reported this method for the first time for the production of nanotubes.

The CVD method deposits hydrocarbon molecules on top of heated catalyst material where the metal catalysts dissociate the hydrocarbon molecules as shown in Figure 5. The CVD method which uses hydrocarbons as the carbon source produces both single-wall and multi-wall nanotubes after heating the Hydrocarbons that are flowing through the quartz tube to high temperature [Sinnot et al., 1999]. At the high temperatures, the hydrocarbon molecules are cracked by this energy source into reactive atomic carbon. Following that, the carbon disperses to the substrate, which is heated and covered with a catalyst (typically a first row transition metal such as Ni, Fe or Co) and if the proper parameters are sustained, the catalyst will bind and carbon nanotubes will be shaped. By using CVD, superb alignment as well as positional control on nanometer scale can be attained. Moreover, it can maintain control over the diameter as well as the growth rate of the nanotubes [Yudasaka et al., 1995; Ren et al., 1999].

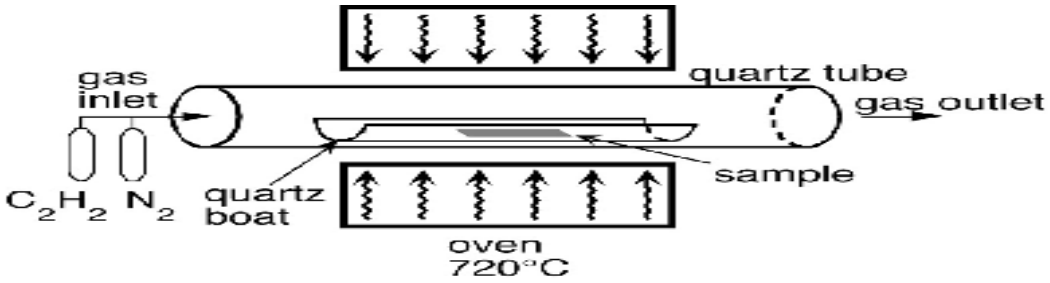

Figure 5: Schematics drawings of a CVD deposition oven

In a CVD reactor, there have been different techniques developed for the last ten years for the carbon nanotubes production such as thermal chemical, alcohol catalytic, enhanced plasma, vapor phase growth, laser- assisted CVD and aero gel-supported CVD.

2.7 Equipment for Characterization of Nano Tubes

To evaluate comprehensively CNT materials, techniques such as scanning electronic microscopy (SEM), transmission electron microscopy (TEM), energy dispersive x-ray analysis, Raman spectroscopy, TGA, and ultraviolet-visible-near infrared (UV-Vis-NIR) spectroscopy are all characterization tools that can be used for this purpose. However, among all electrons beam instruments, SEM is the most commonly used to obtain Nano scale information from various Nano materials. High-quality images are obtained with an image resolution of 0.5 nm. TEM determines the atomic structure of interfaces and defects with high position accuracy. The resolution of TEM reaches as high as 0.1 nm. Another advantage of electron microscope is that it offers the accessibility of associated spectroscopy and diffraction. Both SEM and TEM provide quantitative analysis and chemical composition determination when combined with energy dispersive X-ray spectrometry (EDS).

The various characterization methods will determine various properties and morphologies of CNT such as diameter, length, Single and Multi tubes, homogeneity, dispersion stability, and impurity constituents. In addition, there are other techniques that can be used to characterize CNT such as x-ray photoelectron spectroscopy (XPS), electron beam diffraction, inductively coupled plasmas (ICPs), high-pressure liquid chromatography, x-ray diffraction, and laser

desorption ionization (LDI) to investigate the various properties of CNT material. From the characterization of Nano materials, it was found that CNT varies significantly in its properties, depending on the parameters under which the material is produced or processed.

2.8 Optimization of Carbon Nano Tubes

As mentioned earlier, there are many literatures that are addressing the nano tubes from all aspects, however only few literatures in the open media were found addressing the optimization of nano tubes by adopting statistical factorial design. In the following section, we are summarizing those literatures limiting only to those that have attempted to optimize CNT's operating conditions as well as quality of CNTs by adopting the factorial design approach.

In 2005, Á. Kukovecz et al used statistical design of experiments (DoE) for Catalytic Chemical Vapor Deposition (CCVD) set for single-wall carbon nanotubes to assess and optimize CNT's production, catalyst composition, amount, reaction temperature, reaction time, preheating time, C_2H_2 flow rate, and inert gas flow rate. FeMo/MgO was used as a carbon source for the Catalytic Chemical Vapor Deposition (CCVD). Mass of carbonaceous material formed and SWCNT content as calculated from FT-Raman spectra which are quantitative descriptors were used to assess performance.

In 2005, Chien-Sheng Kuo et al, studied Diameter control of multiwalled carbon nanotubes using DOE. Chemical vapor deposition floating feed method in a vertical reactor was used to synthesis Multiwalled carbon nanotubes (MWNTs). The effects on the average diameter of carbon nanotubes by the preparation variables were analytically studied using the fractional factorial design (FFD). The

FFD study shows that, the key factors impacting the diameter of MWNTs were found to be the main and interactive effects of reaction temperature, chamber pressure, and methane flow rate. The dependence of the diameter of carbon nanotubes at the neighborhoods around extreme (420 nm) and lowest (15 nm) on the reaction temperature and methane flow rate were represented in empirical models. These models indicated that the diameter of carbon nanotubes normally augmented with growing reaction temperature and methane flow rate. According to the empirical models, the continuous CVD fabrication method can be used to accurately control the diameter of MWNTs from 15 to 420 nm.

In 2011, N.M. Mubarak, et al used two-stage chemical vapor deposition to study synthesizing carbon nanotubes and their potential use in protein purification. Ferrocene as a catalyst, and acetylene (C_2H_2) and hydrogen (H_2) as precursor gases were used in the gas phase two-stage chemical vapor deposition to produce Carbon nanotubes (CNTs). Field emission scanning electron microscopy (FESEM), transmission electron microscopy (TEM), and thermo gravimetric analysis (TGA) were used to characterize the CNTs. Design-Expert software was used to optimize process parameters such as reaction time, reaction temperature and C_2H_2 and H_2 flow rates. The optimum conditions for the CNT production were found to be reaction temperature at 850 C^o, reaction time at 60 min and gases flow rates at 40 and 150 mL/min for C_2H_2 and H_2, respectively. Acid treatment was used to purify and functionalize the optimum CNTs.

In 2011, Siang-Piao Chaia et al, studied production of carbon nanotubes by methane decomposition over Co–Mo/Al_2O_3. Three-level factorial design with integrated response surface methodology in a CVD reactor was used to methodically study various process variables effect on the formation of carbon

nanotubes (CNTs). Multiple-regression analysis was used to obtain a quadratic polynomial model for carbon yield. The effects of reaction temperature (T), methane partial pressure (PCH_4) and catalyst weight loaded into the reactor (W) on methane decomposition were assessed. Reaction temperature of 761 C^o, methane partial pressure of 0.75 atm and catalyst weight of 0.4 g were concluded to be the optimum conditions for CNT production within the experimental ranges.

In 2012, Oscar M. Dunens et al, used a high-throughput methodology for screening and optimizing the single and double walled carbon nanotube parameter space. An automated micro-chemical vapor deposition (CVD) reactor and statistical design of experiments contains the high-throughput methodology. It was used for screening and the first pass optimization of the single- (SWCNT) and double-walled carbon nanotube (DWCNT) parameter space using an alumina supported iron-molybdenum catalyst. The most significant reaction parameters were initially explored using an L18 experimental design to find those parameters which are reaction temperature, bi-metallic ratio, metal loading, gas flow ratio and total gas flow rate. Product characterization metrics included carbon yield by TGA, IG/ID from Raman spectroscopy, the presence of SWCNTs/ DWCNTs from radial breathing modes and transmission electron microscopy (TEM). The optimum metal loading of 4.9 wt% and a synthesis temperature of 900 C^o were found to be the most significant variables.

The following table summarizes the papers review in the literatures that have optimized CNT production in the past few years:

Year	**Author**	**Title**	**Process**	**Feed gas/catalyst**	**Parameters**	**DOE/ Characterization**	**Findings**
2005	A. Kikovecz, et al	Optimization of CCVD synthesis conditions for single-wall carbon nanotubes by statistical design of experiments (DoE)	Catalytic chemical vapor deposition (CCVD)	Acetylene (C_2H_2) FeMo/MgO catalyst	Catalyst composition, & amount, reaction temp & time, preheating time, C2H2 flow rate, inert gas flow rate	2^{7-4} Fractional factorial design FT-Raman spectra	The optimum was found at Fe:MgO = 0.149, T = 863 °C, Ar flow = 372 cm3/min
2005	Chien-Sheng Kuo, et al	Diameter control of multiwalled carbon nanotubes using experimental strategies	Chemical vapor deposition floating feed method in a vertical reactor	(CH4) and N2 carrier gas A mixture of Fe(CO)5 as the catalyst precursor	Temp, CH4 rate, & chamber pressure	Fractional factorial design	Main and interactive effects of temp, CH_4 rate, & chamber pressure were key factors influencing diameter of MWNTs
2011	N.M. Mubarak, et al	Production of carbon nanotubes using two-stage chemical vapor	Two-stage chemical vapor deposition	Acetylene (C_2H_2) and hydrogen (H_2) as	Reaction temperature, reaction time and gas flow	Full Factorial Design-(Expert software)	Optimum were reaction temperature of 850 C^o, reaction time of 60 min and

		deposition and their potential use in protein purification		precursor gases. Ferrocene as a catalyst	rates of C_2H_2 and H_2	Emission Scanning Electron Microscopy (FESEM), (TEM), and Thermo Gravimetric Analysis (TGA)	gases flow rates of 40 and 150 ml/min.
2011	Siang-Piao Chaia et	Synthesis of carbon nanotubes by methane decomposition over Co–Mo/Al2O3	CVD reactor	Methane decomposition over a Co–Mo/Al2O3 catalyst	Reaction temperature, Methane partial pressure and catalyst weight	Optimum conditions were reaction temperature of 761 ◦C, a methane partial pressure of 0.75 atm and a catalyst weight of 0.4 g	
2012	Oscar M. Dunens et al	Screening and optimization of the single and double walled carbon nanotube parameter space using a high-throughput methodology	Automated vertical micro-chemical vapour deposition (CVD)	CH_4/Argon gas. Alumina supported iron-molybdenum catalyst	Reaction temperature, metal loading, bi-metallic ratio, total gas flow, and gas flow ratio	L18 experimental design(Raman spectroscopy) and transmission electron microscopy (TEM)	The temperature and metal loading were found to be the most influential variables

Table 1: Literature review of CNTs published optimization papers

CHAPTER 3

Research Methodology

Chemical Vapor Deposition process was used to produce the CNT's as the CVD process is attracting the attention of researchers in this field due to its ability to produce large scale catalytic synthesis of CNT's. Moreover, the CNT's synthesis can be achieved under relatively moderate conditions by catalytic techniques giving more control over the growth process. Therefore, in this section we will describe in depth the system model used to produce CNT's, the catalyst used, characterization selected to characterize the yield from the experimental runs, and give some back ground about the Design of experiment and factorial design which we have used to optimize the operating conditions of the CVD process.

3.1 Systems Model (Chemical Vapor Deposition Process)

A Vertical Chemical Vapor Deposition (V-CVD) reactor was used for CNT's production through gas phase. Figure 6 shows the CVD reactor schematic diagram and Figure 7 shows a photo of the CVD setup. In this system, the CNT deposition experiments were performed via hot-wall, vertical, down-stream reactor.

The vertical reactor consists of a quartz tube with a diameter of 100 mm and a length of 1200 mm with top and bottom flanges and heated by two furnaces. Gas inlet port and a port for feeding catalysts are provided in the top flange. A bottle for accumulating the CNT material is provided in the bottom flange. The hydrocarbon liquid is introduced from the top flange via a syringe pump. The

pressurized hydrogen is also introduced from the top flange and its flow rate is set and controlled via flow meter.

The great ability for high production of nanotubes material and the ability to control growth of carbon nanotubes are considered to be the main advantages of the CVD reactors. Argon (Ar) gas was used as flushing gas into the (V-CVD) reactor to prevent the oxidation of catalytic metal while elevating the temperature to the desired reaction temperature. When the desired temperature is reached, the liquid solution (P-xylene & Ferrocene) is started to be injected via the syringe pump where it disperse into a fluid-like spray. The fluid is atomized or dispersed as fine droplets that come into immediate contact with a flow of hot hydrogen gas. The Ferrocene vapor will decompose first to form atomic iron, which will agglomerate into iron clusters or iron particles for the growth of carbon nanotubes.

Production conditions were varied in order to study the optimum conditions to produce the most suitable carbon nanotubes. Amongst these is reaction temperature from 700 C^o to 1000 C^o, Hydrogen flow rates from 100 mL/min to 3000 mL/min and P-xylene flow rate from 5 to 40 mL/hr where the reaction was allowed to take place for 1 hour for all the runs. After the growth of carbon nanotubes, the reactor was allowed to cool down to room temperature filled in Argon gas and the CNT's are collected from the bottom flange and its weight is measured.

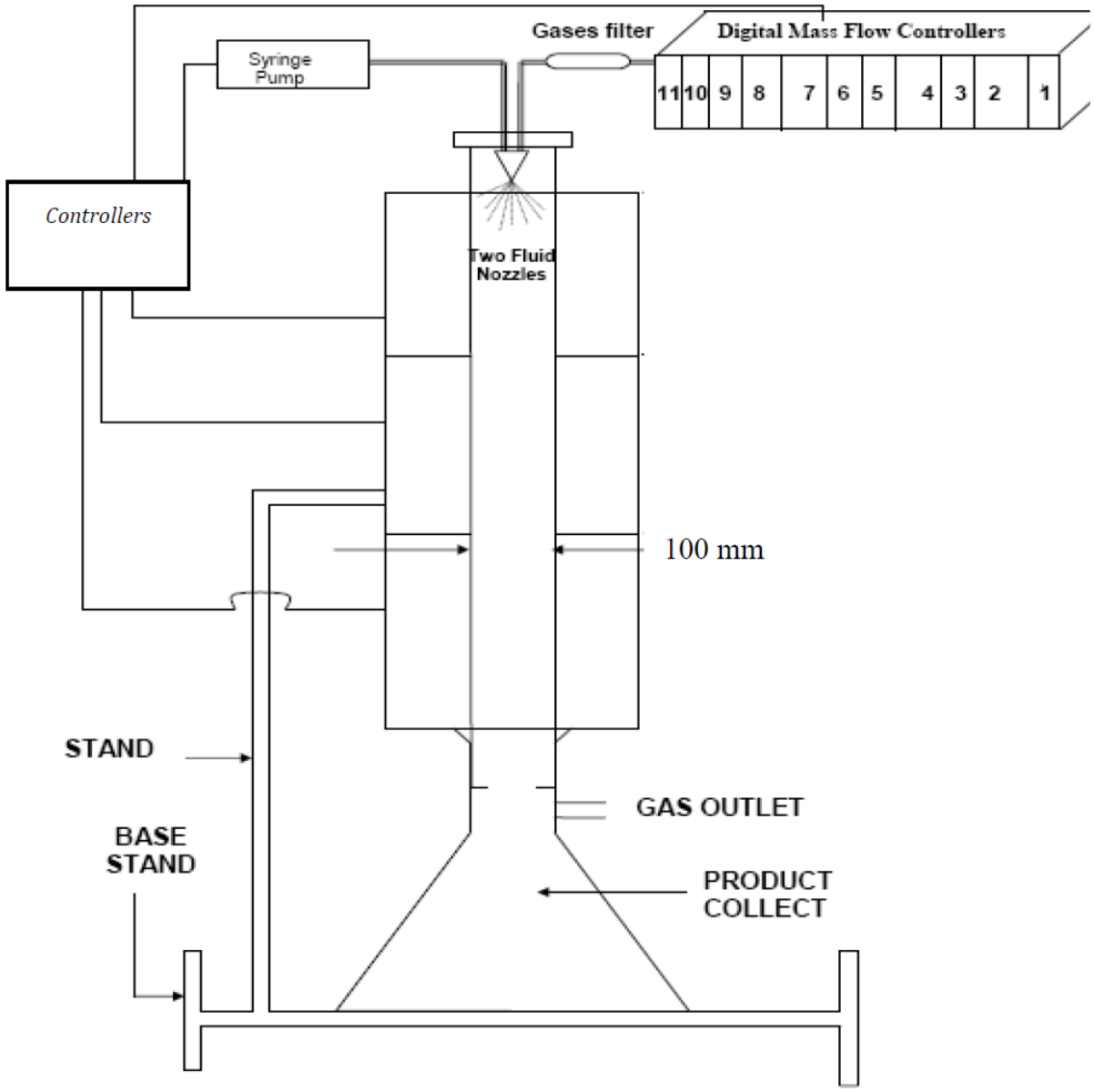

Figure 6: Schematic Diagram of the designed I-CVD Reactor

a b

Figure 7: Photo of the reactor at different locations (a) the whole reactor (b) two vertical furnaces with quartz tube at the middle

3.2 Catalyst Used

The thermal decomposition which is the breaking of hydrocarbons bonds at high temperatures is called Pyrolysis. The decomposition temperature of the hydrocarbons can be lowered by the use of appropriate metal catalysts where it is called in this case catalytic pyrolysis. It should be noted that, the hydrocarbon decomposition must take place on the metal surface alone to prevent unstructured aerial pyrolysis (prevent the hydrocarbon to break un-catalyzed, outside the catalyst surface). The proper selection of hydrocarbon, catalyst materials, vapor pressure of the hydrocarbon, concentration of the catalyst, and the CVD reaction

temperature can restrict pyrolysis to the catalyst surface. Besides the catalyst material, concentration of the catalyst plays an essential role in the CNT growth.

In this system, the catalyst that was used in the process is Ferrocene [Fe $(C_5H_5)^2$] in the form of powder which is mixed and dissolved with P-xylene. The ratio of catalyst to the hydrocarbon was maintained in all runs at 1% of Fe (50 mL solvent, 1.6 g Ferrocene) while the volume of P-xylene was injected to the CVD along with the catalyst at a flow rate of 5, 22.5 and 40 mL/hour for the various runs. In all CVD reactions, the precursor/catalyst solution was decomposed in a hydrogen/argon carrier gas at temperatures that varies between 700 to 1000 C^o.

3.3 Characterization of CNTs

In this study, we have used Scanning Electron Microscopy (SEM) to characterize the produced CNT for all the samples collected to verify the CNT's yield and quality. To understand properties of CNTs, it is quite necessary to characterize their structure at an atomic level. Various analytic methods have been employed to investigate the structure of Nano materials. For instance, scanning electron microscope (SEM) and transmission electron microscopy (TEM) are very useful tools for imaging and structure analysis. Among all electron beam instruments, SEM is the most commonly used to obtain Nano scale information from various Nano materials. High-quality images are obtained with an image resolution of 0.5 nm.

A concentrated beam of high-energy electrons is used in the scanning electron microscope (SEM) to produce a diversity of signals at the surface of solid samples. Information about the sample including chemical composition, external

morphology, and crystalline structure and orientation of materials forming the sample are obtained from the signals that resulting from electron-sample interfaces. Informations are collected over a particular area of the surface of the sample in most applications, and a 2-dimensional image is produced that shows three-dimensional variations in these properties. Using conventional SEM techniques in a scanning mode where magnification can range from 20X to nearly 30,000X, it can image areas ranging from approximately 1 cm to 5 microns in width. Therefore, fine structures of materials and nanoparticles synthesized by the nanotechnology can be imaged by the powerful SEM instrument at high resolution. Important data such as surface morphology of the sample, chemical composition with energy dispersion x-ray (SEM-EDS), size of carbon particles and the diameter and length of bundles can be obtained by the SEM.

3.4 Design Of Experiments (DOE)

DOE was used to design the experiment with a full factorial design to predict the mathematical model and optimize the process parameters of CNT production with respect to high purity and yield. The Carbon Nano Tubes was produced using the Chemical Vapor Disposition Process (V-CVD) described in figure 6.

The least square method initially was used for regression to fit the model. To improve the mathematical model, a software design package was used for the generation and evaluation of statistical experimental designs where the mathematical model was fit by Multiple Linear Regression (MLR) method. The quality of CNT yield from the experiments was verified using the Scanning Electron Microscope (SEM).

The objectives of an experiment and selecting the appropriate process factors for the study are the starting steps of DOE. The Design of Experimental is basically a thorough experimental plan in advance of performing the experiment. It is normally start with a process model called black box with some discrete or continuous input factors that can be controlled and one or more measured output responses where the output responses are assumed continuous. The outputs and inputs responses are connected by developing an empirical model from the experimental data. These empirical models generally contain first and second-order terms.

The methodology of optimizing each factor discretely normally requires many experiments over the course of several days. Conversely, significant reduction of the number of experiments involved can be achieved by the DOE and consequently wastage of chemicals, reagents, manpower and instrument time are reduced. They are meant to get maximum data from the least amount of experimental runs.

In order to observe the effect on the response variables in an experiment, we usually alter one or more process variables (or factors). At the end of the DOE, the outcome of the statistical design of experiments can be examined to obtain right and objective conclusions. Frequently the experiment has to consider a number of uncontrolled factors that are discrete such as different operators or equipment's or continuous such as humidity or ambient temperature. Figure 8 illustrates this situation.

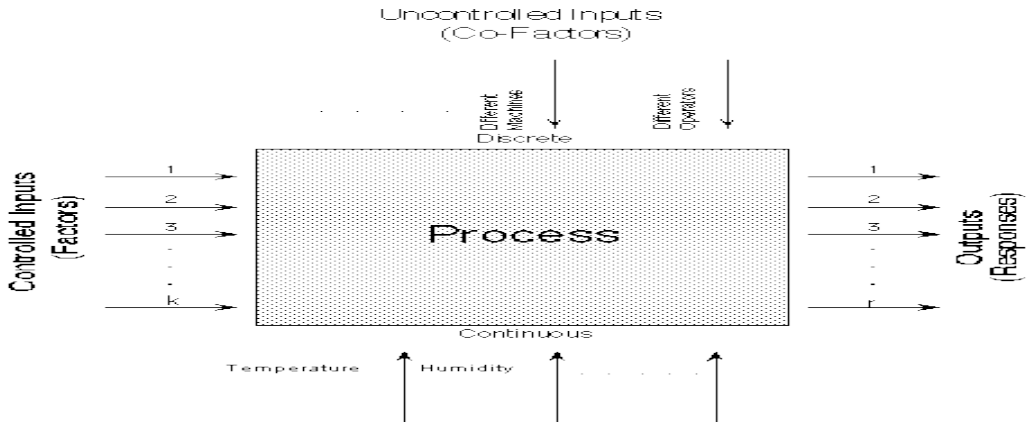

Figure 8: DOE black box

3.5 Factorial Design

The factorial design is a procedure for determining the optimal yield by analyzing in a statistically manner the relationship between the factors and the responses using regression method. It is a valuable statistical tool that supports the analytical scientist achieves process optimization experiments in a way that can achieve maximum data in a slight number of experiments. In factorial design, the parameters are systematically planned and experiments are conducted in which all of the variables are changed simultaneously rather than one at a time. Main effects for the factors being studied as well as disclose any existing interactions among factors can be identified by these designs. Generally, factorial designs comprise the study of two or more factors or variables in which each factor is assigned discreet values or levels and each potential factor-level variation is tested over several experimental trials or runs.

The simplest form of factorial designs is the full factorial designs where the entire possible factor-level combinations are verified. The number of factors being examined determines the number of experimental runs needed for a full factorial design and is equal to n^K, where n stand for the level of the factorial design and k

stand for the number of factors. For example, a full factorial design with 2 levels and three factors would require 2^3 or eight runs while a full factorial design with 3 levels and three factors would require 3^3 or twenty seven runs. For the 2 level, a high and low, +1 and -1 exist to indicate the high and the low level of each factor. For the 3 level, a high, medium and low, +1, 0 and -1 exist to indicate the high, medium and the low level of each factor.

To study the effects of two to four factors by the optimization of analytical techniques, full factorial design is a proper choice. Other factorial designs with less number of runs such as fractional factorial or Plackett-Burman designs may be considered for more than four factors. In this project, we have considered three factors to study the system at three levels or 3^3 designs to predict coefficients of parameters that are affecting the yield of CNT. The selected parameters to be optimized were reaction temperature, flow rate of hydrocarbon with dissolved catalyst and the flow rate of hydrogen and therefore, the number of experimental runs required is twenty seven runs.

The 3^K design is superior to other factorial designs in our case because it has the ability to model possible curvature in the response function and to facilitate investigation of a quadratic relationship between the response and each of the factors. The coefficients of parameters that are affecting the yield of CNT were then calculated to predict the model and optimum parameters. As an example of the full factorial matrix, a three factor, two-level, full factorial statistically design matrix is shown in figure 9.

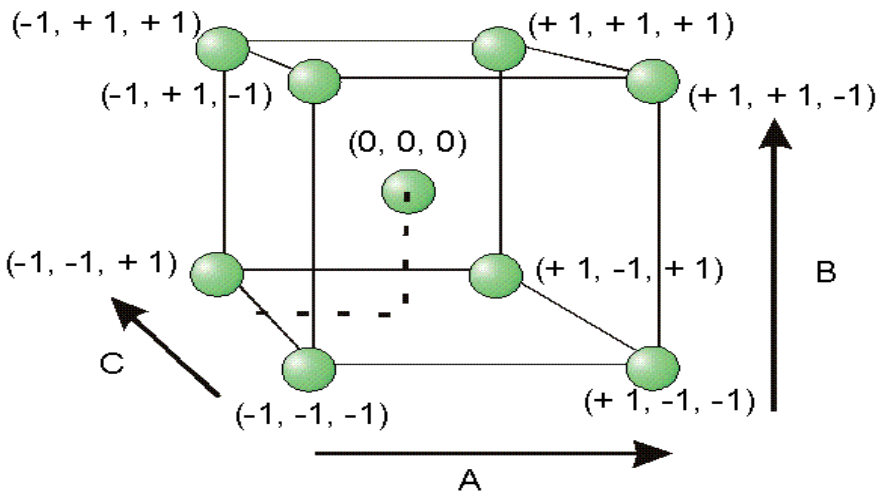

Figure 9: Design matrix (2^3)

Consequently, for the two level and two factors example, a linear mathematical model with two factors, X1 and X2, can be written as

$$Y = \beta_0 + \beta_1 X_1 + \beta_2 X_2 + \beta_{12} X_1 X_2 + \text{experimental error} \quad \ldots\ldots\ldots\ldots\ldots(1)$$

Where, Y is the response for certain levels of the main effects X1 and X2 and the X1 X2 term is comprised to account for a likely interaction effect between X1 and X2. The main effects are referred to the effect of a single factor on a particular experimental response, averaged across the levels of any other independent factors. In contrary, factor interactions take place when the effect of a factor is contingent on the level setting of another factor. Every factorial designs are capable to find main effects as well as factor interactions. The constant $\beta 0$ is the response of Y when both main effects are 0. For more illustration, a linear model with three factors X1, X2, X3 and one response at three levels Y, if all possible terms were included in the model would look like the following:

$$Y = \beta_0 + \beta_1 X_1 + \beta_2 X_2 + \beta_3 X_3 + \beta_{12} X_1 X_2 + \beta_{13} X_1 X_3 + \beta_{23} X_2 X_3 + \beta_{123} X_1 X_2 X_3 + \text{experimental error} \quad \text{.....(2)}$$

When the experimental data are investigated, the entire unknown "β" parameters are calculated and the coefficients of the "X" terms are verified to see which ones are considerably different from 0.

CHAPTER 4

Experimentation and Experimental Results

As described in the previous chapter, we have used the CVD to produce CNT's at various operating conditions. The experimental runs that we have conducted and the results such as the obtained yields for every run and the characterization we have performed are presented in the following sections.

4.1 Experimental Runs

As stated earlier, experimental designs were generated using experimental design software. The 3^K experimental design matrix consisted of 27 experiments to investigate the three parameters (temperature, total gas flow rate, and hydrogen flow rate). The experiments were performed utilizing the equipment described in figure-6 above where we have conducted according to the 3^K matrix 27 runs at various conditions for temperature, Hydrogen flow rates and Hydrocarbon injection rates. The number of experimental runs required for a full factorial design for the three factors being studied is equal to n^K. Consequently, we have assigned the levels for each factor in every run as high, medium and low, +1, 0 and -1 to indicate the high, medium and the low level of each factor (Table 2). The levels were then translated to the operating conditions that were set to conduct the experimentations as shown in Table-3. For every run, the weight was collected and measured while the quality and purity were verified using the Scanning Electron Microscope (SEM) and Thermal Gravity Analyzer (TGA).

Run #	T	F	I	TF	TI	FI	TFI
1	-1	-1	-1	1	1	1	-1
2	-1	-1	0	1	0	0	0
3	-1	-1	1	1	-1	-1	1
4	-1	0	-1	0	1	0	0
5	-1	0	0	0	0	0	0
6	-1	0	1	0	-1	0	0
7	-1	1	-1	-1	1	-1	1
8	-1	1	0	-1	0	0	0
9	-1	1	1	-1	-1	1	-1
10	0	-1	-1	0	0	1	0
11	0	-1	0	0	0	0	0
12	0	-1	1	0	0	-1	0
13	0	0	-1	0	0	0	0
14	0	0	0	0	0	0	0
15	0	0	1	0	0	0	0
16	0	1	-1	0	0	-1	0
17	0	1	0	0	0	0	0
18	0	1	1	0	0	1	0
19	1	-1	-1	-1	-1	1	1
20	1	-1	0	-1	0	0	0
21	1	-1	1	-1	1	-1	-1
22	1	0	-1	0	-1	0	0
23	1	0	0	0	0	0	0
24	1	0	1	0	1	0	0
25	1	1	-1	1	-1	-1	-1
26	1	1	0	1	0	0	0
27	1	1	1	1	1	1	1

Table 2: factors assigned low medium and high level for the different runs

In the CVD reactor, once the temperature had reached to the reaction temperature, the hydrocarbon liquid with Ferrocene catalyst is injected into the first reaction chamber at different injection rates (5 mL /min, 22.5 mL/min and 40 mL /min). The hydrogen gas was flown to the system during the reaction period. The hydrogen gas was used as activation agent to activate the surface of the catalyst.

The reaction time was fixed at one hour since it was found that this reaction time is the optimum time per Attiah, et al. The optimum reaction time of one hour is attributed to the available space for the catalyst that are depositing at the quartz tube walls which are acting as a substrate for the CNT's growth during the reaction time.

In the experimental set up, the reactor walls were used as substrates for CNT growth where the iron nanoparticles deposited on the reactor wall act as the catalyst base for CNT growth. It was found that, in one hour the catalyst will occupy all the available space in the quartz tube walls at the various P-xylene rates where the growth of CNT's starts. Extending the reaction time beyond one hour will not improve the growth of CNT's since the catalyst is not forming a base for the growth of CNTs due to unavailable space in the reactor walls used as substrate that is responsible for the growth of the CNT's.

The reaction temperature was varied from 700 C^o to 1000 C^o while the hydrogen flow rate was varied from 100 to 3000 mL /min. The effects of reaction temperature and different hydrogen on the morphology, quality and quantity of the product were investigated. Table 3 shows the parameters that were set for every run along with the measured CNT's weights, calculated yields, average diameter, average length and the calculated average aspect ratio for the produced CNT's.

The yield is defined as the weight of the produced CNT in grams divided by the weight of the P-xylene fed to the reactor per the following:

$$CNT\ Yield\ (\%) = \frac{Wight\ of\ CNT\ (g)}{Wight\ of\ P-x\ (g)} * 100 \qquad (3)$$

#	Temp (C°)	H2 Flow (ML/ Min)	Cat. H.C Inject (ML/hr)	Prod. Experim. (g)	Yield Experim. (wt%)	Average Diameter (nm)	Average Length (um)	Average L/D
1	700	100	5.0	0.130	3.00	250	100	400
2	700	100	22.5	0.187	0.96	200	250	1250
3	700	100	40.0	0.198	0.57	130	150	1153
4	700	1550	5.0	0.430	10.00	130	150	1153
5	700	1550	22.5	0.660	3.39	130	150	1154
6	700	1550	40.0	0.850	2.45	170	200	1176
7	700	3000	5.0	0.220	5.00	100	250	2500
8	700	3000	22.5	0.468	2.40	100	100	1000
9	700	3000	40.0	0.219	0.63	150	120	800
10	850	100	5.0	0.505	11.66	200	300	1500
11	850	100	22.5	1.045	5.36	200	150	750
12	850	100	40.0	1.590	4.59	170	200	1176
13	850	1550	5.0	0.780	18.00	120	130	1083
14	850	1550	22.5	1.660	8.50	100	230	2300
15	850	1550	40.0	2.180	6.29	100	200	2000
16	850	3000	5.0	0.604	13.94	150	430	2867
17	850	3000	22.5	1.610	8.26	180	300	1667
18	850	3000	40.0	1.710	4.93	200	400	2000
19	1000	100	5.0	0.620	14.31	150	100	667
20	1000	100	22.5	0.630	3.23	200	135	675
21	1000	100	40.0	0.997	2.88	200	200	1000
22	1000	1550	5.0	0.480	11.00	150	200	1333
23	1000	1550	22.5	1.100	5.64	100	200	2000
24	1000	1550	40.0	1.350	3.89	150	230	1533
25	1000	3000	5.0	0.350	8.00	130	230	1769
26	1000	3000	22.5	0.874	4.48	100	230	2300
27	1000	3000	40.0	1.450	4.18	250	200	800

Table 3: CNTs yield of the experimental runs at various conditions

4.2 Experimental data reproducibility and accuracy

To ensure reproducibility of the experimental runs, selected runs were repeated and the results were compared to the initial runs. Table 4 shows the selected runs and deviations of the repeated runs from the initial runs. The results of the repeated runs are deviating from the original runs in the range between 9 to 27%. In general, the deviation is relatively acceptable and indicates that the experimental results are reliable and can be used to analyze the CVD process. The subject of whether the calculated deviation represents satisfactory analytical performance is not so simple. The decision on suitability is contingent on what amount of analytical error is permissible without impacting or limiting the use and explanation of a test result. As a reference guideline for defining the amount of error that is allowable, the requirements for analytical quality criteria for acceptability shows variations ranges from 5 to about 30% depends on the process itself. The results were also compared to Attiah, et al study in a similar experiment set up and indicated reasonable agreement to this study in the range between 10 to 30%.

Run#	Yield Experimental (wt%)	Reproduced Run (wt%)	% Deviation
1	3.00	2.24	25.3
11	5.36	6.41	16.4
15	6.29	5.74	8.7
25	8.00	5.82	27.3

Table 4: CNTs yield of the selected repeated runs

4.3 Characterization Results

We have performed SEM for all the samples collected to verify the CNT's yield and quality. In addition, SEM was carried out for the repeated runs to ensure reproducibility of the morphologies and size of the Nano tubes at the various operating conditions. The morphologies of the CNTs of some of the samples examined by SEM as well as the reproduced runs at different growth temperatures are presented in figures 10 -15. It is clear that the CNT's produced vary in length and alignment depending on the operating conditions at which the CNT's were produced.

The examined samples indicated that the diameter of the CNT's produced vary from about 100 nm to 250 nm. The diameter size was found to be in the range of 150 and higher up to 250 nm at temperatures of 700 C^o and then get reduced to the level of 100 nm in the temperature range of 850 C^o while it increases back to the 150 and higher at temperature of 1000 C^o. On the other hand, the length of the Nano tubes exhibited almost opposite behavior to the diameter size trend. The length obtained varied between 100 to about 450 µm. At temperatures of 850 C^o, long and aligned CNTs (200 to 430 µm) were produced as bundles. The diameter and length minimum and maximum, respectively occurred at the temperature range of 850 C^o. In addition, the aspect ratio which is the length over the diameter appears at the 850 C^o range. In many applications, a high aspect ratio of CNT's is always desirable and therefore, it is of commercial interest to have a scalable method to produce aligned CNT's with high aspect ratios.

a)

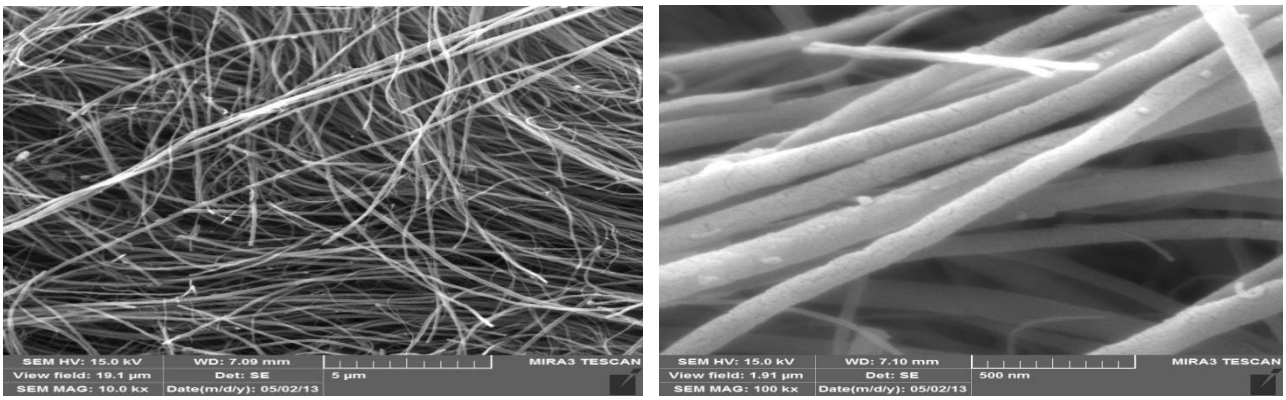

(b)

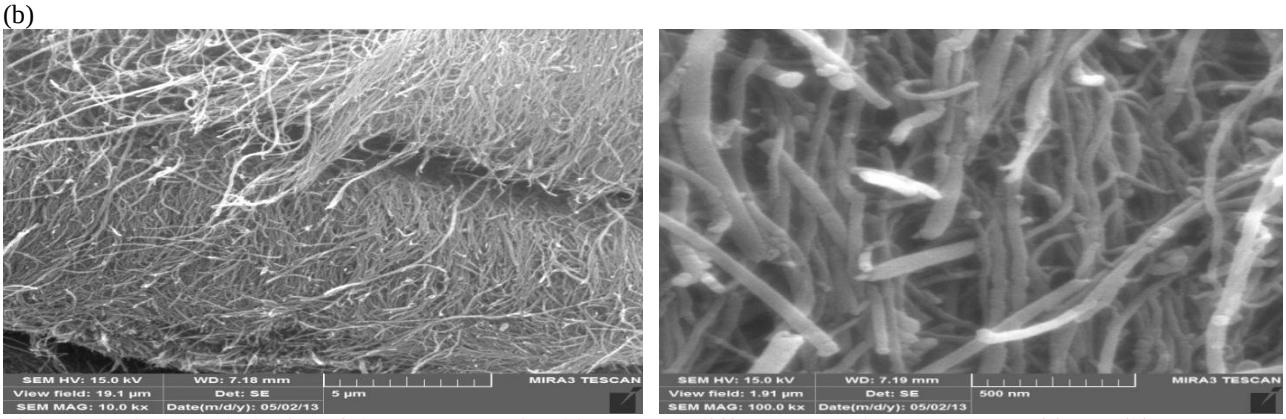

Figure 10: The morphologies of the CNTs examined by SEM at different growth temperatures: (a) R#1 (b) R#8

(c)

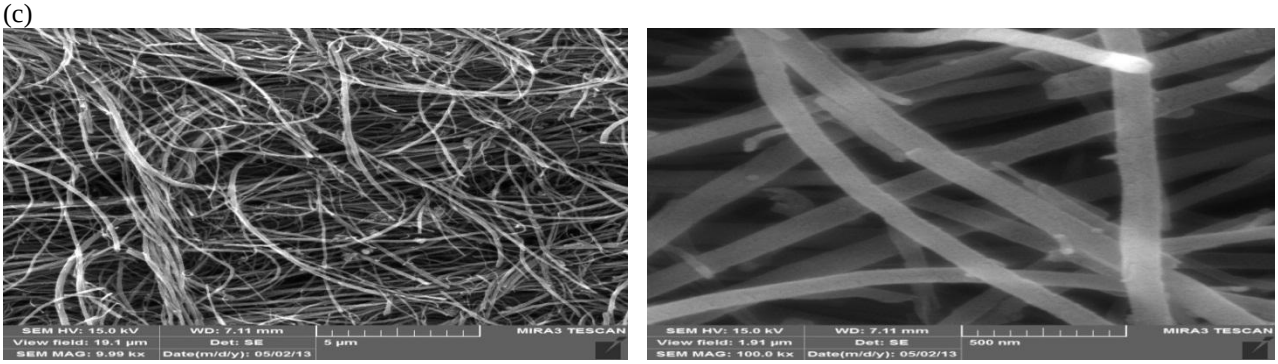

(d)

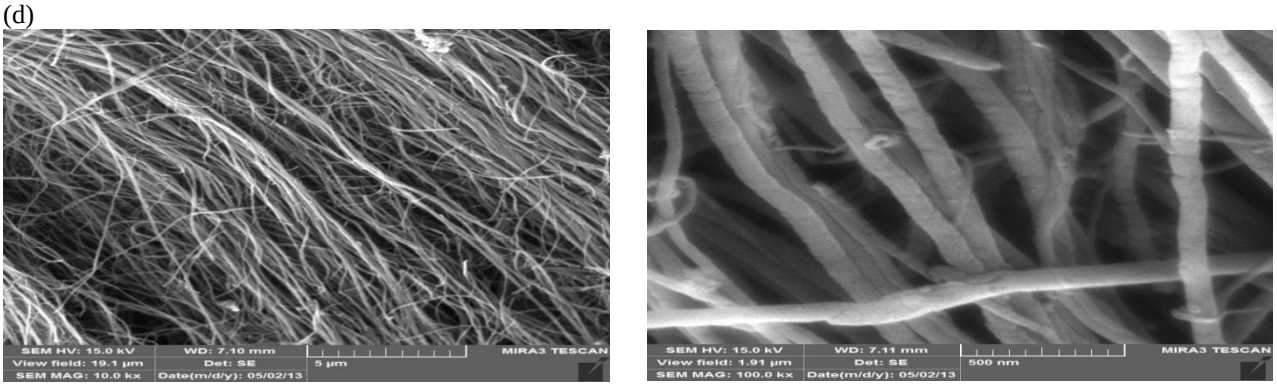

Figure 11: The morphologies of the CNTs examined at different growth temperatures: (a) R#15 (d) R#16

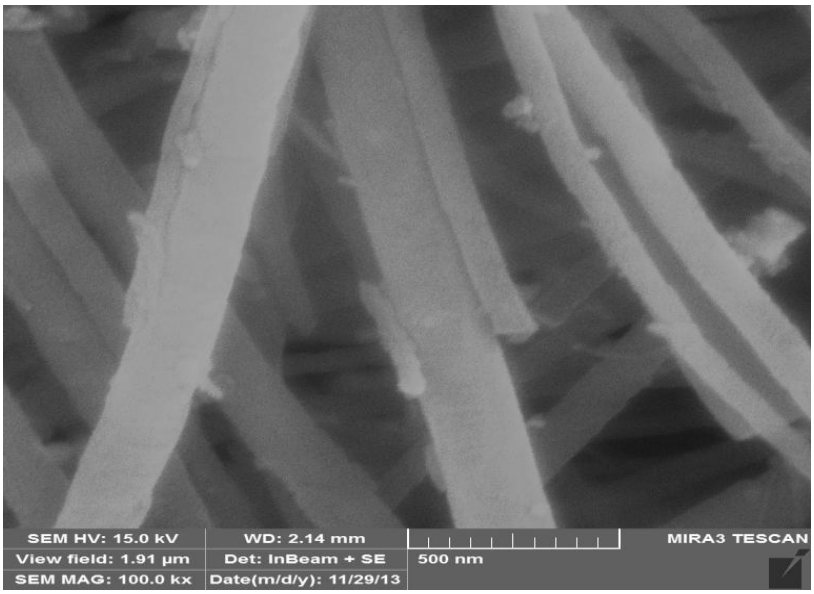

Figure 12: Run#1 reproduced morphologies examined by SEM

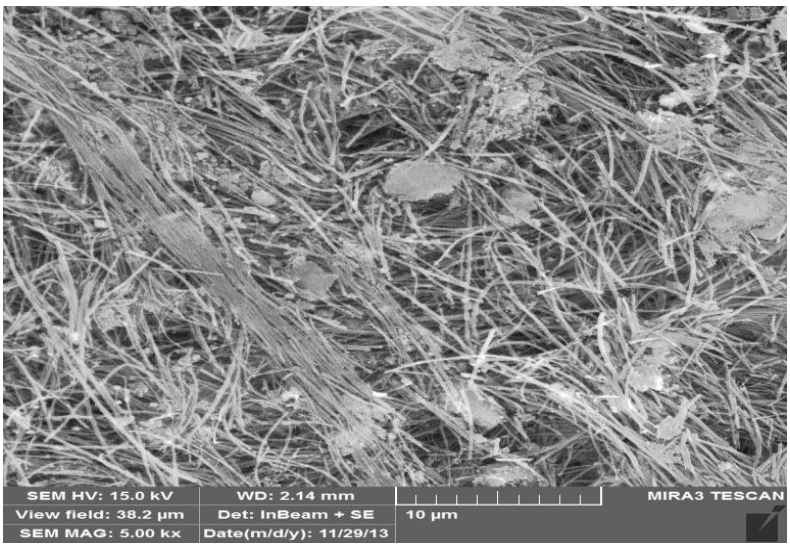

Figure 13: Run#1 reproduced morphologies examined by SEM

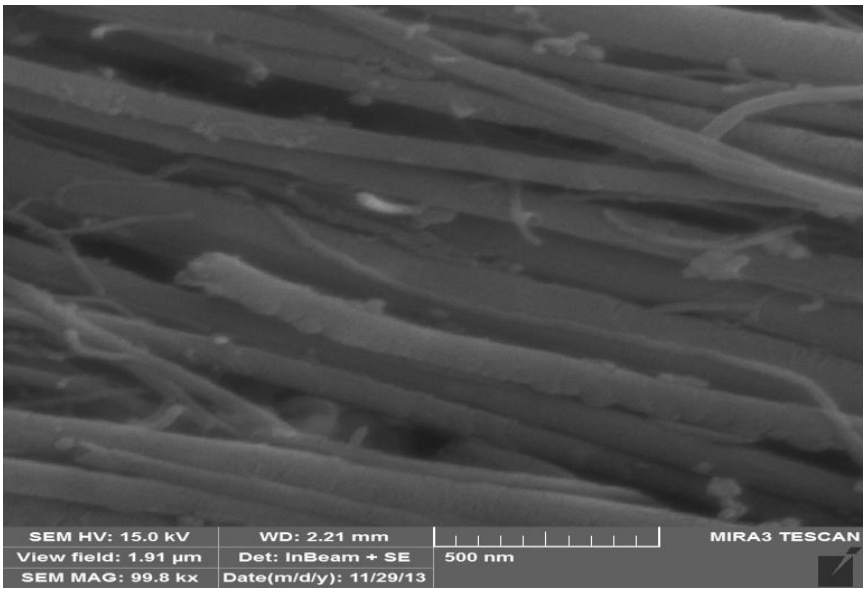

Figure 14: Run#11 reproduced morphologies examined by SEM

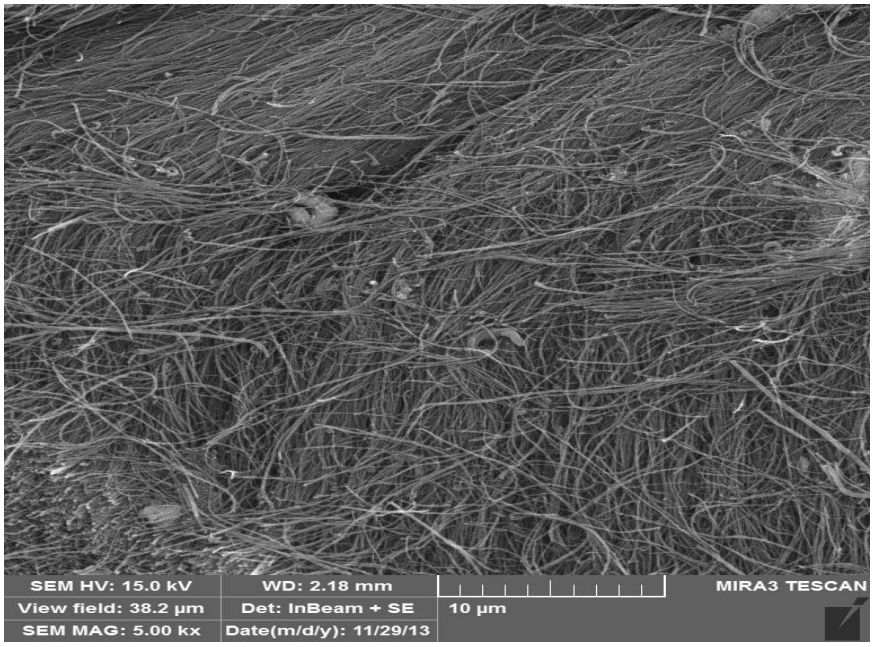

Figure 15: Run#11 reproduced morphologies examined by SEM

4.4 Results of Thermal Gravity Analyzer (TGA)

The purity of the CNT was determined using the Thermal Gravimetry Analyzer (TGA). This is to study the thermal stability of the products in order to distinguish the deposited carbons according to their different thermal stability level. Figure 16 shows the TGA of CNTs obtained at R_T=700 C^o and H_2 flow of 3000 mL/min. It is observed that the sample decomposition starts at 200 C^o indicating impurity of the produced CNT.

Figure 17, show the TGA of CNTs obtained at R_T=850 C^o, and H_2 flow of 3000 ml/min and P-x rate of 40 mL/hr. The CNT decomposition in this case behaves little bit differently where it starts at 500 C^o and then rapidly decompose at 500 C^o. In addition, the TGA graph shows a single step decomposition which is an indication of the CNT purity. Figure 18, shows the TGA of CNTs obtained at R_T=1000 C^o, and H_2 flow of 3000 mL/min and P-x rate of 22.5 mL/hr. The CNT decomposition starts in this case at 400 C^o and then decomposes rapidly at 500 C^o indicating less purity.

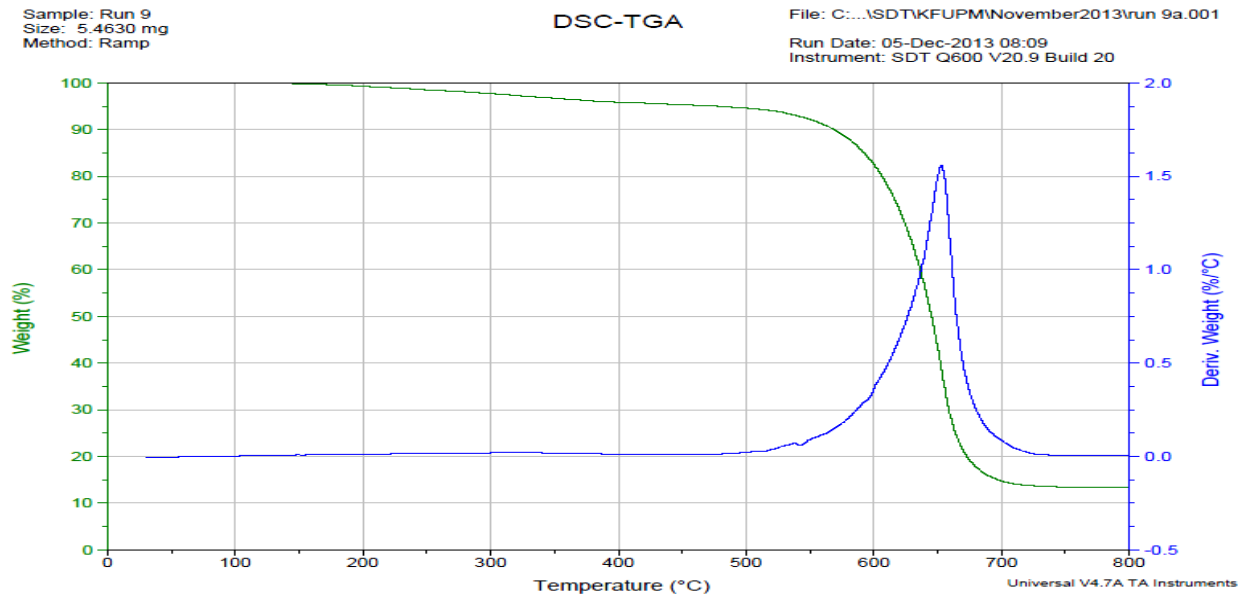

Figure 16: TGA for Run#9

In TGA, the CNT is burned under air where normally the CNT will not burn before a temperature of about 480 C^o (SWCNT) followed by MWCNT that will burn at approximately 500 C^o and finally by the CNF which starts burning at approximately 600 C^o. The carbon and catalyst contents determined by the TGA profile in figure 16 were 95% and 12%, respectively. From this data, the purity of the sample can be estimated to be 83%. The purity of the random samples that were performed is listed in Table 5 where it shows that the purity is ranging from 65% to about 91%.

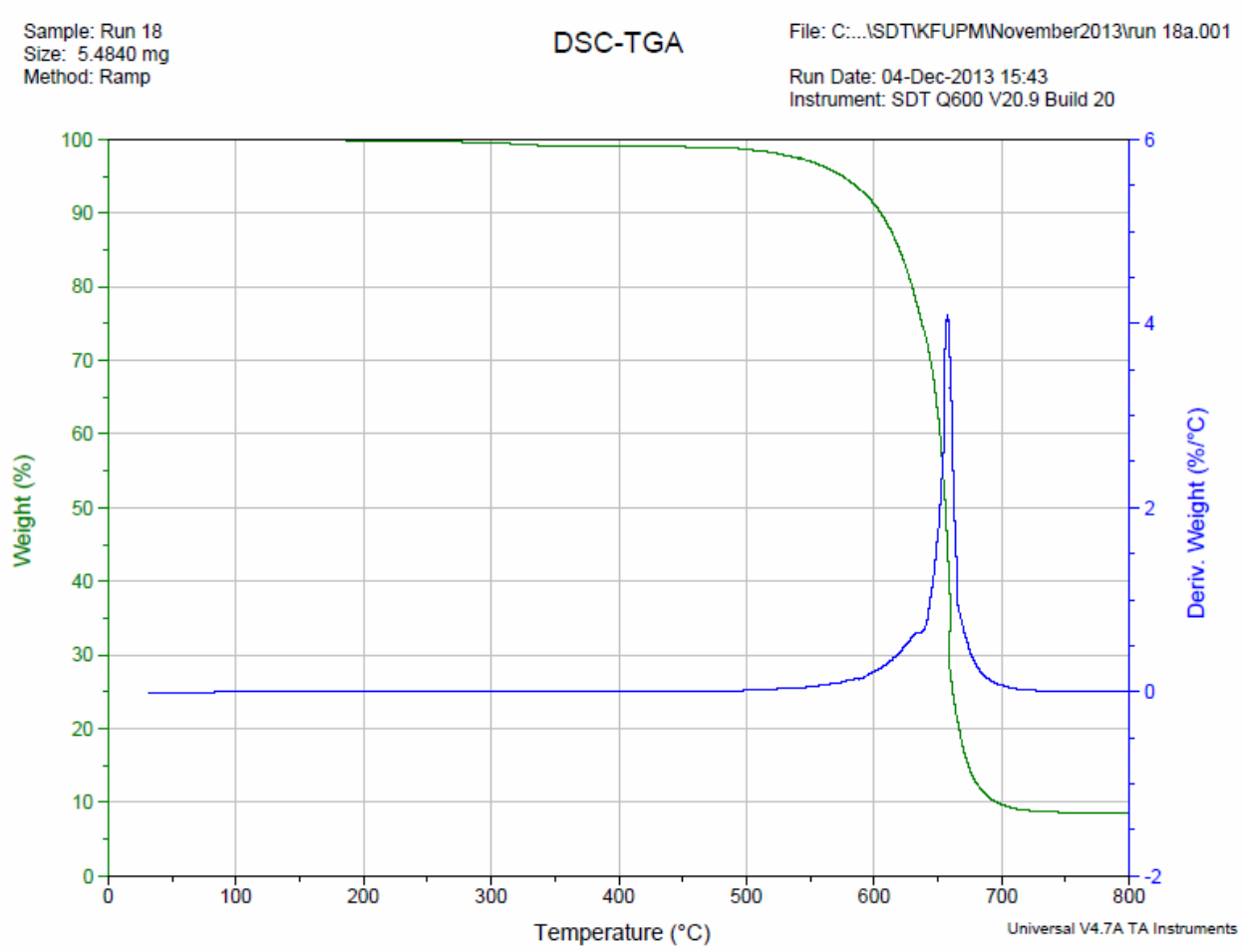

Figure 17: TGA for Run#18

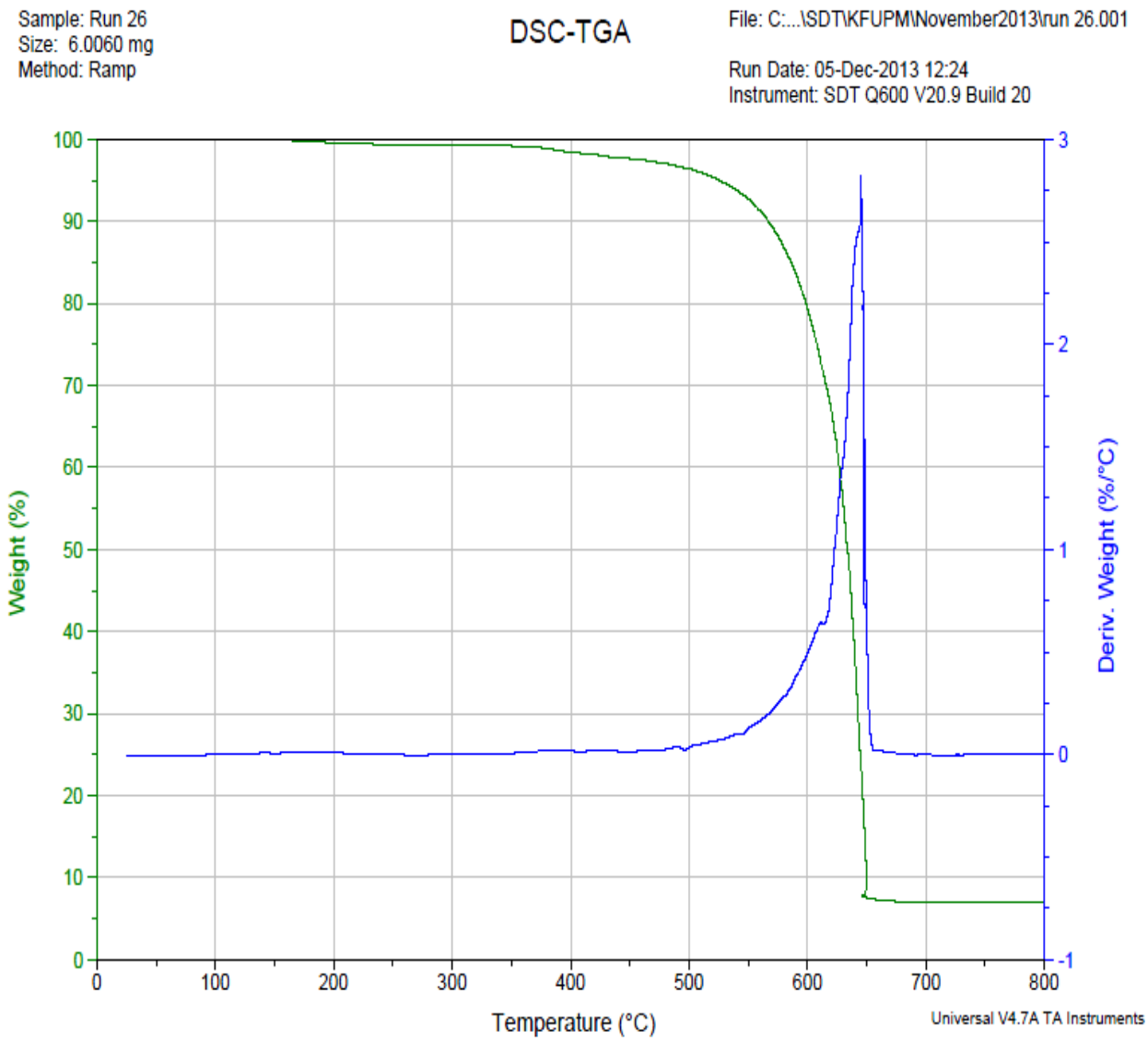

Figure 18: TGA for Run#26

Table 5 shows the purity from the TGA conducted for all the experimental runs.

#	Temp	H2 Flow	P-x Flow	Purity (%)
1	700	100	5	**78**
2	700	100	22.5	**60**
3	700	100	40	**65**
4	700	1550	5	**80**
5	700	1550	22.5	**77**
6	700	1550	40	**78**
7	700	3000	5	**82**
8	700	3000	22.5	**83**
9	700	3000	40	**83**
10	850	100	5	**80**
11	850	100	22.5	**77**
12	850	100	40	**90**
13	850	1550	5	**82**
14	850	1550	22.5	**89**
15	850	1550	40	**89**
16	850	3000	5	**85**
17	850	3000	22.5	**87**
18	850	3000	40	**91**
19	1000	100	5	**82**
20	1000	100	22.5	**83**
21	1000	100	40	**83**
22	1000	1550	5	**85**
23	1000	1550	22.5	**89**
24	1000	1550	40	**91**
25	1000	3000	5	**76**
26	1000	3000	22.5	**89**
27	1000	3000	40	**80**

Table: 5 Purity from TGA of various runs

CHAPTER 5

Modeling and Parametric Optimization

To model the response variables and then perform parametric optimization, regression was employed to develop models that are best fit the experimental data. In statistical, regression is an attempt to determine the strength of the relationship between one dependent variable typically represented by Y and a series of other changing variables identified as independent variables. The two basic types of regression are linear regression and multiple regressions where linear regression uses one independent variable to describe and the outcome of Y. The multiple regressions use two or more independent variables to predict the outcome. Regression takes a set of arbitrary variables, supposed to be estimating Y, and attempts to identify a mathematical link between them. This link is usually represented in a mathematical model that best describes all the individual data points. In the following sections, we will show two methods of regressions namely least square and multiple linear regression methods which are both multiple regression that we have applied to describe the experimental data for the yield and prove that the MLR gives a better model to describe our experimental values. Hence, the MLR is then adopted to develop the models for the other parameters which are CNT purity and dimensions. The Analysis Of Variance (ANOVA) and other statistical measures are presented in this chapter to show the significance of the models that were used to develop the contours and 3D diagrams as well as the objective functions to find optimum conditions.

5.1 Least Square Method (LS)

Initially, the least square estimation was used to calculate the values of the model coefficients for the CNT yield only from the above experimental data in table 2. The three factor, three-level, full factorial statistically design matrix is shown in figure 19. In addition, the levels that were assigned for the factors (temperature, gas flow and hydrogen flow) with its interactions for every run with high, medium and low levels were presented in Table 2 in section 4.1.

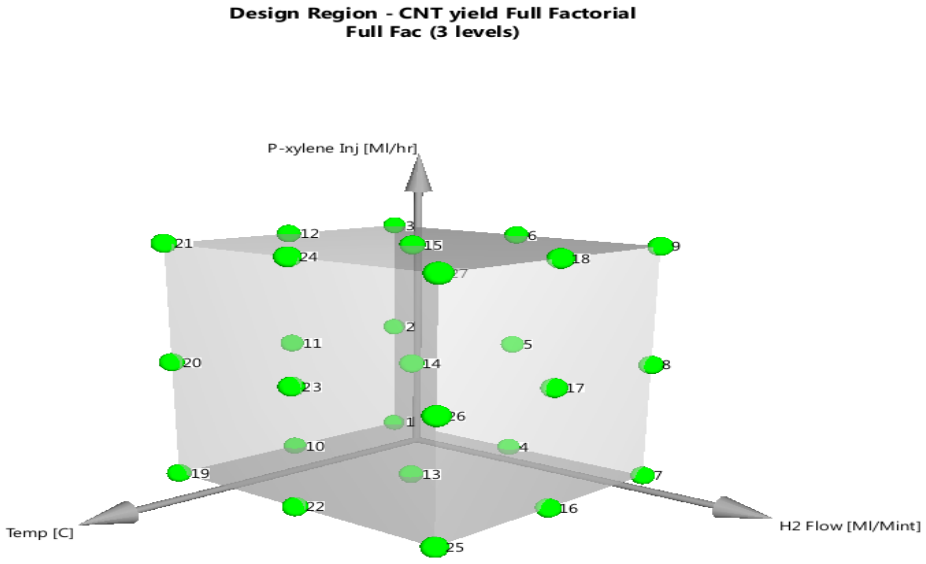

Figure 19: Three levels full factorial design matrix

The coefficients were then calculated after solving the matrices per the following equation:

$$\beta=(X^{T}X)^{-1}X^{T}Y \quad \ldots\ldots\ldots\ldots\ldots\ldots\ldots(3)$$

The calculated coefficients based on solving the above matrix are presented in the following table:

βo	6.205
$\beta 1$	1.623
$\beta 2$	0.292
$\beta 3$	−3.583
$\beta 4$	−0.605
$\beta 5$	−0.667
$\beta 6$	0.311
$\beta 7$	1.194

Table 6: calculated coefficients by LS

Accordingly, the empirical equation with the interaction effects was obtained to be as follows:

$Y_{Model\ (LS)} = 6.205 + 1.623\ T + 0.292F - 3.583\ I - 0.605\ TF - 0.667\ TI +$
$0.311\ FI + 1.194\ TFI$ …….....(4)

Figure 20 is a plot of Y_{obs} versus Y_{model} which shows deviation particularly in the mid points between the observed and experimental values. The observed versus predicted yields are analyzed, compared and presented in Table 7. Comparing the above Y_{model} versus observed data revealed some deviations. The obtained mathematical model was evaluated based on statistical criteria such as coefficient of determination (R^2) and the estimate of the predictive ability of the model (Q^2), see appendix-A for more details about the definition of some of the statistical measures. The obtained R^2 is 0.581 and therefore, to improve the model, a more

rigorous method such as Multiple Linear Regression (MLR) was used to estimate the mathematical models.

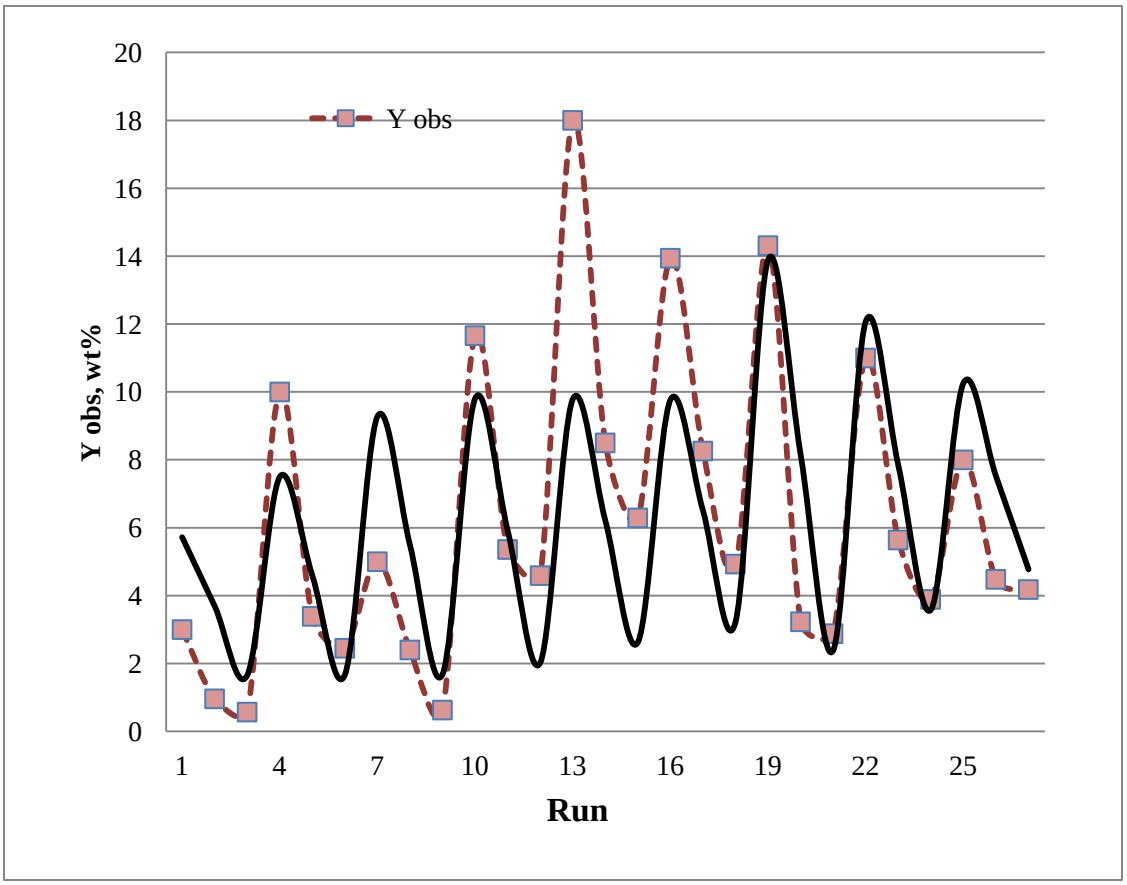

Figure 20: Plot of Y_{obs} versus Y_{model} by Least Square (LS) method

Run #	Y obs (g)	Y obs (wt%)	Y Model	% Error
1	1.130	3.00	5.718	47.5
2	0.187	0.96	3.685	73.9
3	0.198	0.57	1.652	65.5
4	0.430	10.00	7.498	33.4
5	0.660	3.39	4.582	26.0
6	0.850	2.45	1.666	47.1
7	0.220	5.00	9.278	46.1
8	0.468	2.40	5.479	56.2
9	0.219	0.63	1.680	62.5
10	0.505	11.66	9.807	18.9
11	1.045	5.36	5.913	9.4
12	1.590	4.59	2.019	127.3
13	0.780	18.00	9.788	83.9
14	1.660	8.50	6.205	37.0
15	2.180	6.29	2.622	139.9
16	0.604	13.94	9.769	42.7
17	1.610	8.26	6.497	27.1
18	1.710	4.93	3.225	52.9
19	0.620	14.31	13.896	3.0
20	0.630	3.23	8.141	60.3
21	0.997	2.88	2.386	20.7
22	0.480	11.00	12.078	8.9
23	1.100	5.64	7.828	28.0
24	1.350	3.89	3.578	8.7
25	0.350	8.00	10.260	22.0
26	0.874	4.48	7.515	40.4
27	1.450	4.18	4.770	12.4
Avg.				44.5

Table 7: CNTs yield experimental various calculated (LS)

5.2 Multiple Linear Regression (MLR) Method for CNT Yield

We have utilized design of experiment software to design the experiment and estimate the coefficients of the terms in the model using Multiple Linear Regression. The software is effective in achieving product and process efficiency and optimization that help scientists, engineers and statisticians understand complex processes and products when designing experiments. It guides through the setup of the Design of Experiments (DOE) and supports subsequent data analysis.

In MLR, the coefficients of the model are calculated to minimize the sum of squares of the residuals, i.e. the sum of squared deviations between the experimental and fitted values of each response. It is should be noted that, MLR distinctly fits one response at a time and therefore assumes them to be independent. For the CNT yield empirical model, the resulted MLR model fitting incorporating R^2, Q^2, and model validity indicates excellent model fit. The model shows good fit for the three parameters that were selected for analysis as they meet required statistical limits such as R^2 and Q^2. The computed coefficients of the yield fitted model are shown in Table 8.

Yield	Coeff. SC
Constant	9.02556
Temp	1.62278
H2 Flow	0.292222
P-xylene Inj	-3.58278
T*T	-4.28167
F*F	-2.22
I*I	2.27167
T*F	-0.605
T*I	-0.6675
F*I	0.310833

Table 8:MLR Yield Coefficients values

Accordingly, the yield mathematical model obtained with the above coefficients is as follows:

$$Y_{pred} =$$

$$9.02556 + 1.62278T + 0.292222F - 3.58278I - 4.28167TT - 2.22FF + 2.27167II - 0.605TF - 0.6675TI + 0.310833FI \quad \ldots\ldots\ldots\ldots\ldots\ldots\ldots\ldots\ldots\ldots\ldots(5)$$

The observed yield versus predicted or calculated is presented in figure 21 which shows close relation with an R^2 of 0.886 and Q^2 of 0.645. The mathematical model is representing about 89 % of the experimental data and therefore, the model statistically is adequate to be used for analyzing the specified parameters according to statistical guidelines.

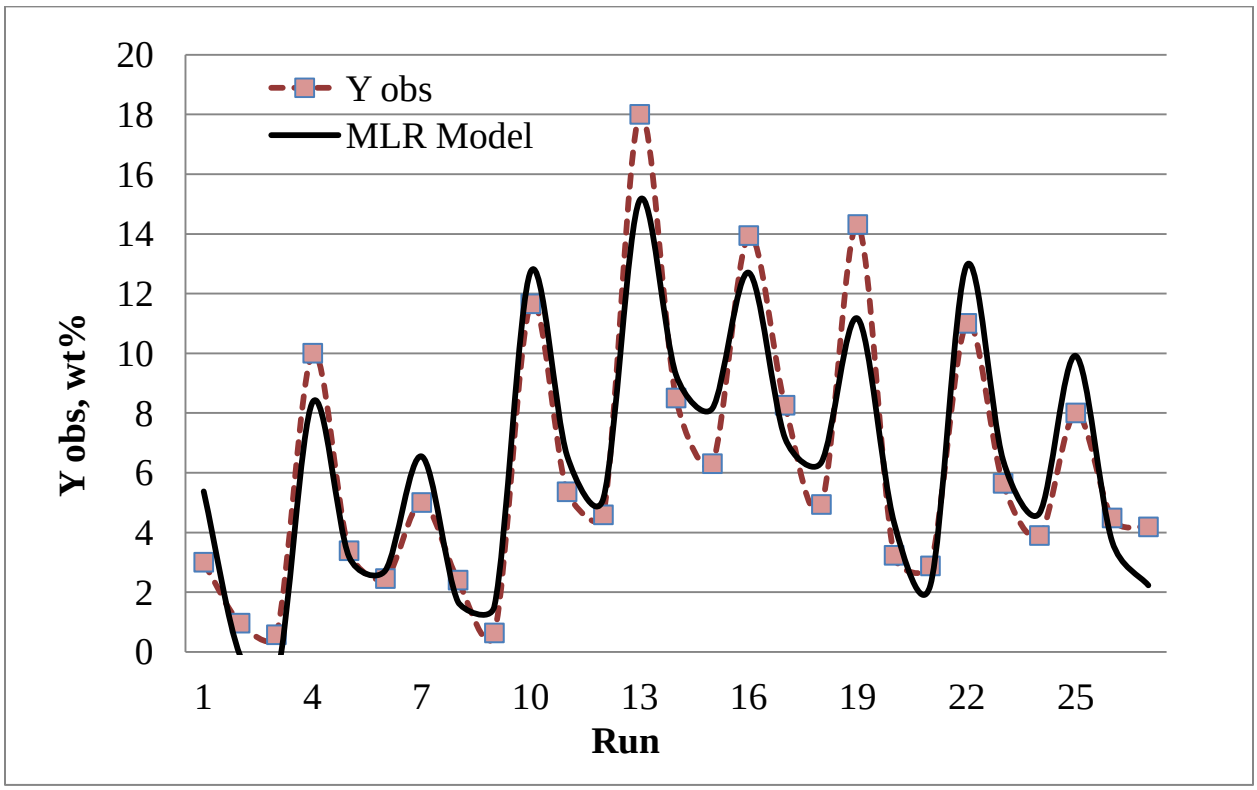

Figure 21: experimental yield versus model by MLR

Table 9 shows Y_{obs} versus predicted with the confidence of interval for every run indicating good model fitting. Additional data on the results of the statistical package for the CNT yield is presented in appendix-B.

Yield	Observed	Predicted	Obs - Pred	Conf. int(±)
1	3	5.50167	-2.50167	2.81144
2	0.96	0.00388805	0.956112	2.30594
3	0.57	-0.950556	1.52056	2.81144
4	10	8.30806	1.69194	2.30594
5	3.39	3.12111	0.268888	2.00598
6	2.45	2.4775	-0.0274982	2.30594
7	5	6.67444	-1.67444	2.81144
8	2.4	1.79833	0.601667	2.30594
9	0.63	1.46555	-0.835555	2.81144
10	11.66	12.6786	-1.01861	2.30594
11	5.36	6.51333	-1.15333	2.00598
12	4.59	4.89139	-0.301389	2.30594
13	18	14.88	3.12	2.00598
14	8.5	9.02556	-0.525558	2.00598
15	6.3	7.71445	-1.41445	2.00598
16	13.94	12.6414	1.29861	2.30594
17	8.26	7.09778	1.16222	2.00598
18	4.93	6.0975	-1.1675	2.30594
19	14.31	11.2922	3.01778	2.81144
20	3.23	4.45945	-1.22945	2.30594
21	2.88	2.17	0.71	2.81144
22	11	12.8886	-1.88861	2.30594
23	5.64	6.36667	-0.726669	2.00598
24	3.89	4.38805	-0.498055	2.30594
25	8	10.045	-2.045	2.81144
26	4.48	3.83389	0.646111	2.30594
27	4.18	2.16611	2.01389	2.81144

Table 9: Yobs versus predicted (MLR)

5.3 MLR for CNT Purity, Diameter, Length & L/D

Similarly, the empirical equations were developed for the other CNT parameters such as Purity (P), Diameter (D), Length (L) and Aspect ratio (L/D). The mathematical models for these parameters are as follows:

$$P_{pred} = 88.667 + 4.55556T + 3.05556F - 1.05556I - 3.33334TT - 5.16667FF - 2.83333\,II - 0.833332TF + 1.5TI + 0.999998FI \quad \ldots\ldots(6)$$

$$D_{pred} = 119.259 + 3.8889T - 18.8889F + 7.77777I - 2.77778TT + 42.2222FF + 15.5556\,II + 13.3333TF + 16.6667TI + 26.6667FI \quad \ldots\ldots(7)$$

$$L/D_{pred} = 1.91885 + 0.183167T + 0.453889F - 0.105778I - 0.546056TT - 0.149556FF - 0.171556II - 0.000666746TF + 0.0631666TI - 0.271667FI \quad \ldots\ldots(8)$$

$$L_{pred} = 237.963 + 27.2222T + 45F - 1.3889I - 95.5556TT + 29.4444FF + 3.61111II + 9.99999TF + 13.75TI - 8.75001FI \quad \ldots\ldots(9)$$

Accordingly the plots of the observed versus predicted for the purity and the various CNTs dimensions are presented in the following charts.

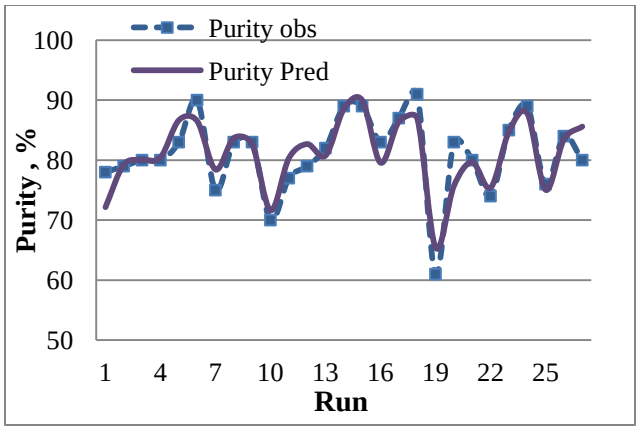

Figure 22- a

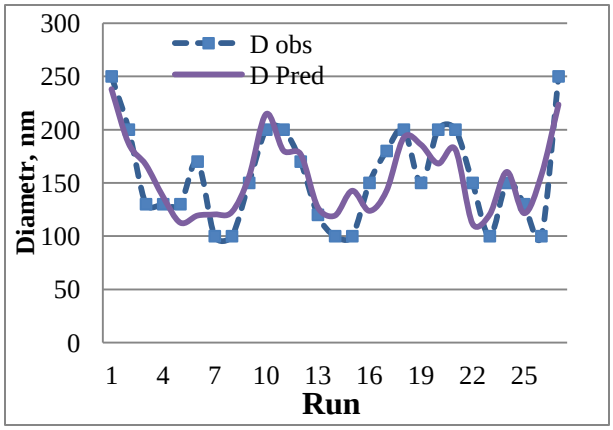

Figure 22-b

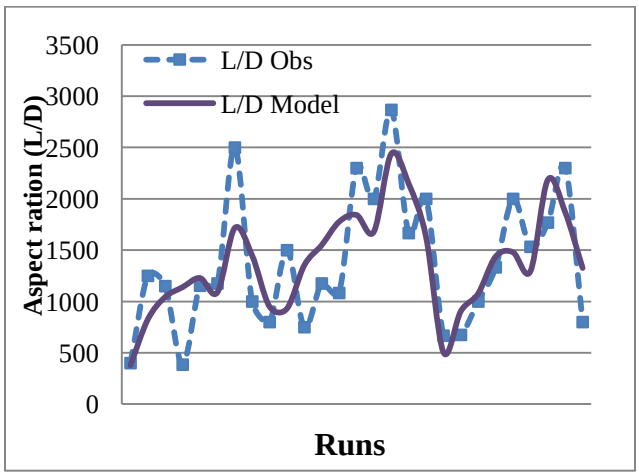

Figure 22- c

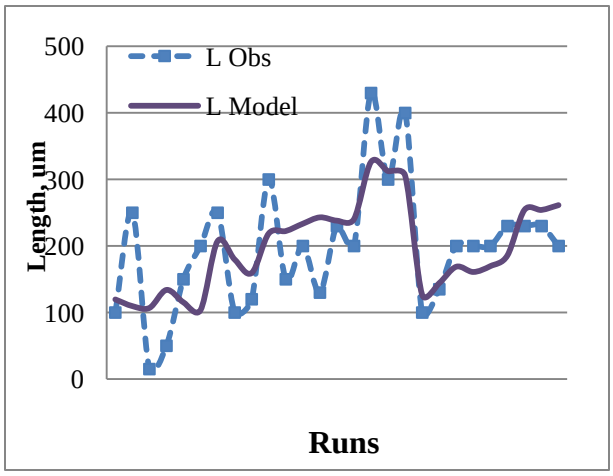

Figure 22- d

Figure 22: (a,b,c,d): Purity, Diameter, Length and L/D plots of obs versus model (MLR)

5.4 Model predictions and ANOVA analysis

The Analysis Of Variance (ANOVA) for each model are shown in Appendix B. The ANOVA analysis is performed in order to further evaluate the models and compare them to statistical criterions to find out whether we have a statistically significant difference between each parameter group means. We can see that the significance levels for the specified parameters such as the p-value ranges from almost 0 to 0.034 except for the Aspect ratio (p=0.123). These p-values are less

than $\propto$ of 0.05 implying clearly that the models are significant. The Fisher F-test value signifies how the mean square of the regressed model compares to the mean square of the residuals (errors) and in our case the highest was found to be 14.7 for yield while the other parameter are in the range between 1.9 to 7.0 indicating strong significant model for the yield and less significance for the remaining parameters.

Note that, the greater the F value, the more efficient the model. Meanwhile, lower probability (p value) demonstrates higher significance for the regression model. Furthermore, the values of the coefficients of determination (R^2) are ranging from 0.500 to 0.886 indicating high significance for the yield and less significance for the other parameters, see appendix-A for more details about the statistical definition.

Review of the literatures addressing optimization of CNT's by factorial design indicated that the models at such level of statistical measures can be satisfactorily used for further analysis and optimization. However, further improvement particularly for the Length can be achieved by the eliminations of insignificant factors in the empirical equations which are beyond the scope of this research. The ANOVA analyses for CNT yield, purity and the other CNT dimensions such as Diameter, Aspect ratio and Length are all shown in Appendix B.

In addition, it was found that according to the model performance indicators that the most significant factors are temperature and its interaction as well as the P-xylene injection rates with its interaction. Figures 23 (a-e) show the plots of regression coefficients of the fitted models to the response variables of the data set.

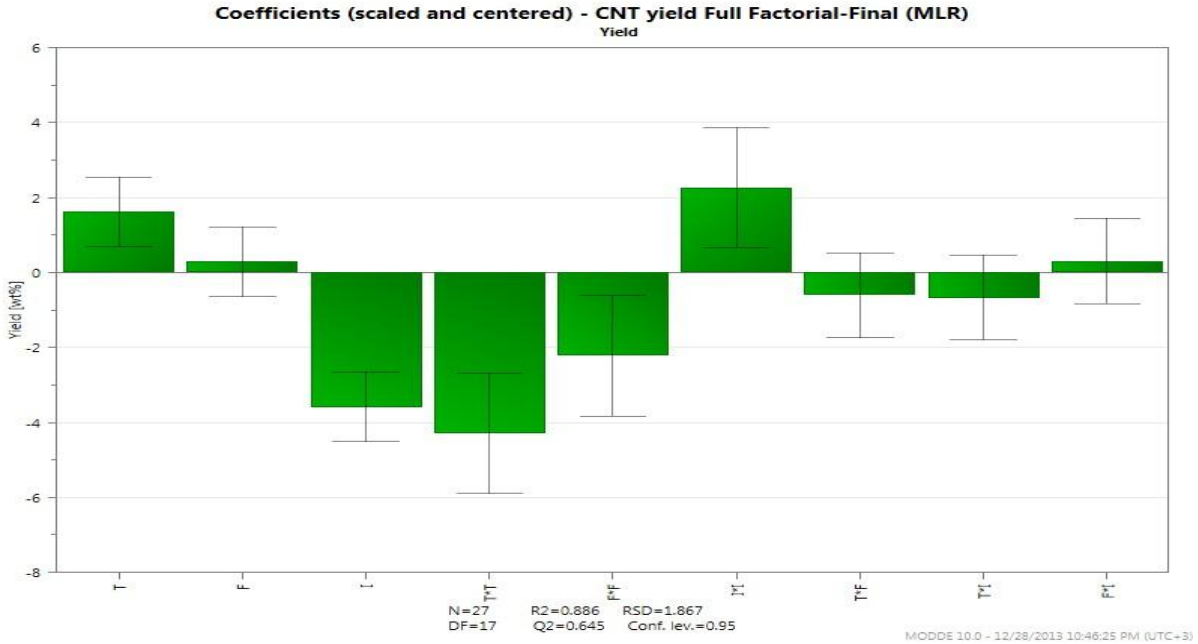

Figure 23-a: Model performance indicators for Yield

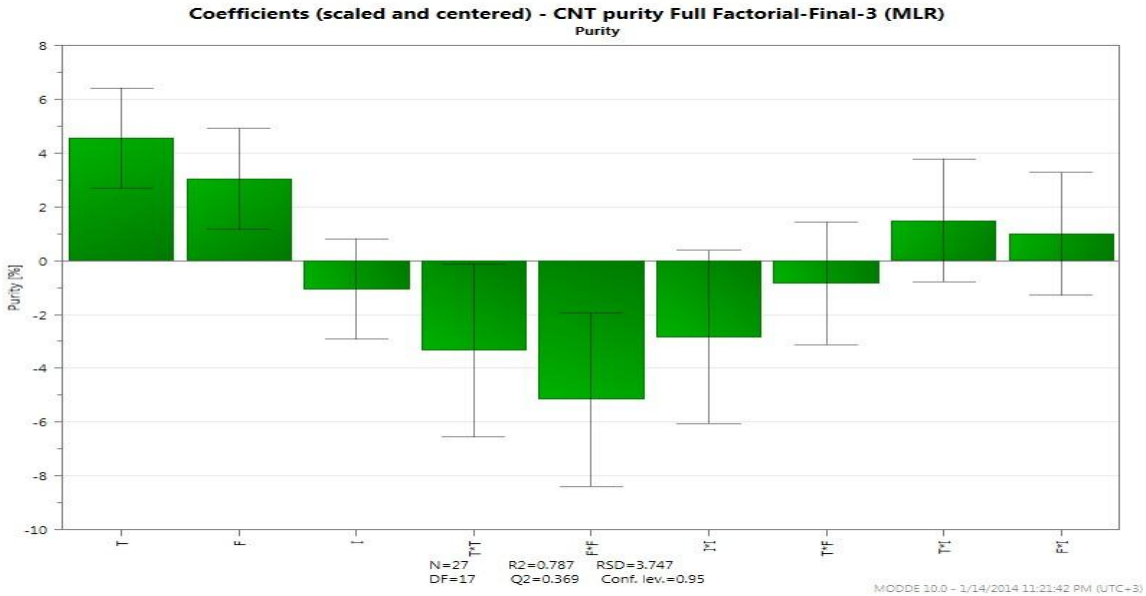

Figure 23-b: Model performance indicators for Purity

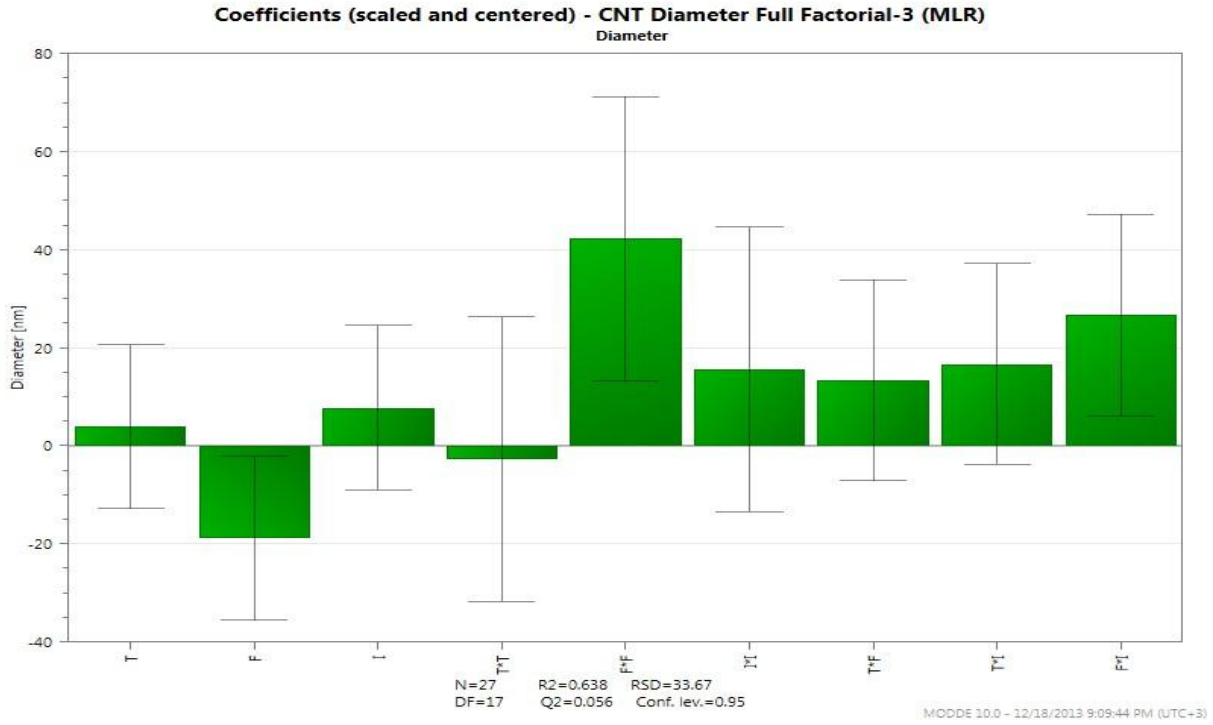

Figure 23-c: Model performance indicators for Diameter

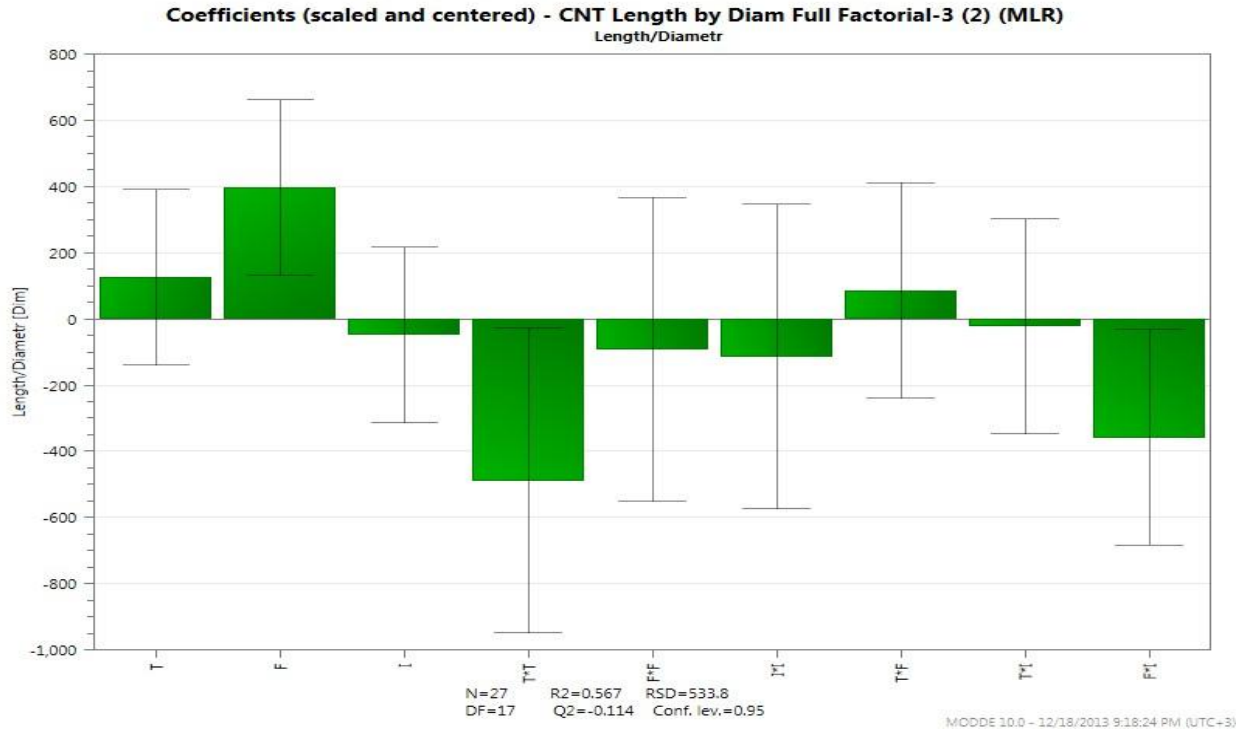

Figure 23-d: Model performance indicators for Aspect ratio

For the Length response, the P-x injection rate and its interactions with temperature and Hydrogen flow rate are the most insignificant factors. These factors can be eliminated for further improving the empirical equation for the Length response model.

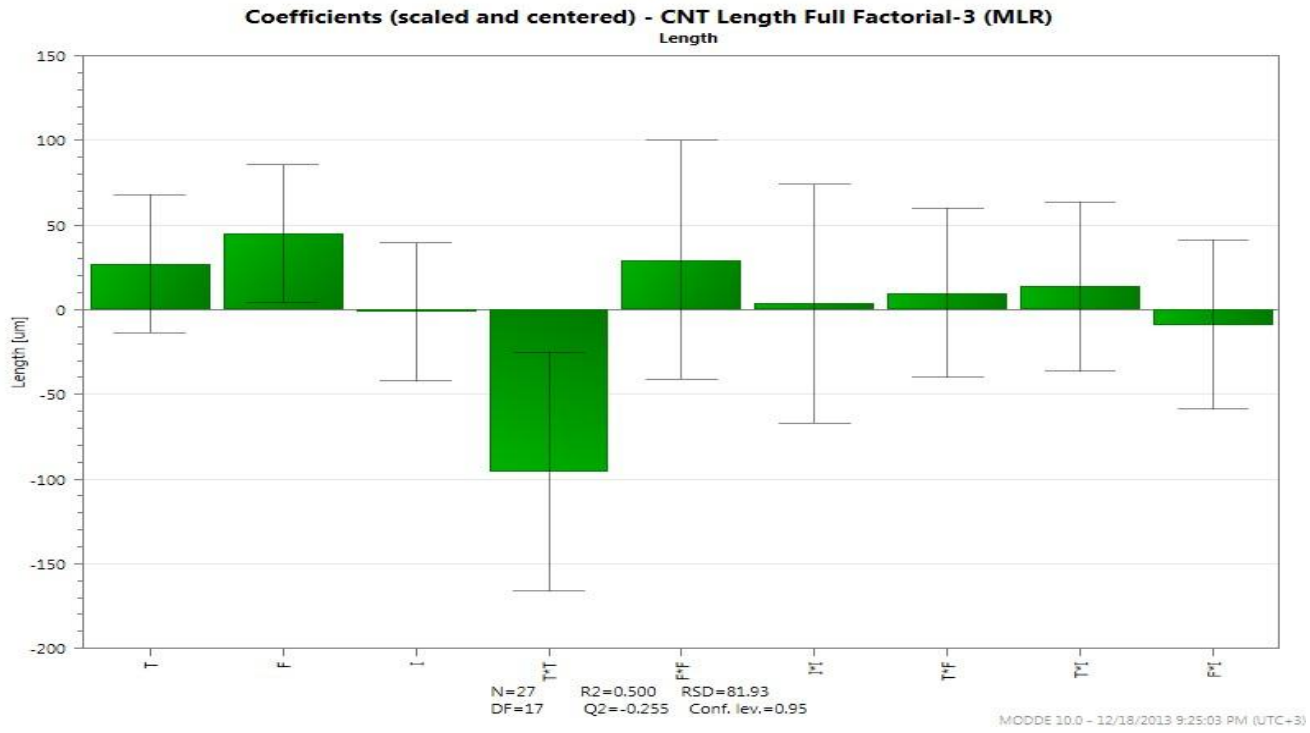

Figure 23-e: Model performance indicators for Length

Figure 23(a,b,c,d,e): Model performance indicators (MLR)

5.5 Response contour and 3 D plots

Factors with good model fit can be used to construct response contour plots. Response contour plots for CNT yield as a function of temperature and hydrogen flow rates at the various hydrocarbon flow rates are shown in Figures 24. The maximum CNT yield is laying in the temperature range of 800 to 950 and at hydrogen flow rate ranging from 500 to 3000 mL/mint.

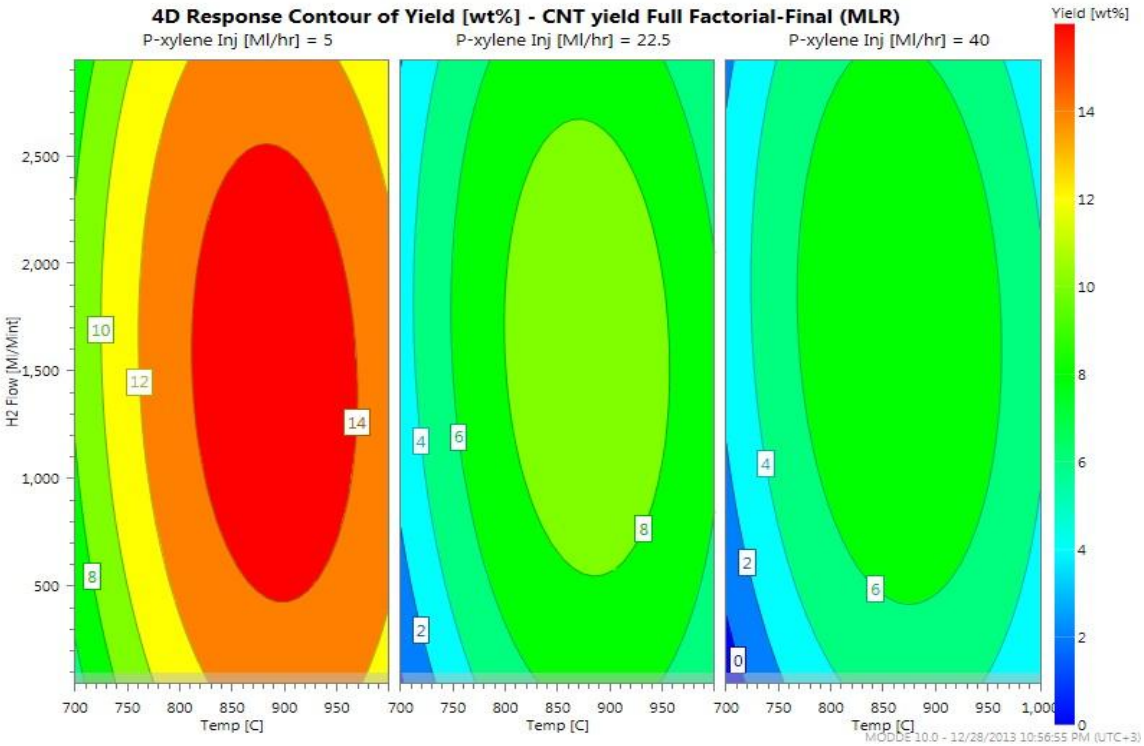

Figure 24: Yield contour plots at various hydrocarbon flow rates

The response contour plots for purity in figure 25 clearly show maximum purities are produced at higher H_2 flow while P-x flow rate is at minimum of 5 mL/hr.

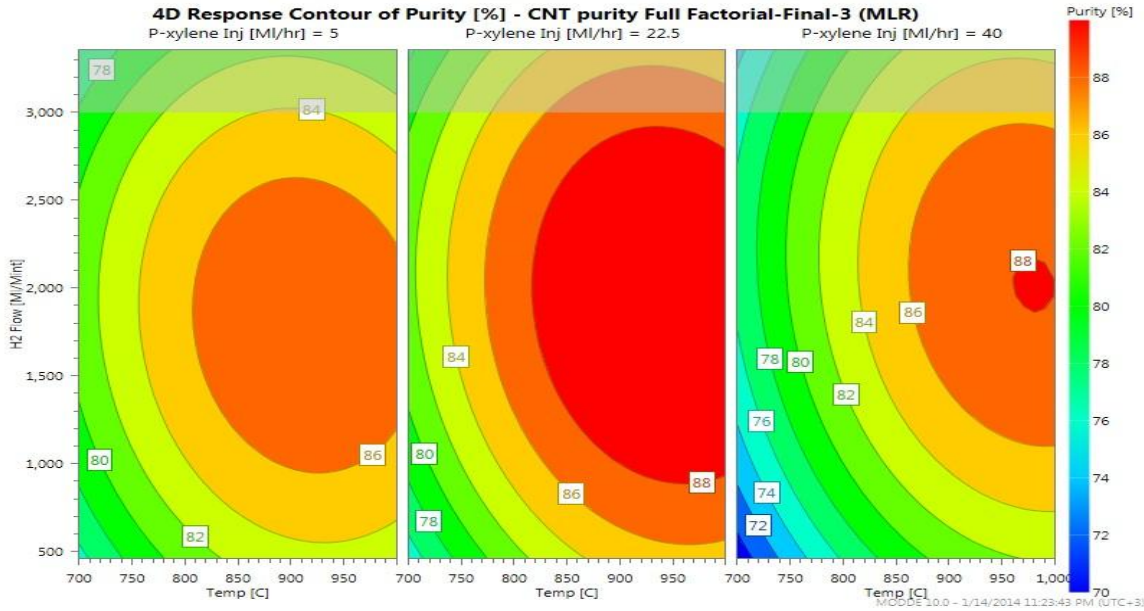

Figure 25 Purity contour plots at various hydrocarbon flow rates

The response contour plots for the diameter presented in figure 26 clearly show minimum diameters are produced at higher H_2 flow rates while P-x flow rate is at the minimum of 5 mL/hr.

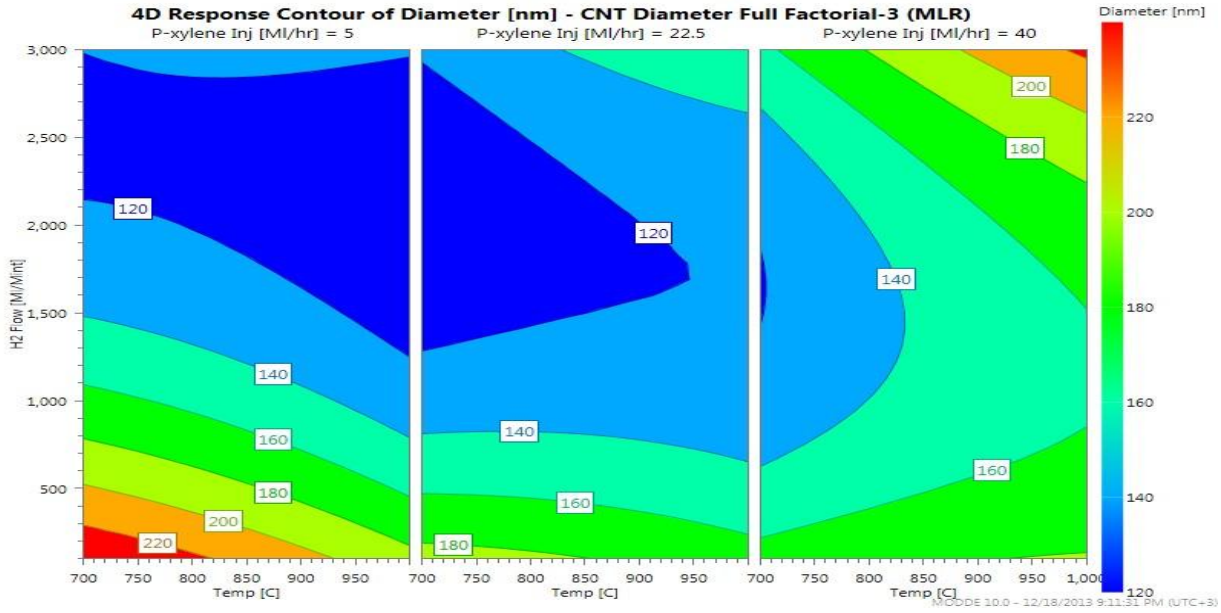

Figure 26: Diameter contour plots at various hydrocarbon flow rates

Similarly, the highest aspect ratio from the contour (Figure: 27) apparently is produced at the minimum P-x flow rate of 5 mL/hr in the temperature range between 800 to 950 C^o. Similar behavior is observed for the Length from the contour of Figure: 28.

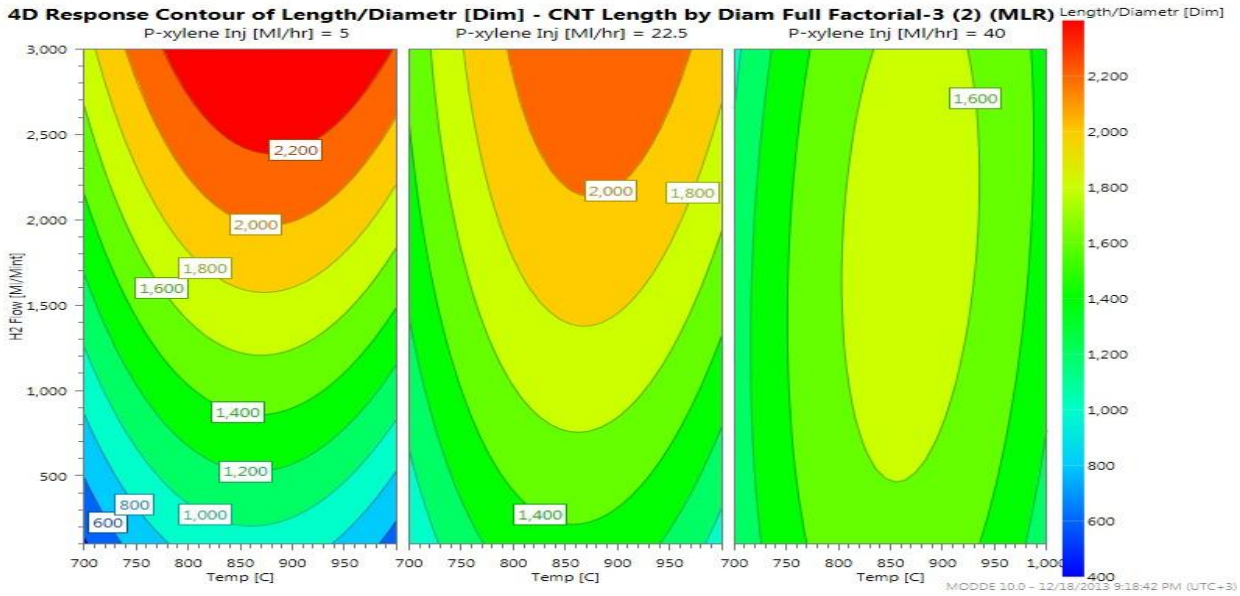

Figure 27: Aspect ratio contour plots at various hydrocarbon flow rates

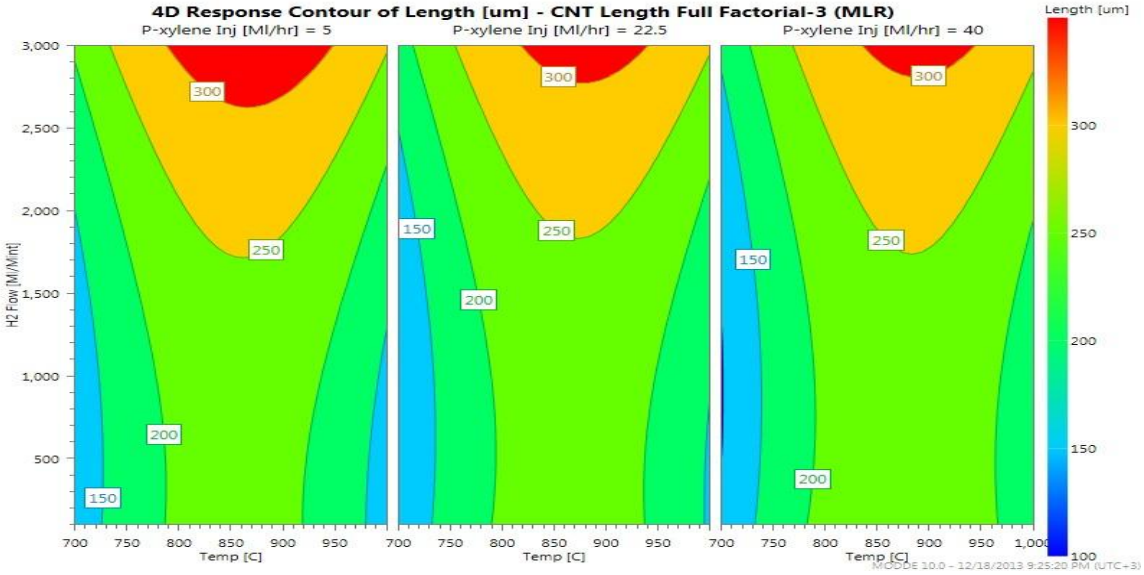

Figure 28 Length contour plots at various hydrocarbon flow rates

Moreover, the response 3D plots for CNT yield as a function of temperature and hydrogen flow rates at the various hydrocarbon flow rates are shown in Figures 29, a, b and c, respectively. It is clear that, poor growth is observed at low reaction

temperatures at the various P-x flow rates resulting from insufficient energy required to crack the hydrocarbon bonds.

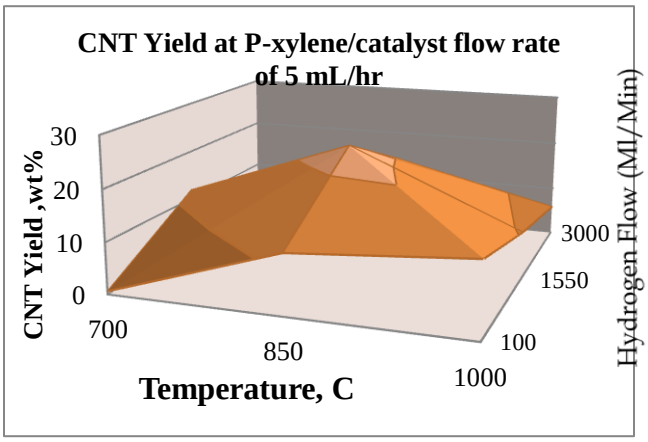

Figure 29 (a)

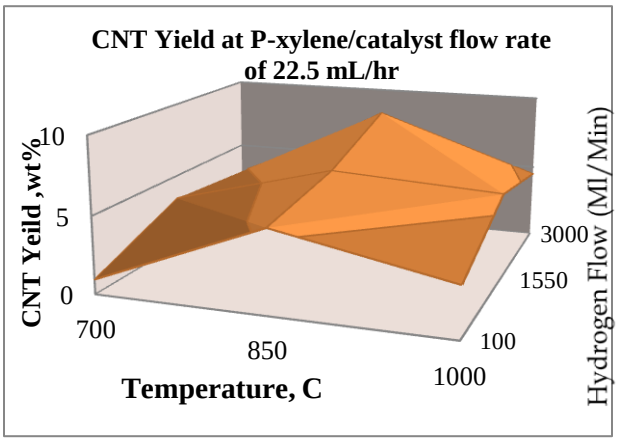

Figure 29 (b)

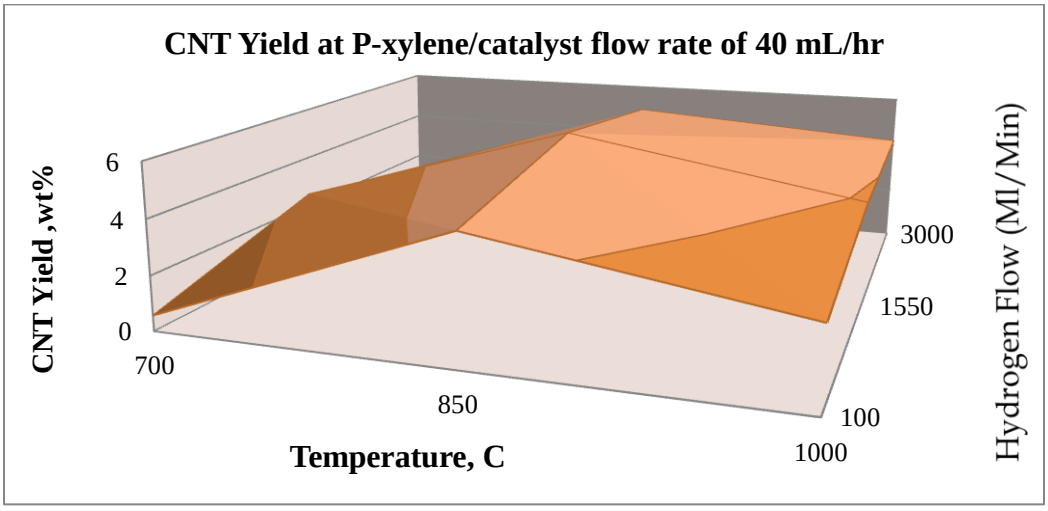

Figure 29: a, b &c, 3D plots of CNT yield at the various P-xylene flow rate mL/hr

Similarly, the response 3D plots for CNT purity and dimensions (D, L/D, L) as a function of temperature and hydrogen flow rates at the various hydrocarbon flow rates are shown in Figures 30-33, respectively.

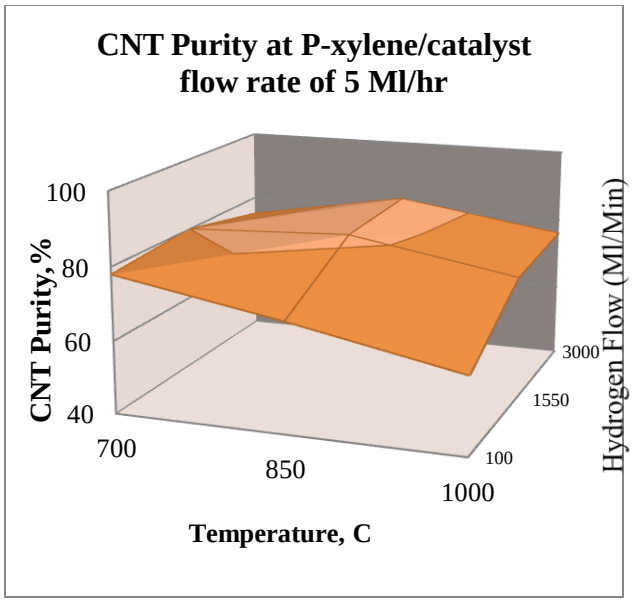

Figure 30 (a)

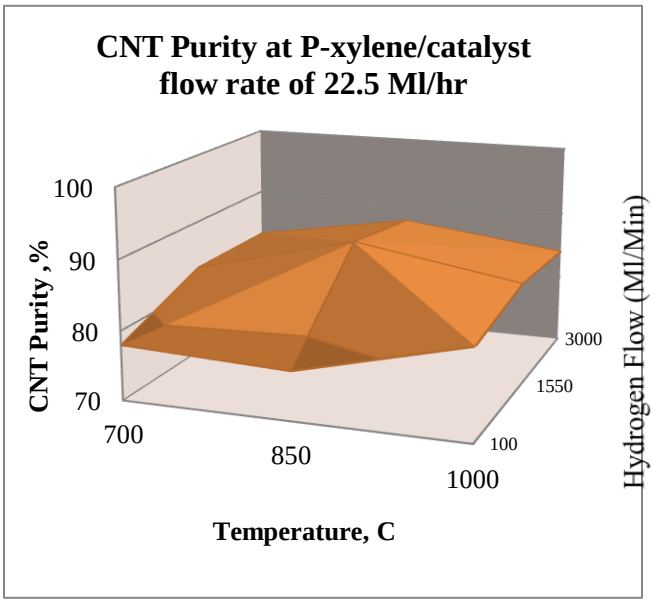

Figure 30 (b)

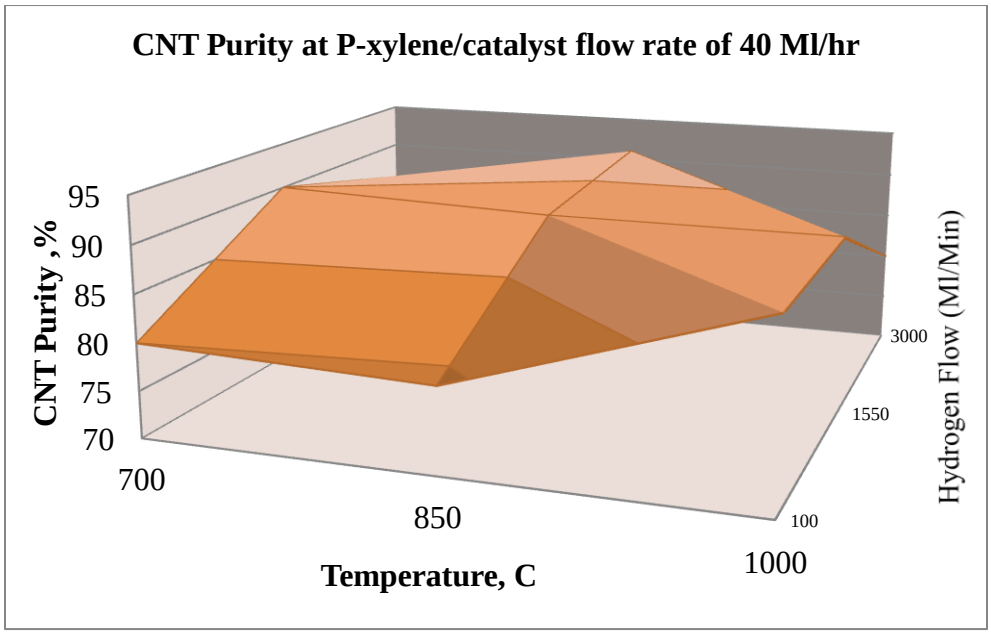

Figure 30 (c)

Figure 30 (a,b,c): 3D plots (Purity of CNT's at various P-x flow rates)

In all cases, poor quality is observed at low reaction temperatures at the various P-x flow rates and show improvement as the temperature increases towards 900 C^{o}

range while hydrogen flow rates from 1500 to 2500 mL/mint produced better CNT's quality.

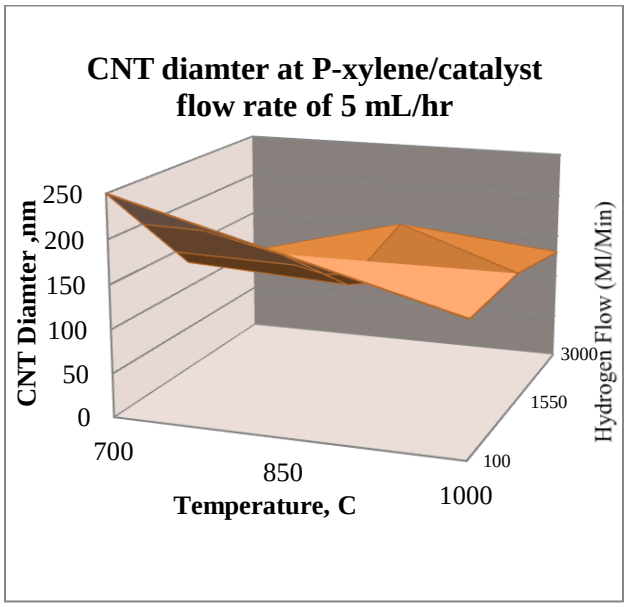

Figure 31 (a)

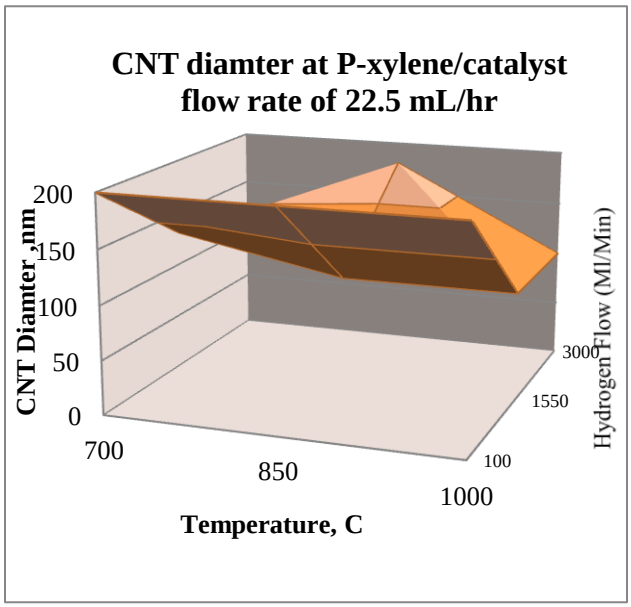

Figure 31 (b)

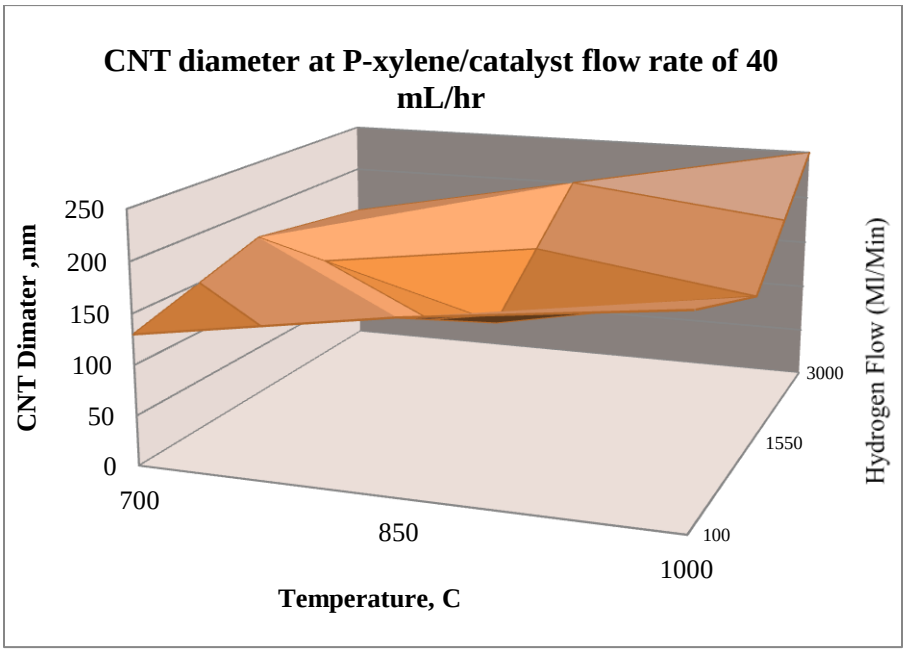

Figure 31 (c)

Figure 31 (a,b,c): 3D plots (Diameter of CNT's at various P-x flow rates)

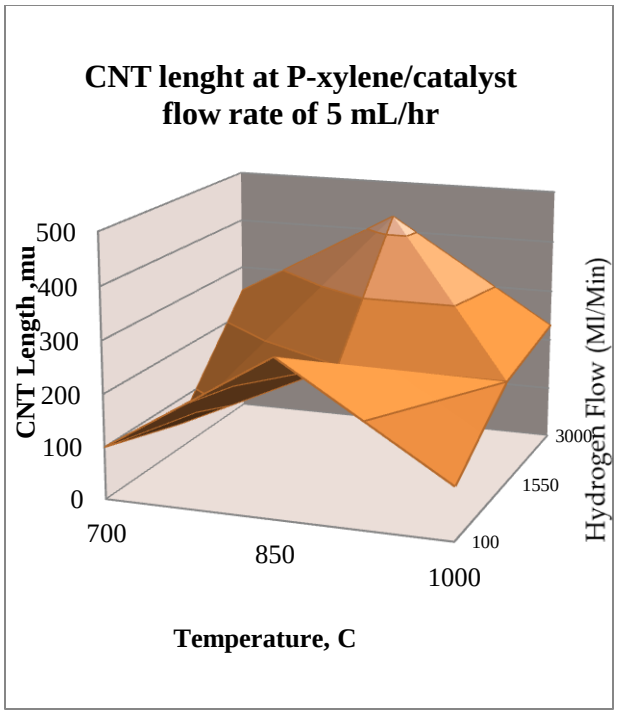

Figure 32 (a)

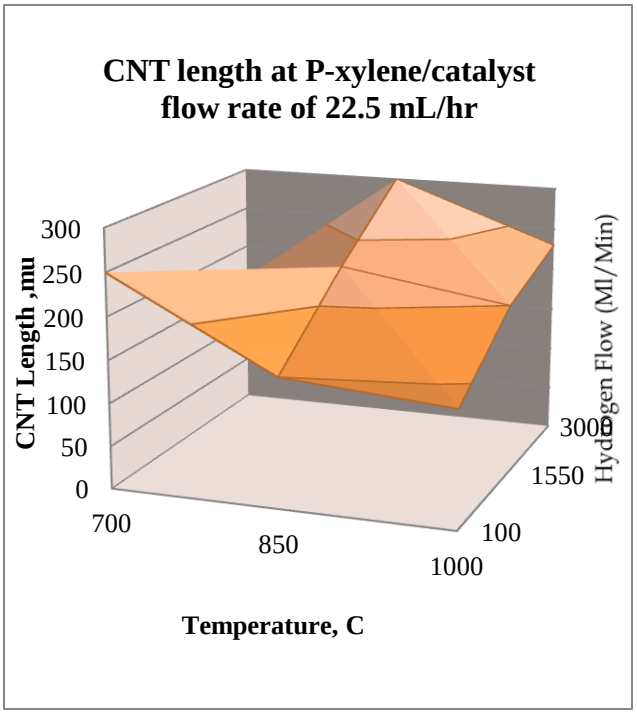

Figure 32 (b)

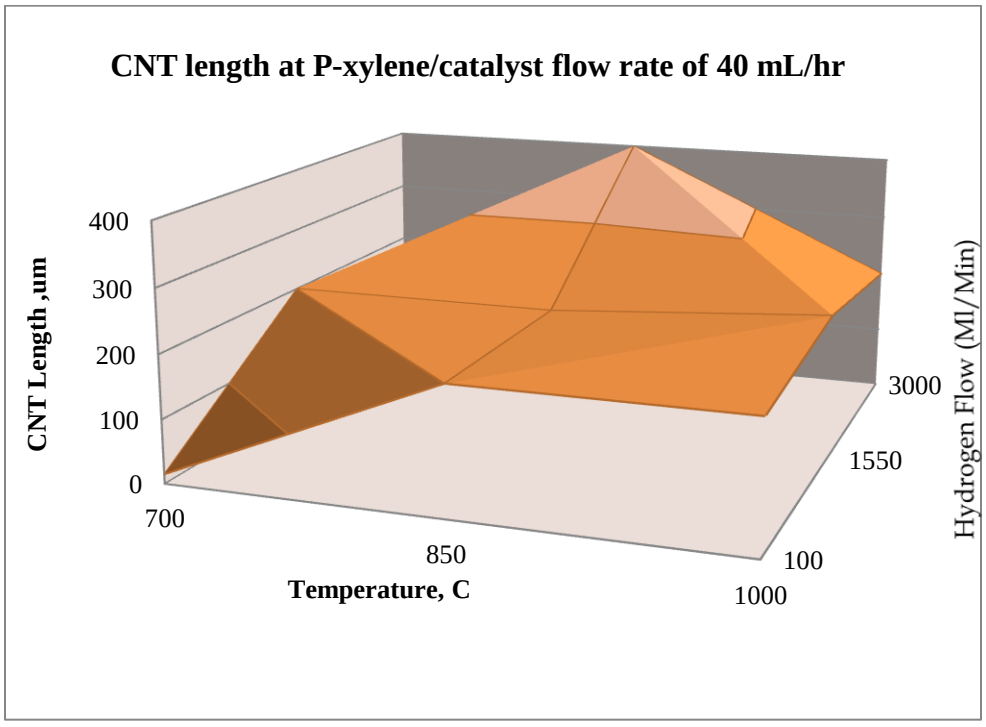

Figure 32- (c)

Figure 32 (a,b,c): 3D plots (Length of CNT's at various P-x flow rates)

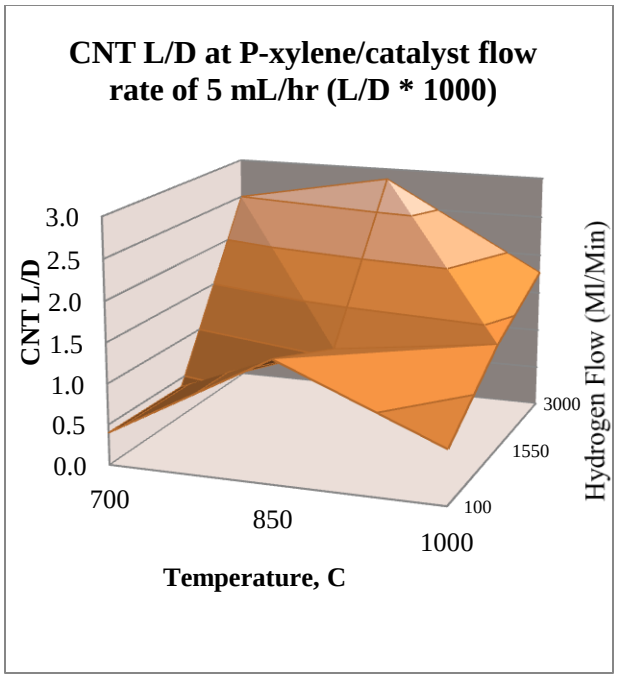

Figure 33 (a)

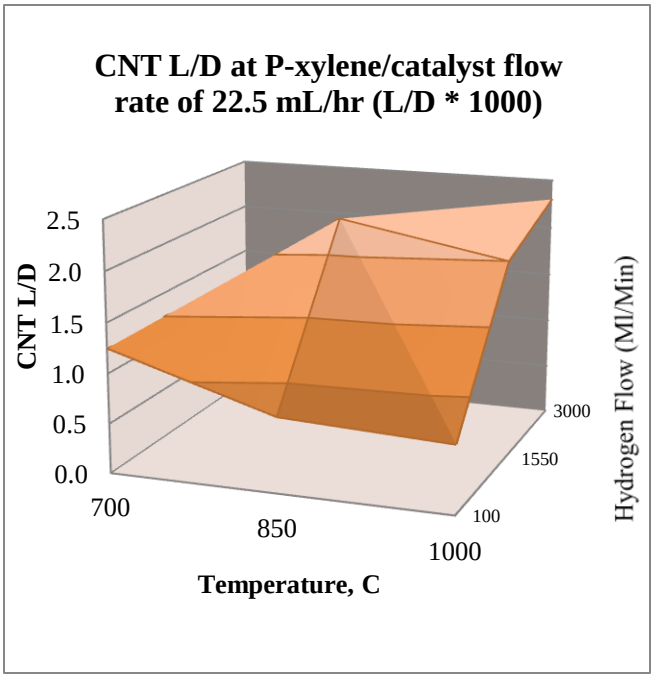

Figure 33 (b)

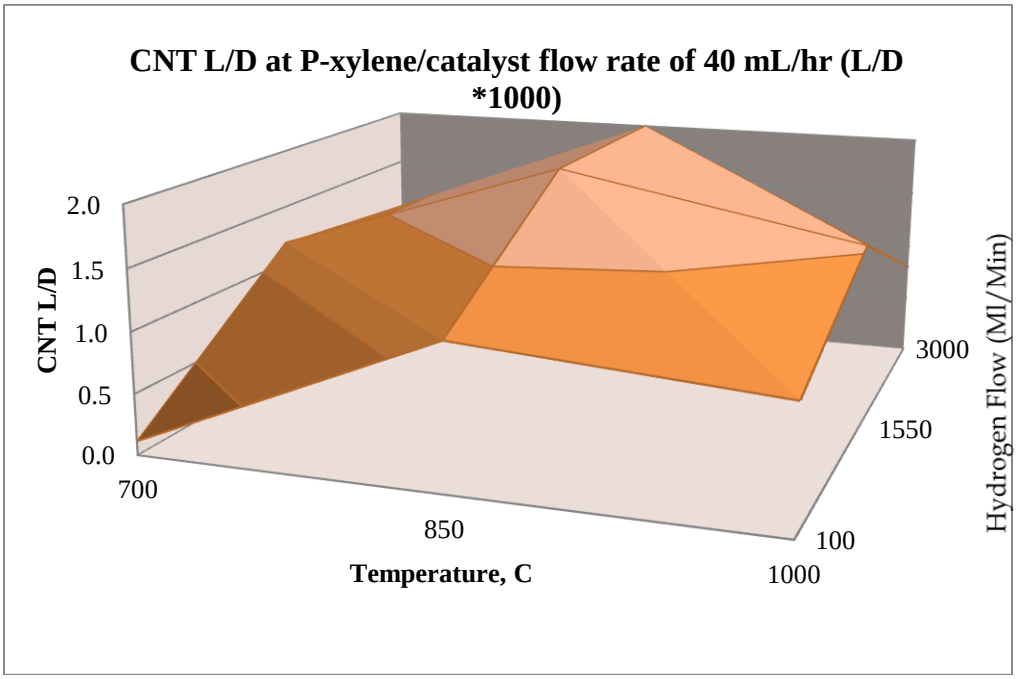

Figure 33 (c)

Figure 33 (a,b,c): 3D plots (L/D of CNT's at various P-x flow rates

5.6 Optimum Conditions

The set of empirical equations (Equations 5 to 9) were used as the objective functions in the design of experiment software optimizer to find out the optimum conditions for each parameter. The objectives were to maximize the response factors for all parameters except for the diameter where the objective was to minimize the CNT diameter. The mathematical models were shown to reasonably fit the experimental data where they were compared to statistical measures that indicated significant models particularly for the yield and purity. We can now comfortably use these mathematical models to optimize the CVD process of our system.

The optimizer uses a multidimensional Sim-plex method. Running the optimizer with the objective to maximize yield, we have obtained maximum CNT yield of 15.2 wt% at a temperature of 892 C^{o}, Hydrogen flow rate of 1497 mL/min and 5 mL/hr of P-xylene flow rate with the optimizer contour plot shown in figure 34. Additional data and outputs of the optimizer are referenced in the attached appendix-C. This conclusion and optimum conditions can also be seen from the contour and 3D plots presented in the previous section.

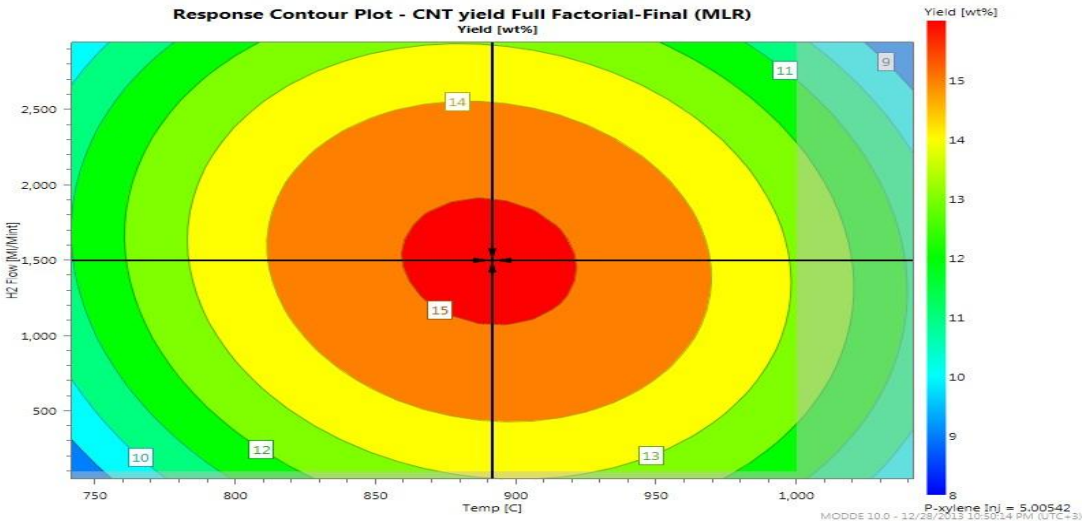

Figure 34: Optimizer contour plot for the yield

Similarly, the optimizer was run to find out the optimum Purity, Diameter, Aspect ratio and Length. The optimizer contour plots are shown in figure 35- 38. The results are summarized in Tables 10-13. It can be seen that, the optimum conditions for all parameters are at the P-x flow of 5 mL/hr and temperatures and H_2 flow rates above 850 C and 1500 mL/mint, respectively except for the purity where optimum conditions was found at higher P-x flow rate (23 mL/hr).

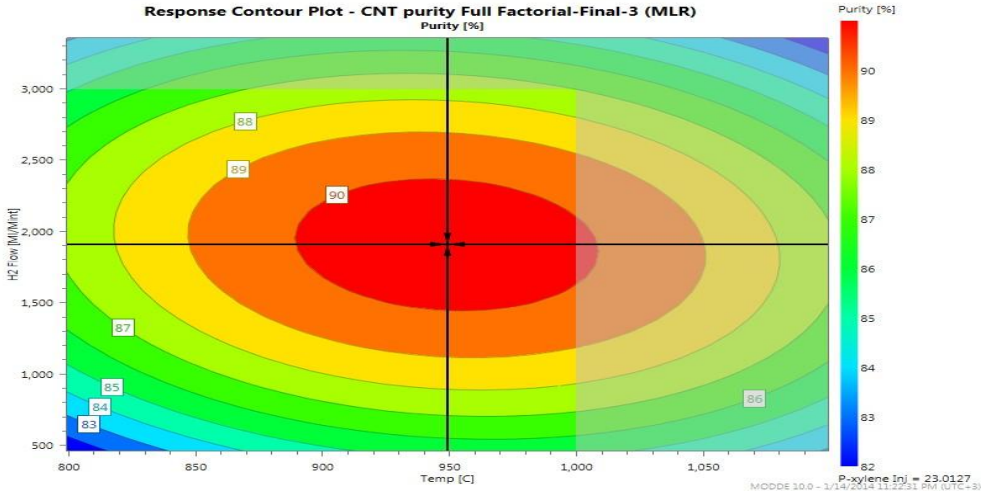

Figure 35: Optimizer contour plot for the Purity

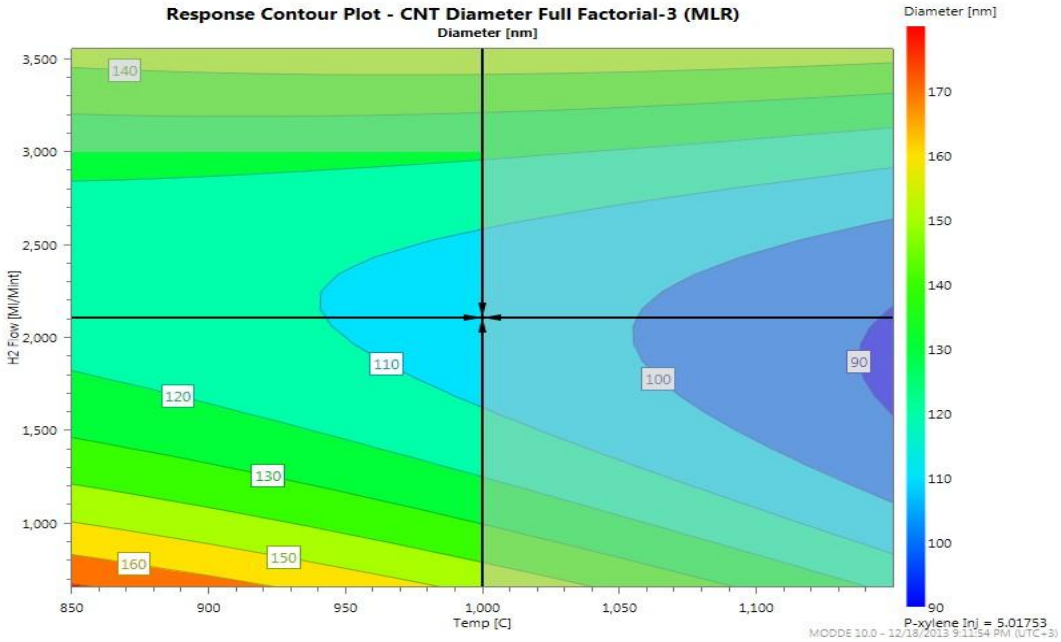

Figure 36: Optimizer contour plot for the Diameter

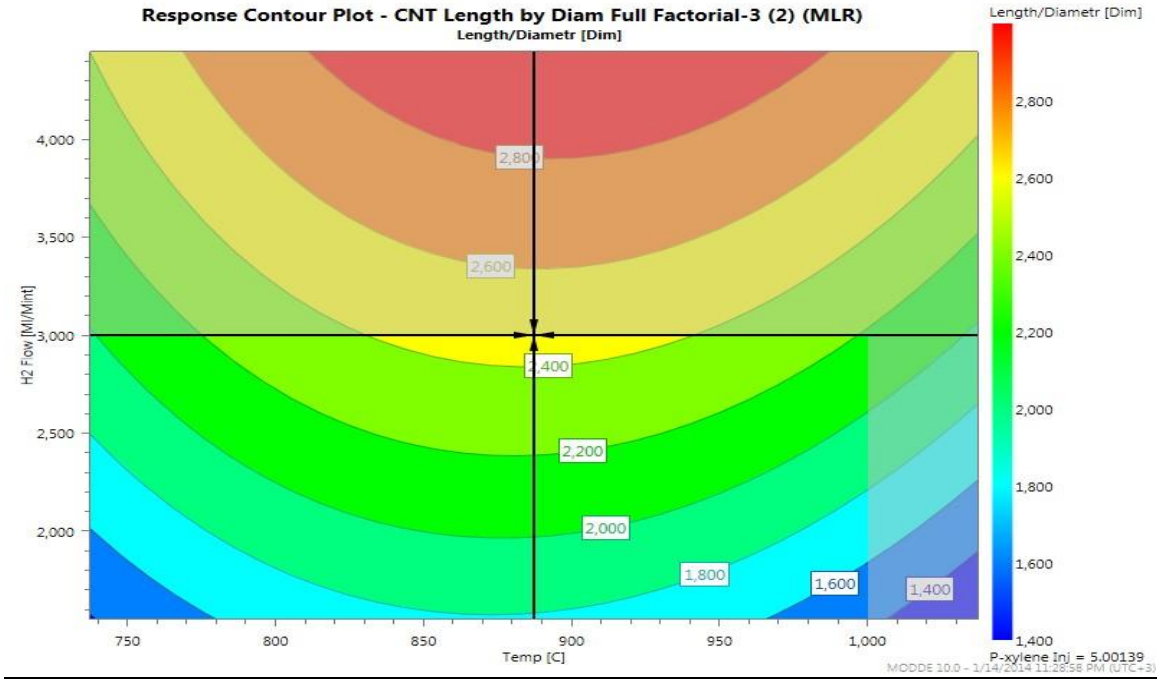

Figure 37: Optimizer contour plot for Aspect ratio

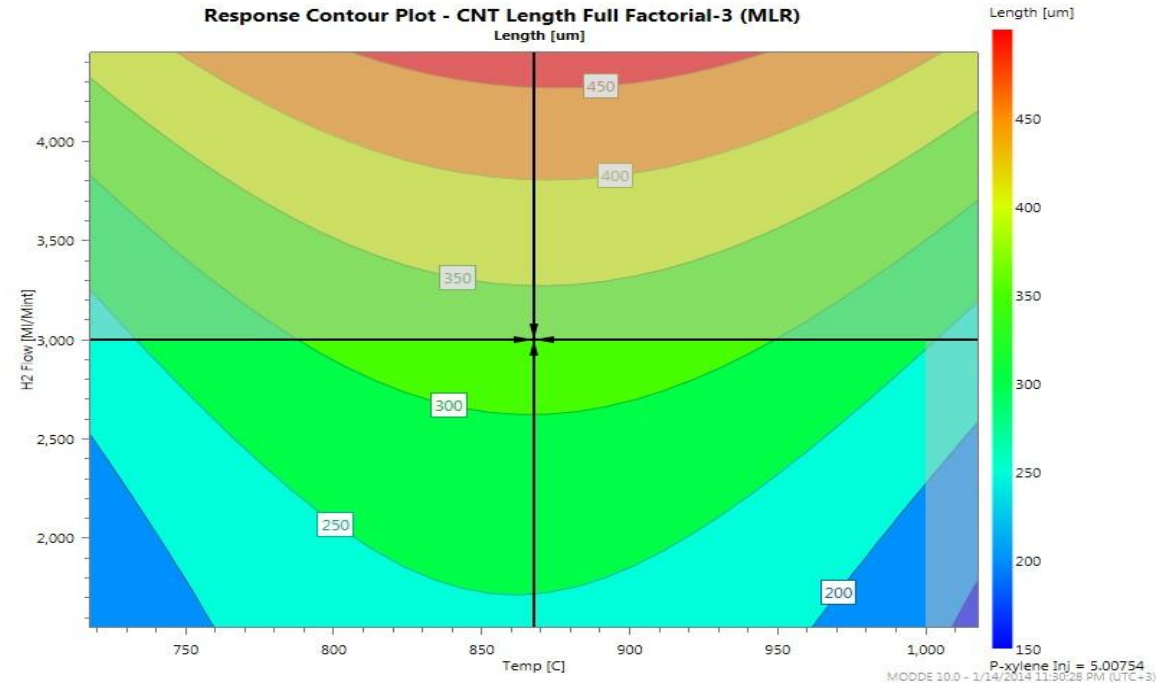

Figure 38: Optimizer contour plot for the Length

Purity (%)	Maximize	90.5
Temp	Free	949.2
H2 Flow	Free	1908.5
P-xylene Inj	Free	23.0

Table 10: optimum conditions for Purity

Diameter (nm)	Minimize	105.3
Temp	Free	1000
H2 Flow	Free	2105.8
P-xylene Inj	Free	5.0

Table 11: optimum conditions for Diameter

Aspect Ratio	Maximize	2435.6
Temp	Free	865.6
H2 Flow	Free	3000
P-xylene Inj	Free	5.0

Table 12: optimum conditions for L/D

Length (um)	Maximize	328.3
Temp	Free	868.0
H2 Flow	Free	3000
P-xylene Inj	Free	5.0

Table 13: optimum conditions for Length

CHAPTER 6

Discussions of results

Following sections will discuss effects of P-xylene flow rates, Hydrogen flow rates and temperature on the CNT's quantity and quality.

6.1 P-xylene flow rate effects

The effect of varying P-xylene concentrations at various operating temperatures from 700 to 1000 C^o is presented in the contour and the 3D plots where they show that the maximum yield is obtained at a P-xylene flow rate of 5 mL/hr and temperature of 892 C^o (contour plots and optimizer results). Therefore, it is clear that the yield of CNT is higher at lower hydrocarbon flow rates. At higher hydrocarbon flow rates, the catalysts depositing in the quartz tube walls and acting as a base for CNT growth occupies all available surface area and therefore any further increase of hydrocarbon rate with the dissolved catalyst will not improve CNT growth due to unavailable substrates in the reaction chamber.

At this P-x flow rate of 5 mL/hr, it was found from the optimizer that the best CNT's quality with respect to Diameter, Length and Aspect ratio will be produced except for the Purity where it was found that the optimum purity will be produced at higher P-x flow rate of 23 mL/hr as can also be seen from the SEM images of figures 39 (a,b,c).

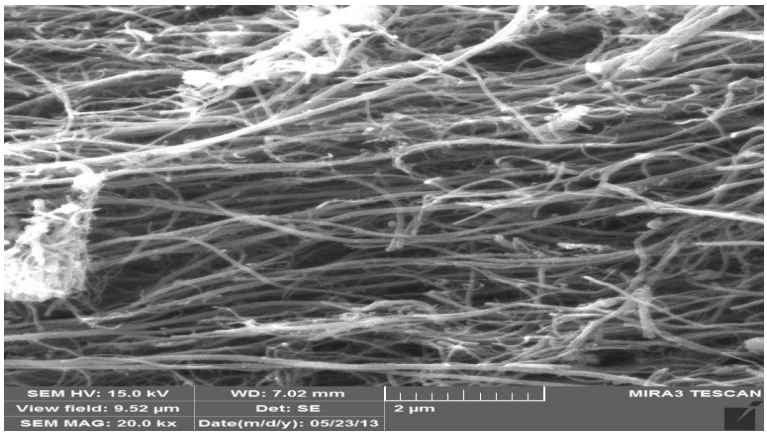

Figure 39 (a)

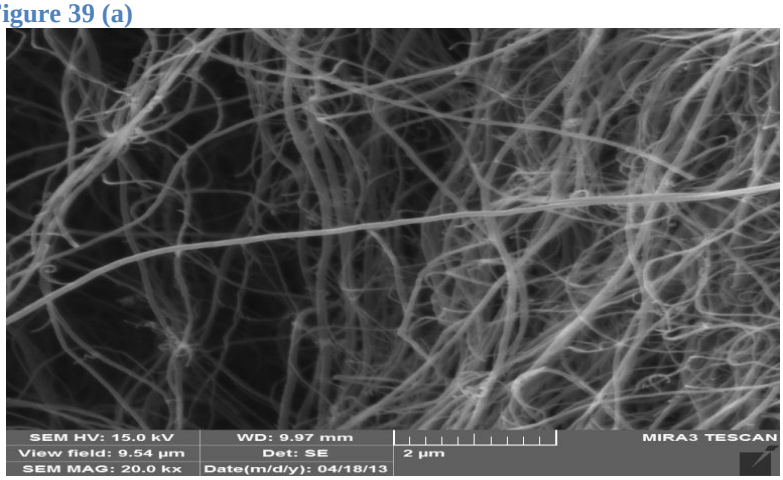

Figure 39 (b)

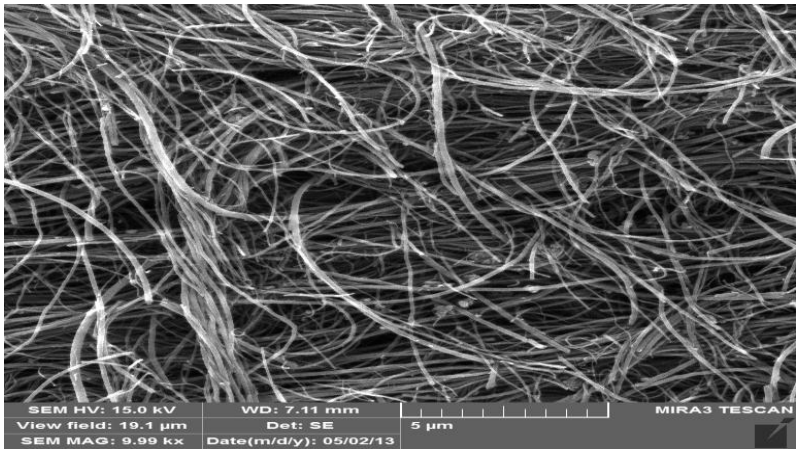

Figure 39 (c)

Figure 39 (a,b,c):

R#13 morphologies R#13 Fixed temperature at 850 and H_2 flow rate at 1550 mL/Min and varying P-xylene flow rates. Figure (a) show P-xylene flow rate of 5 mL/hr (Run#13), Figure (b) shows a flow of 22.5 (Run#14) and figure (c) shows a flow of 40 Ml/hr (Run#15).

6.2 Temperature Effect

The CNT yield, purity and other dimensions as a function of temperature and hydrogen flow rates at the various P-x flow rates also can be seen in the contour and the 3D plots. It can be seen that, a poor yield, purity and quality in terms of dimensions were obtained at temperature of 700 C^o, possibly due to slow catalytic decomposition of P-xylene, while CNT growth and quality have improved and became significant at temperatures above 850 C^o. Increasing temperature enhances growth, which reaches an optimum at around 892 C^o and then starts dropping afterwards. This type of growth versus temperature profile and the appearance of a growth maximum are attributed to transformation of the catalyst morphology as temperature increases. At lower reaction temperature, small amount of CNT is produced due to the low heating energy needed to crack the hydrocarbon bonds. On the other hand, at higher reaction temperature more than 892 C^o, the CNT yields reduces due to the hydrogenation process in the system where the hydrogen gas will react with carbon atoms and forms different hydrocarbon gases. The SEM images of CNT's produced at different temperatures are presented in Figures 40 (a,b,c).

Similar trend was observed for the purity, dimensions except for the diameter where optimum diameter was found at the maximum temperature of 1000 C^o. The explanation to the observed behavior with the growth temperature is that, at low temperatures (below 850 C^o), supplied energy is not sufficient to decompose all P-x into carbon and hydrogen. At moderate temperatures (850°C - 875 C^o) most of the P-x is disassociated supplying carbon for CNT formation. At high temperatures (above 900 C^o) supplied energy is sufficient to disassociate P-xylene into carbon and hydrogen. Thus, the available carbon is plentiful to have longer

CNTs and added hydrogen along with the disassociated hydrogen from P-xylene is effectively shaping catalyst film into desired smaller nanoparticles.

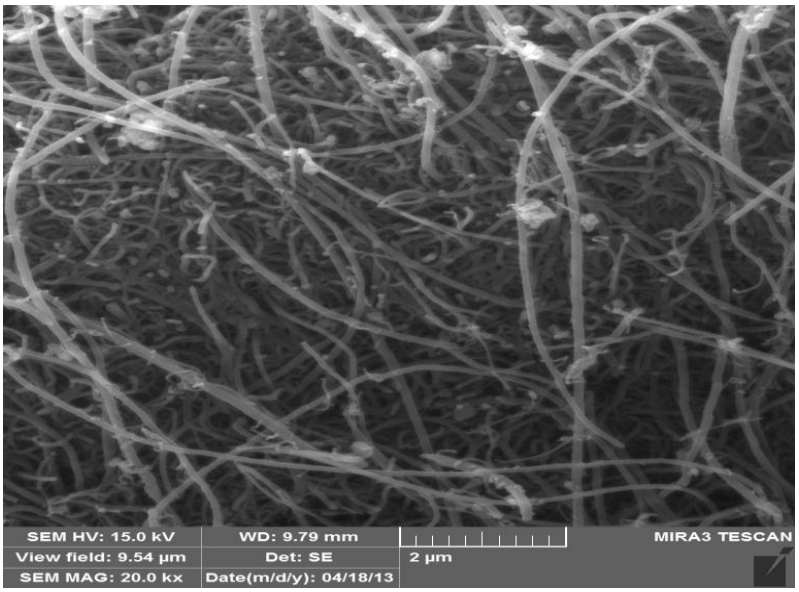

Figure 40 (a)

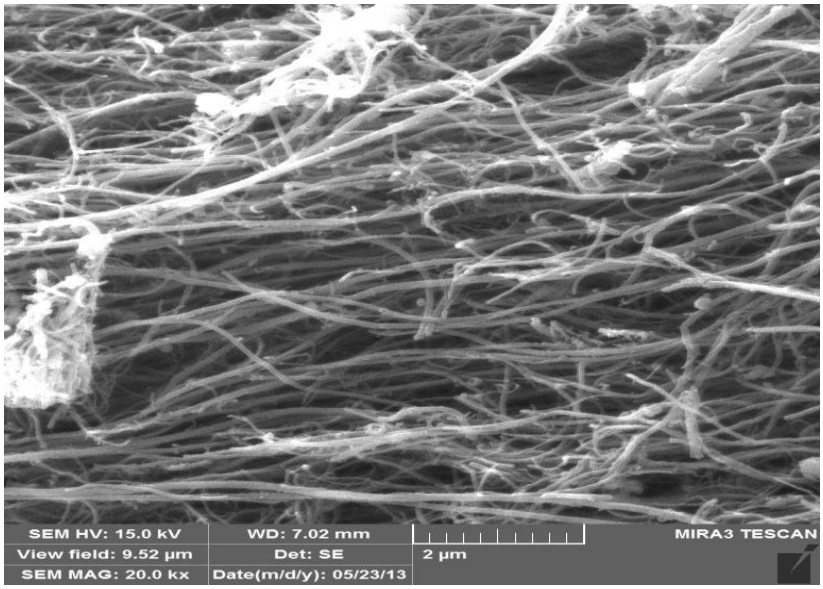

Figure 40 (b)

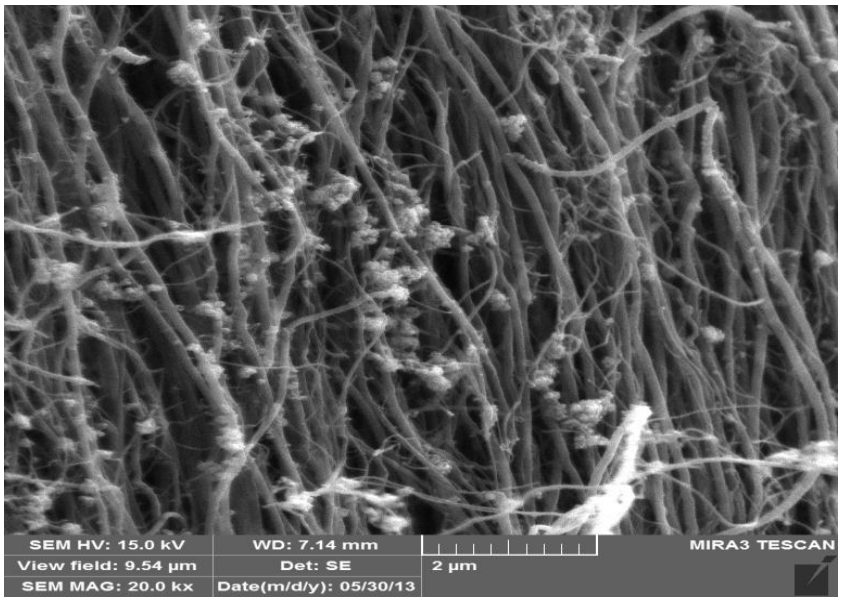

Figure 40 (c)

Figure 40 (a,bc):

Fixed H_2 flow rate at 1550 mL/Min and P-xylene flow rates at 22.5 mL/hr while changing temperature. Figure (a) shows temperature at 700 C^o, (Run#5), Figure (b) shows temperature at 850 C^o (Run#13) and figure (c) shows temperature at 1000 C^o (Run#23).

6.3 Hydrogen Effect

Hydrogen has the ability to either suppress or accelerate the formation of CNTs as it affects the formation of the catalyst and the growth of CNTs. It is observed from the figures that as the hydrogen flow rate increases from 100 to 1497 mL/min (optimizer results and shown in the contours), the yield of CNTs increases at the various temperatures range of 700 C^o to 1000 C^o and beyond a flow rate of 1497 mL/min, the yield decreases. According to the findings of Singh et al., (2003) suggest that the reduction in rate of yield of CNTs at higher hydrogen flow rate could be attributed to a low residence time of P-xylene in the reactor as a result of a high velocity profile created by high hydrogen flow rate which suppresses the

formation of CNTs by removing P-xylene at a faster rate from the reaction zone of the reactor.

The effect of hydrogen on P-xylene decomposition in a CVD reactor used to produce CNTs has been examined by the SEM images. It was evident that hydrogen concentration inside CVD reactor has an effect on the nature and quality of the synthesized materials. Low hydrogen flow resulted in lower purity, quality and smaller CNTs in length figure 41 (a,b,c). Increasing hydrogen concentration resulted in the appearance of CNTs in the synthesized materials and the percentage and quality of these CNTs increased with hydrogen concentration at 1497 mL/min (observed and shown in the SEM of figure 41) and then started to reduce towards higher Hydrogen flow rates up to 3000 mL/mint except for the length and consequently aspect ratio. The figures show that, increasing the hydrogen flow rate increases the purity of the product. The optimum purity was found to be at 1908 mL/min. This was also proven by the referenced study "Attiah, et al" where they have shown that maximum purity was reached at H_2 flow rate of 2000 mL/mint.

As stated above, the hydrogen gas helps in sustaining the catalytic activity of the iron particles. However, further increase in hydrogen flow above 1497 mL/min, reduces the amount of CNT due to the hydrogenation process which takes place in the reaction chamber.

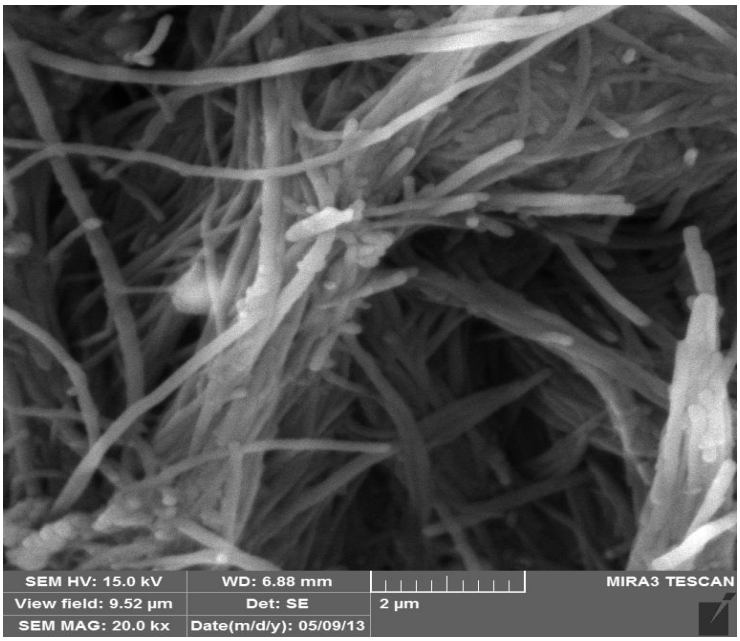

Figure 41 (a)

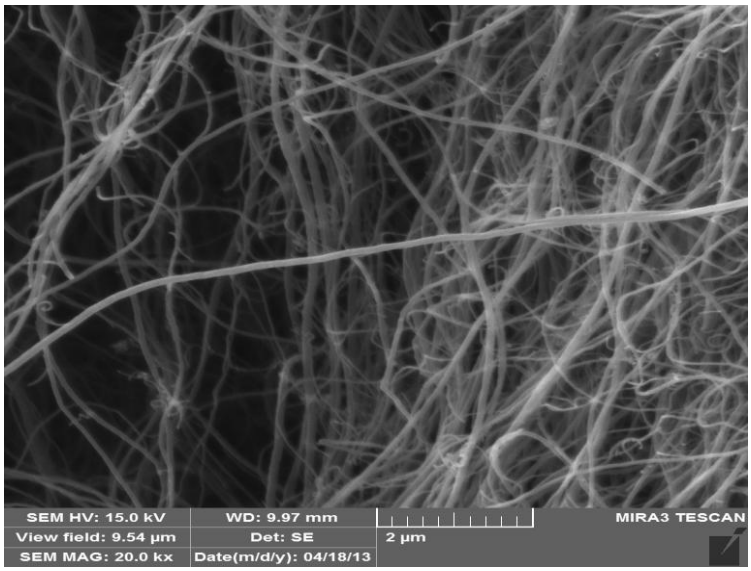

Figure 41 (b)

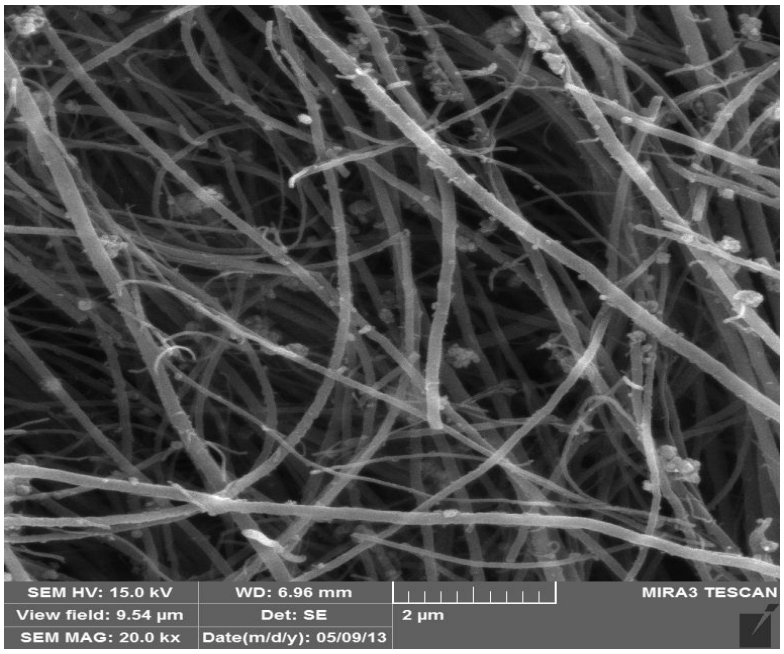

Figure 41 (c)

Figure 41 (a,b,c):

Fixed Temperature at 850 C^{o} and P-xylene flow rates at 22.5 Ml/hr while changing Hydrogen rate. Figure (a) shows hydrogen rate at 100 mL/Min, (Run#11), Figure (b) shows hydrogen rate at 1550 mL/Min (Run#14) and figure (c) Shows hydrogen rate at 3000 mL/Min (Run#17).

Conclusions

Using CVD system with P-xylene and Ferrocene as catalyst, the reaction parameters of temperature, hydrogen and hydrocarbon flow rates were investigated via 3^K experimental design. Statistical analysis indicated good models fit (R^2 ranging from 0.886 to 0.500) as well as meeting other statistical measures such as p values of less than acceptable measure of 0.05 and relatively high F test except for the CNT's Length. To improve the empirical models further, the insignificant factors affecting the accuracy of the models can be eliminated to improve the models accuracy which is beyond the scope of this research.

The optimum conditions using design of experiment software optimizer revealed maximum CNT yield of 15.2 wt% at a temperature of 892 C^o, Hydrogen flow rate of 1497 mL/mint and 5 mL/hr of P-xylene flow rate. The purity and quality of CNT's were found to be optimum at the minimum P-xylene flow rate of 5 mL/hr as well except for the purity while both the purity and quality of CNT's showed improvement at higher CNT growth temperature above 850 C^o.

The analysis shows that, increasing temperature enhances growth, purity and quality which reaches an optimum at around 892 C^o for the yield and above 850 C^o for the purity and dimensions and then starts dropping afterwards except for the diameter where the optimum was found to be at the maximum temperature of 1000 C^o. This type of growth versus temperature profile and the appearance of a growth maximum are attributed to transformation of the catalyst morphology as temperature increases. For the yield, at low reaction temperature, small amount of CNT is produced due to the low heating energy needed to crack the hydrocarbon bonds while at high reaction temperature more than 892 C^o, the CNT yields

reduces due to the hydrogenation process. For the CNT's quality, at low temperatures (below 850 C^o), supplied energy is not sufficient to decompose all P-x into carbon and hydrogen while at high temperatures (above 900 C^o) supplied energy is sufficient to disassociate P-xylene into carbon and hydrogen sufficient to have longer CNTs and the desired smaller nanoparticles

As the hydrogen flow rate increases from 100 to 1497 mL/min, the yield of CNTs increases at the various temperatures range of 700 C^o to 892 C^o and beyond a flow rate of 1497 mL/min, it decreases. The effect of hydrogen on P-xylene decomposition in a CVD reactor used to produce CNTs has been examined by the SEM images. Low hydrogen flow resulted in lower quality and smaller CNTs in length. Increasing hydrogen concentration resulted in the appearance of CNTs in the synthesized materials and the percentage and quality of these CNTs increased with hydrogen concentration at the observed value of 1550 mL/mint and then started to reduce towards higher Hydrogen flow rates up to 3000 mL/mint except for the length where optimum was found to be at the maximum hydrogen flow rate.

Recommendations

- To produce high yield and purity of CNT's in a CVD reactor (100 mm diameter and 1200 mm length) using P-xylene as a hydrocarbon source and Ferrocene as a catalyst precursor, the CVD need to be operated at a temperature range of 865-892 C^o and Hydrogen flow rate of about 1500-2000 mL/mint. The P-x flow rate need to be maintained at a flow rate of 5 mL/hr for higher yield while to improve the purity, the P-x flow need to be increased to about 23 mL/hr at the same temperature and H_2 operating

conditions. On the other hand, to control the diameter and aspect ratio of the produced CNT's, higher hydrogen flow rate need to be considered and maximum temperature for smaller nano tubes diameter.

- As a future work, the insignificant factors in the empirical models particularly for Length and Aspect ratio can be eliminated to improve the accuracy of the empirical models.

- The CNT's yield can be increased significantly by increasing the surface area of the reactor tube walls used as a substrate for the CNT's growth. This could be achieved by several ways such as enlarging the diameter of the quartz tube or other options such as doubling quartz tube walls or considering serious of quartz tubes. In any of the cases, experimental runs can be performed to verify the produced CNT's quantity and quality.

Appendix-A

ANOVA

The analysis of variance (ANOVA) partitions the total variation of a selected response SS (Sum of Squares corrected for the mean) into a part due to the regression model and a part due to the residuals.

$$SS = SS_{regr} + SS_{resid}$$

If there are replicated observations (experiments), the residual sum of squares is further partitioned into pure error SS_{pe} and Lack of fit SS_{lof}.

$$SS_{resid} = SS_{pe} + SS_{lof}$$

$$DF_{resid} = (n - p)$$

$$SS_{pe} = \sum (e_{ki} - e_k)^2$$

$$DF_{pe} = \sum (n_k - 1)^2$$

$$DF_{lof} = n - p - \sum (n_k - 1)^2$$

1. where the $\sum$ loops over ki resp k.
2. n = number of experimental runs (excluding missing values)
3. n_k = number of replicates in the k^{th} set
4. p = number of terms in the model, including the constant
5. e_k = average of the n_k residuals in the k^{th} set of replicates
6. j = j^{th} residual in the k^{th} set of replicates

A goodness of fit test is performed by comparing the MS (mean square) of lack of fit to the MS of pure error:

Two ANOVA plots are displayed:

1. The regression goodness of fit test
2. The LoF goodness of fit test

Appendix-A

Measures of goodness of fit

MODDE computes and displays the following:

Q2

$Q^2 = (SS - PRESS)/SS$

with

$$PRESS = \sum_i \frac{(Y_i - \hat{Y}_i)^2}{(1 - h_i)^2}$$

where h_i is the i^{th} diagonal element of the hat matrix:

$X(X'X)^{-1}X'$

R2

$R^2 = (SS - SS_{resid})/SS$

$R^2\ adj = (MS - MS_{resid})/MS$

$MS = SS / (n - 1)$

$MS_{resid} = SS_{resid} / (n - p)$

RSD = Residual Standard Deviation = $\sqrt{MSE_{resid}}$

- ***Residual Sum of Squares*** **(*RSS*)**

It is the sum of the squared difference between the experimental response y and the response calculated by the regression model:

$$RSS = \sum_{i=1}^{n} (y_i - \hat{y}_i)^2 \qquad (1)$$

If *RSS* is equal to zero the model is perfect, i.e. for all the *n* samples, the calculated responses coincide with the experimental responses. Obviously, *RSS* also depends on the measure unit used for the response. In practice, for the same model, if you multiply the experimental response for 10, *RSS* is 100 times greater, being a squared quantity.

Appendix-A

- ***Total Sum of Squares*** *(TSS)*

It is the total variance that a regression model can explain and is used as a reference quantity to calculate standardized quality parameters. Also denoted as *SSY*, it is the sum of the squared differences between the experimental responses and the average experimental response:

$$TSS \equiv SSY = \sum_{i=1}^{n} (y_i - \bar{y})^2 \qquad (2)$$

TSS is assumed as a theoretical reference model where for each experimental response a constant value is calculated as the average experimental response. As for *RSS*, also *TSS* depends on the measure unit used for the response.

- ***Derived regression parameters for evaluating the goodness of fit***

From the previous definitions of *RSS* and *TSS*, the following quantities are usually defined:

$$TSS = MSS + RSS \qquad (3)$$

where *TSS* and *RSS* are the quantities defined above and *MSS* is the ***Model Sum of Squares***. All these three quantities are sums of squares and then are always positive quantities:

$$TSS \geq 0 \quad MSS \geq 0 \quad RSS \geq 0$$

The ***coefficient of determination*** R^2 and the ***multiple correlation coefficient*** R are defined as:

$$R^2 = \frac{MSS}{TSS} = 1 - \frac{RSS}{TSS} = 1 - \frac{\sum_{i=1}^{n} (y_i - \hat{y}_i)^2}{\sum_{i=1}^{n} (y_i - \bar{y})^2} \qquad 0 \leq R^2 \leq 1 \qquad (4)$$

$$R \,(\text{or } r) = \sqrt{R^2} \qquad 0 \leq R \leq 1$$

The ***Mean square error*** (or *residual mean square*) s^2_y and the ***residual standard deviation*** (or *residual standard error*) s_y are defined as:

$$s_y^2 = \frac{RSS}{n - p'} \qquad s_y = \sqrt{\frac{RSS}{n - p'}} \qquad (5)$$

where n is the number of samples, p' the number of model parameters (often given by p variables plus the intercept). Other symbols that can be commonly used for the residual standard deviation are *RSD*, *SE*, and *s*.

Finally, the ***F-ratio test in regression*** is defined as the ratio between the variance explained by the model to the residual variance, both scaled by the corresponding degrees of freedom:

$$F = \frac{MSS\,/\,(p' - 1)}{RSS\,/\,(n - p')} \qquad (6)$$

It must be observed that, for the same number of objects and variables, if *RSS* decreases (i.e. a better model is obtained), then both R^2 and F increase monotonically with *RSS*, while the residual mean square s^2_y decreases monotonically with *RSS*. This means that the best goodness of fit can be equally evaluated by using any of the three parameters (max(R^2), max(F) and min(s^2_y).

Appendix-B

MODDE 10 OUTPUT

Calculated coefficients and confidence of intervals

Yield	Coeff. SC	Std. Err.	P	Conf. int(±)
Constant	9.02556	0.950777	3.30197e-008	2.00598
Temp	1.62278	0.440124	0.00182838	0.928589
H2 Flow	0.292222	0.440124	0.515625	0.928589
P-xylene Inj	-3.58278	0.440124	2.87789e-007	0.928589
T*T	-4.28167	0.762318	3.08158e-005	1.60836
F*F	-2.22	0.762318	0.00970876	1.60836
I*I	2.27167	0.762318	0.00840634	1.60836
T*F	-0.605	0.53904	0.277309	1.13728
T*I	-0.6675	0.53904	0.232428	1.13728
F*I	0.310833	0.53904	0.571738	1.13728

N = 27 Q^2 = 0.645 Cond. no. = 5.23

DF = 17 R^2 = 0.886 RSD = 1.867

R^2 adj. = 0.826

Conf. lev. = 0.95

Purity	Coeff. SC	Std. Err.	P	Conf. int(±)
Constant	88.6667	1.90783	2.33862e-019	4.02519
Temp	4.55556	0.883152	7.879e-005	1.8633
H2 Flow	3.05556	0.883152	0.00299366	1.8633
P-xylene Inj	-1.05556	0.883152	0.24841	1.8633
T*T	-3.33334	1.52966	0.0436788	3.22733
F*F	-5.16667	1.52966	0.0035766	3.22733
I*I	-2.83333	1.52966	0.0814342	3.22733
T*F	-0.833332	1.08164	0.451615	2.28207
T*I	1.5	1.08164	0.183423	2.28207
F*I	0.999998	1.08164	0.368151	2.28207

N = 27 Q^2 = 0.369 Cond. no. = 5.23

DF = 17 R^2 = 0.787 RSD = 3.747

R^2 adj. = 0.675

Conf. lev. = 0.95

Appendix-B

MODDE 10 OUTPUT

Calculated coefficients and confidence of intervals

Diameter	Coeff. SC	Std. Err.	P	Conf. int(±)
Constant	119.259	17.1447	2.31819e-006	36.1724
Temp	3.8889	7.93645	0.630394	16.7446
H2 Flow	-18.8889	7.93644	0.029285	16.7446
P-xylene Inj	7.77777	7.93644	0.340824	16.7446
T*T	-2.77778	13.7463	0.842258	29.0025
F*F	42.2222	13.7463	0.00691346	29.0024
I*I	15.5556	13.7463	0.273507	29.0024
T*F	13.3333	9.72012	0.187983	20.5078
T*I	16.6667	9.72012	0.104579	20.5078
F*I	26.6667	9.72012	0.0138569	20.5078

N = 27 Q^2 = 0.056 Cond. no. = 5.23

DF = 17 R^2 = 0.638 RSD = 33.67

R^2 adj. = 0.446

Conf. lev. = 0.95

Length/Diametr	Coeff. SC	Std. Err.	P	Conf. int(±)
Constant	1842.19	271.822	3.2293e-006	573.499
Temp	125.667	125.829	0.33194	265.478
H2 Flow	396.389	125.829	0.00584028	265.478
P-xylene Inj	-48.2778	125.829	0.705974	265.478
T*T	-488.556	217.942	0.0386147	459.822
F*F	-92.0557	217.942	0.678037	459.822
I*I	-114.056	217.942	0.6075	459.822
T*F	85.5832	154.109	0.585894	325.143
T*I	-23.0833	154.109	0.882695	325.143
F*I	-357.917	154.109	0.0328746	325.143

N = 27 Q^2 = -0.114 Cond. no. = 5.23

DF = 17 R^2 = 0.567 RSD = 533.8

R^2 adj. = 0.338

Conf. lev. = 0.95

Appendix-B

MODDE 10 OUTPUT

Calculated coefficients and confidence of intervals

Length	Coeff. SC	Std. Err.	P	Conf. int(±)
Constant	237.963	41.7149	2.5817e-005	88.0115
Temp	27.2222	19.3103	0.176652	40.7414
H2 Flow	45	19.3103	0.0323604	40.7414
P-xylene Inj	-1.3889	19.3103	0.9435	40.7414
T*T	-95.5556	33.4464	0.0109122	70.5662
F*F	29.4444	33.4464	0.390947	70.5662
I*I	3.61111	33.4464	0.915287	70.5662
T*F	9.99999	23.6501	0.677719	49.8979
T*I	13.75	23.6501	0.568606	49.8979
F*I	-8.75001	23.6502	0.715968	49.8979

N = 27 Q^2 = -0.255 Cond. no. = 5.23

DF = 17 R^2 = 0.500 RSD = 81.93

R^2 adj. = 0.236

Conf. lev. = 0.95

Appendix-B

MODDE 10 OUTPUT

Yield	Observed	Predicted	Obs - Pred	Conf. int(±)
1	3	5.50167	-2.50167	2.81144
2	0.96	0.00388805	0.956112	2.30594
3	0.57	-0.950556	1.52056	2.81144
4	10	8.30806	1.69194	2.30594
5	3.39	3.12111	0.268888	2.00598
6	2.45	2.4775	-0.0274982	2.30594
7	5	6.67444	-1.67444	2.81144
8	2.4	1.79833	0.601667	2.30594
9	0.63	1.46555	-0.835555	2.81144
10	11.66	12.6786	-1.01861	2.30594
11	5.36	6.51333	-1.15333	2.00598
12	4.59	4.89139	-0.301389	2.30594
13	18	14.88	3.12	2.00598
14	8.5	9.02556	-0.525558	2.00598
15	6.3	7.71445	-1.41445	2.00598
16	13.94	12.6414	1.29861	2.30594
17	8.26	7.09778	1.16222	2.00598
18	4.93	6.0975	-1.1675	2.30594
19	14.31	11.2922	3.01778	2.81144
20	3.23	4.45945	-1.22945	2.30594
21	2.88	2.17	0.71	2.81144
22	11	12.8886	-1.88861	2.30594
23	5.64	6.36667	-0.726669	2.00598
24	3.89	4.38805	-0.498055	2.30594
25	8	10.045	-2.045	2.81144
26	4.48	3.83389	0.646111	2.30594
27	4.18	2.16611	2.01389	2.81144

Appendix-B

MODDE 10 OUTPUT

Purity	Observed	Predicted	Obs - Pred	Conf. int(±)
1	78	72.4444	5.55559	5.64143
2	79	79.6666	-0.666649	4.6271
3	80	80.2222	-0.222214	5.64143
4	80	80.5	-0.499992	4.6271
5	83	86.8889	-3.88888	4.02519
6	90	86.6111	3.38888	4.6271
7	75	78.2222	-3.2222	5.64143
8	83	83.7778	-0.777763	4.6271
9	83	82.6667	0.333336	5.64143
10	70	71.7222	-1.72221	4.6271
11	77	80.4444	-3.44444	4.02519
12	79	82.5	-3.5	4.6271
13	82	80.7778	1.22223	4.02519
14	89	88.6667	0.333344	4.02519
15	89	89.8889	-0.888885	4.02519
16	83	79.5	3.50001	4.6271
17	87	86.5556	0.444435	4.02519
18	91	86.9444	4.05556	4.6271
19	61	65.3333	-4.33332	5.64143
20	83	75.5555	7.44446	4.6271
21	80	79.1111	0.888885	5.64143
22	74	75.3889	-1.38887	4.6271
23	85	84.7778	0.222237	4.02519
24	89	87.5	1.50001	4.6271
25	76	75.1111	0.888901	5.64143
26	84	83.6666	0.333351	4.6271
27	80	85.5555	-5.55554	5.64143

Appendix-B

MODDE 10 OUTPUT

Diameter	Observed	Predicted	Obs - Pred	Conf. int(±)
1	250	238.148	11.8519	50.6967
2	200	187.037	12.963	41.5814
3	130	167.037	-37.0371	50.6967
4	130	137.037	-7.03705	41.5814
5	130	112.593	17.4074	36.1724
6	170	119.259	50.7407	41.5814
7	100	120.37	-20.3704	50.6967
8	100	122.593	-22.5926	41.5814
9	150	155.926	-5.9259	50.6967
10	200	214.815	-14.8148	41.5814
11	200	180.37	19.6296	36.1724
12	170	177.037	-7.03706	41.5814
13	120	127.037	-7.03706	36.1724
14	100	119.259	-19.2593	36.1724
15	100	142.593	-42.5926	36.1724
16	150	123.704	26.2963	41.5814
17	180	142.593	37.4074	36.1724
18	200	192.593	7.40741	41.5814
19	150	185.926	-35.926	50.6967
20	200	168.148	31.8518	41.5814
21	200	181.482	18.5184	50.6967
22	150	111.481	38.5185	41.5814
23	100	120.37	-20.3704	36.1724
24	150	160.37	-10.3703	41.5814
25	130	121.481	8.5185	50.6967
26	100	157.037	-57.037	41.5814
27	250	223.704	26.2963	50.6967

Appendix-B

MODDE 10 OUTPUT

Length/Diametr	Observed	Predicted	Obs - Pred	Conf. int(±)
1	400	378.324	21.6761	803.776
2	1250	825.102	424.898	659.256
3	1150	1043.77	106.232	803.776
4	385	1139.1	-754.102	659.256
5	1154	1227.96	-73.963	573.499
6	1176	1088.71	87.2872	659.256
7	2500	1715.77	784.231	803.776
8	1000	1446.71	-446.713	659.256
9	800	949.547	-149.547	803.776
10	1500	930.046	569.954	659.256
11	750	1353.74	-603.741	573.499
12	1176	1549.32	-373.324	659.256
13	1083	1776.41	-693.408	573.499
14	2300	1842.19	457.815	573.499
15	2000	1679.85	320.148	573.499
16	2867	2438.66	428.342	659.256
17	1667	2146.52	-479.519	573.499
18	2000	1626.27	373.731	659.256
19	667	504.658	162.342	803.776
20	675	905.268	-230.268	659.256
21	1000	1077.77	-77.7687	803.776
22	1333	1436.6	-103.602	659.256
23	2000	1479.3	520.703	573.499
24	1533	1293.88	239.12	659.256
25	1769	2184.44	-415.435	803.776
26	2300	1869.21	430.787	659.256
27	800	1325.88	-525.88	803.776

Appendix-B

MODDE 10 OUTPUT

Length	Observed	Predicted	Obs - Pred	Conf. int(±)
1	100	119.63	-19.6296	123.351
2	250	109.63	140.37	101.172
3	15	106.852	-91.8519	123.351
4	50	133.935	-83.9352	101.172
5	150	115.185	34.8148	88.0116
6	200	103.657	96.3426	101.172
7	250	207.13	42.8703	123.351
8	100	179.63	-79.6297	101.172
9	120	159.352	-39.3519	123.351
10	300	218.657	81.3426	101.172
11	150	222.407	-72.4074	88.0116
12	200	233.38	-33.3797	101.172
13	130	242.963	-112.963	88.0116
14	230	237.963	-7.96297	88.0116
15	200	240.185	-40.1852	88.0116
16	430	326.158	103.842	101.172
17	300	312.407	-12.4074	88.0116
18	400	305.88	94.1203	101.172
19	100	126.574	-26.5741	123.351
20	135	144.074	-9.07408	101.172
21	200	168.796	31.2037	123.351
22	200	160.88	39.1204	101.172
23	200	169.63	30.3703	88.0116
24	230	185.602	44.3982	101.172
25	230	254.074	-24.0741	123.351
26	230	254.074	-24.0741	101.172
27	200	261.296	-61.2963	123.351

Appendix-B

MODDE 10 OUTPUT (ANOVA ANALYSIS)

Yield	DF	SS	MS (variance)	F	p	SD
Total	27	1560.4	57.8			
Constant	1	1039.7	1039.7			
Total corrected	26	520.7	20.0			4.5
Regression	9	461.4	51.3	14.7	**0.000**	7.2
Residual	17	59.3	3.5			1.867
N = 27	DF = 17	Q2 =0.645	R2 =0.886	R2 adj. =0.826	Cond. no. =5.23	RSD =1.867

Purity	DF	SS	MS (variance)	F	p	SD
Total	27	178756	6620.59			
Constant	1	177633	177633			
Total corrected	26	1122.7	43.2			6.6
Regression	9	884	98.2	7.0	**0.000**	9.9
Residual	17	238.7	14.0			3.747
N = 27	DF = 17	Q2 =0.369	R2 =0.787	R2 adj. =0.675	Cond. no. =5.23	RSD =3.747

Diameter	DF	SS	MS (variance)	F	p	SD
Total	27	709700	26285.2			
Constant	1	656448	656448			
Total corrected	26	53251.9	2048.15			45.2565
Regression	9	33977.8	3775.31	3.32987	**0.016**	61.4435
Residual	17	19274.1	1133.77			33.6715
N = 27	DF = 17	Q2 =0.056	R2 =0.638	R2 adj. =0.446	Cond. no. =5.23	RSD =33.67

Appendix-B

MODDE 10 OUTPUT (ANOVA ANALYSIS)

Aspect Ratio	DF	SS	MS (variance)	F	p	SD
Total	27	61.2324	2.26787			
Constant	1	48.5348	48.5348			
Total corrected	26	12.6976	0.48837			0.698835
Regression	9	7.54694	0.838549	2.76766	**0.034**	0.915723
Residual	17	5.15068	0.302981			0.550437
N = 27	DF = 17	Q2 =-0.034	R2 =0.594	R2 adj. =0.38	Cond. no. =5.23	RSD =0.5504

Length	DF	SS	MS (variance)	F	p	SD
Total	27	1.27E+06	46990.7			
Constant	1	1.04E+06	1.04E+06			
Total corrected	26	228380	8783.83			93.7221
Regression	9	114276	12697.4	1.89175	**0.123**	112.683
Residual	17	114103	6711.96			81.9265
N = 27	DF = 17	Q2 =-0.255	R2 =0.500	R2 adj. =0.236	Cond. no. =5.23	RSD =81.93

Appendix-B

MODDE 10 OUTPUT

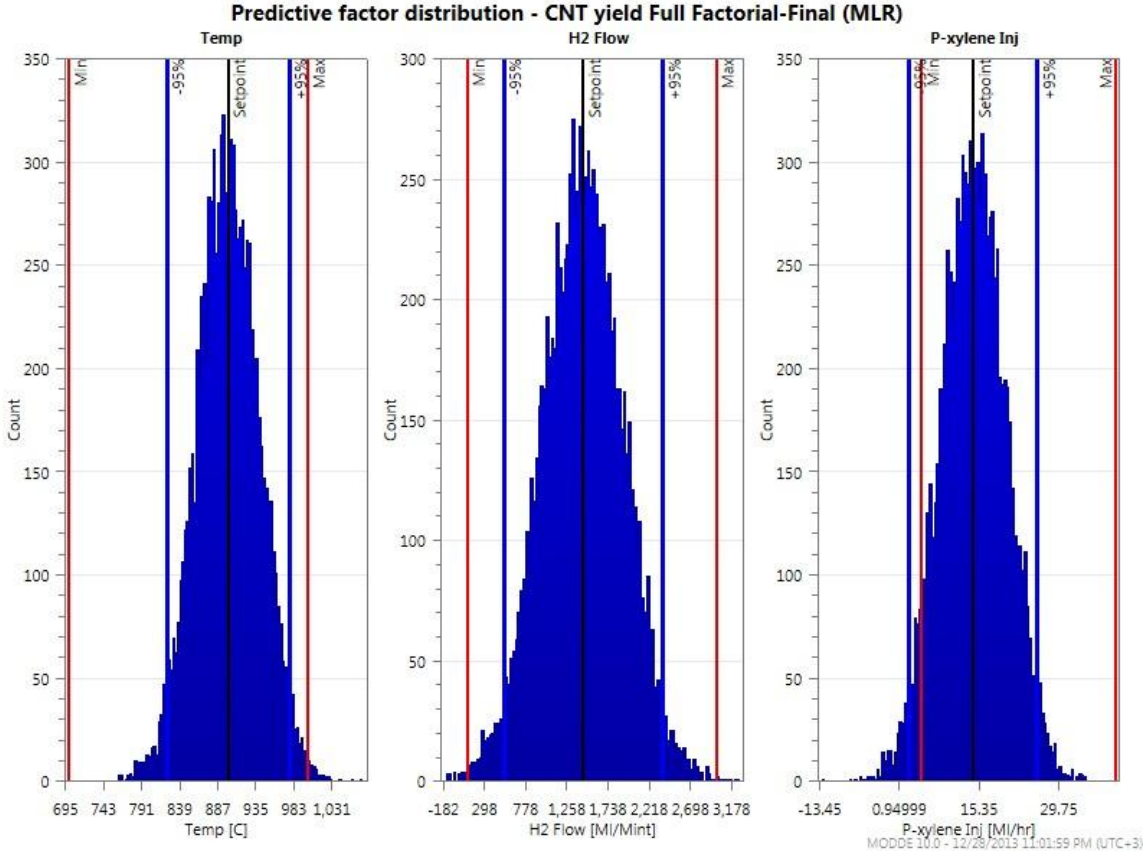

Appendix-B

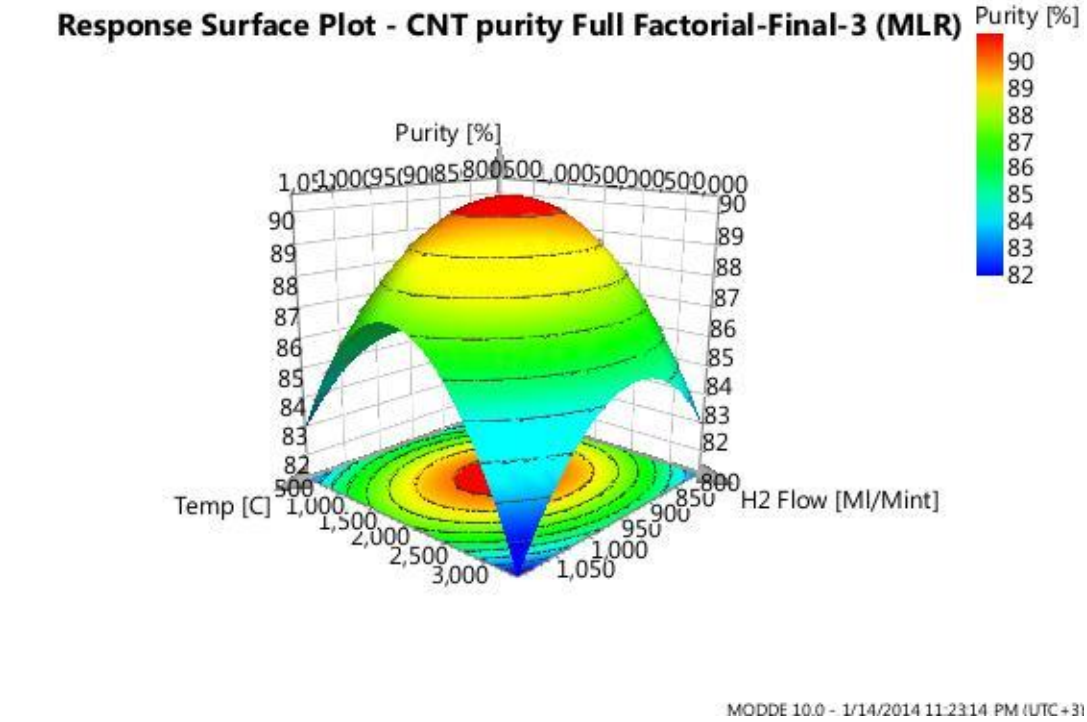
Response Surface Plot - CNT purity Full Factorial-Final-3 (MLR)
Purity [%]
90
89
88
87
86
85
84
83
82
Purity [%]
Temp [C]
H2 Flow [Ml/Mint]
MODDE 10.0 - 1/14/2014 11:23:14 PM (UTC+3)

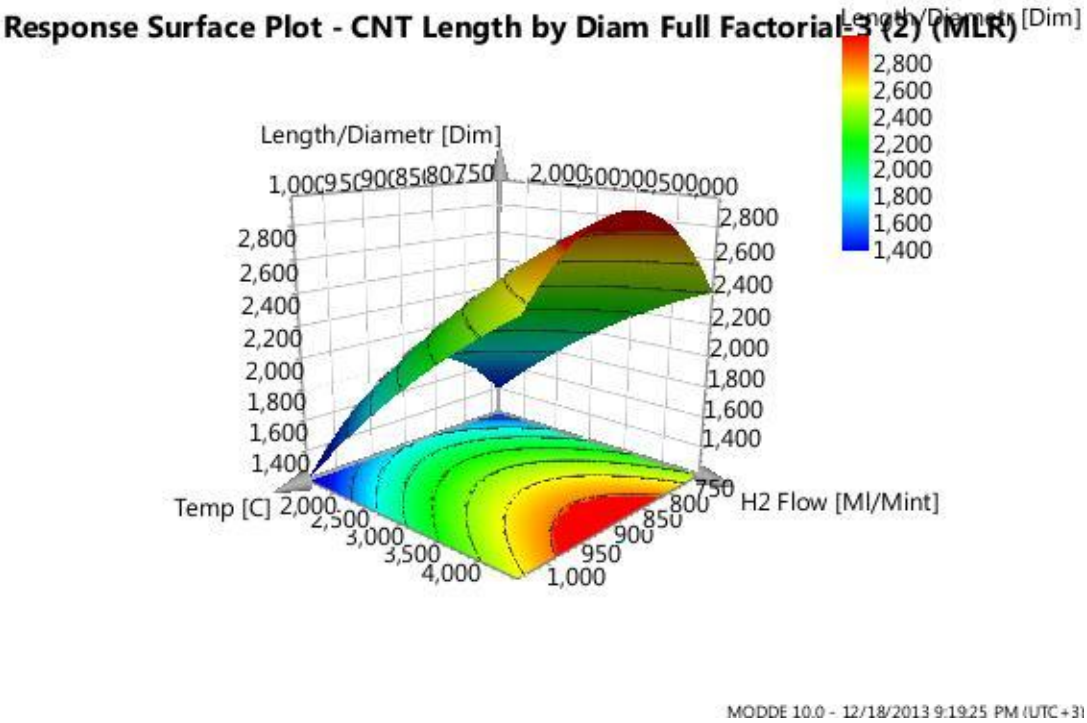
Response Surface Plot - CNT Length by Diam Full Factorial-3 (2) (MLR)
Length/Diametr [Dim]
2,800
2,600
2,400
2,200
2,000
1,800
1,600
1,400
Length/Diametr [Dim]
Temp [C]
H2 Flow [Ml/Mint]
MODDE 10.0 - 12/18/2013 9:19:25 PM (UTC+3)

Appendix-B

MODDE 10 OUTPUT

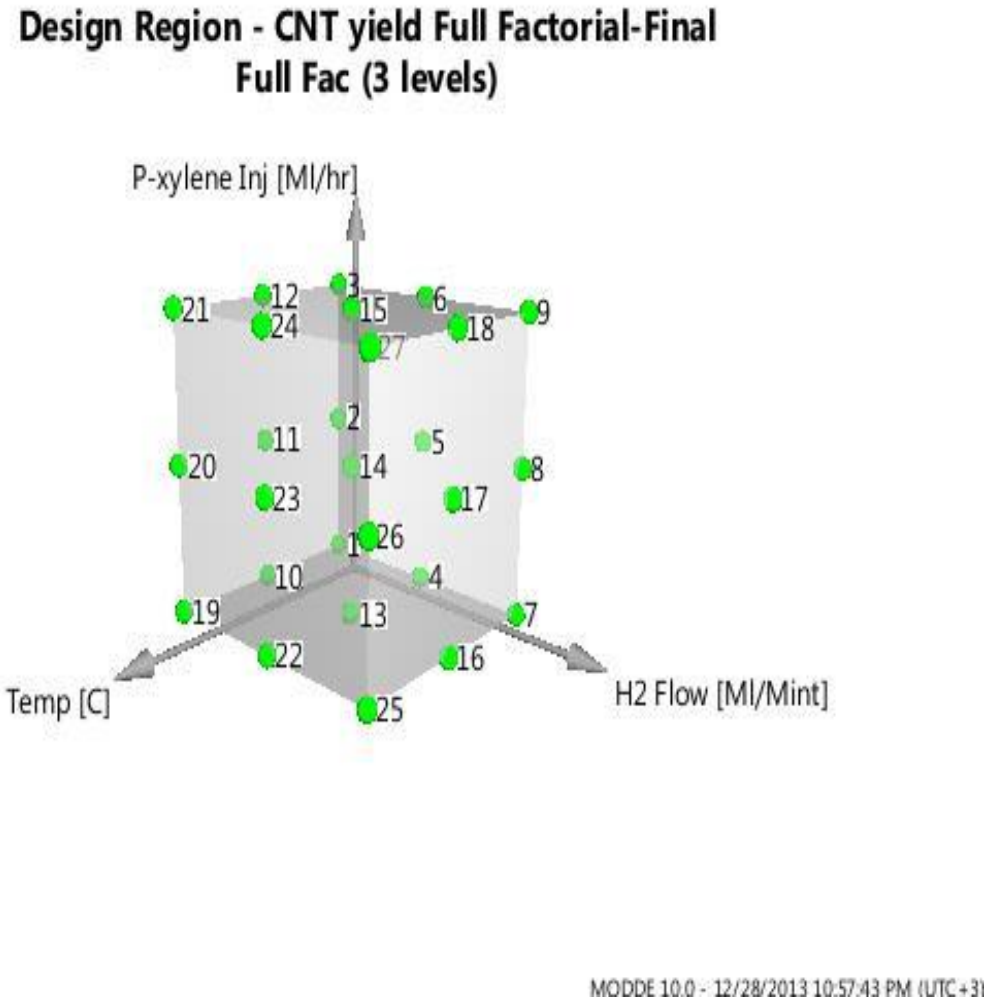

Appendix-B

MODDE 10 OUTPUT

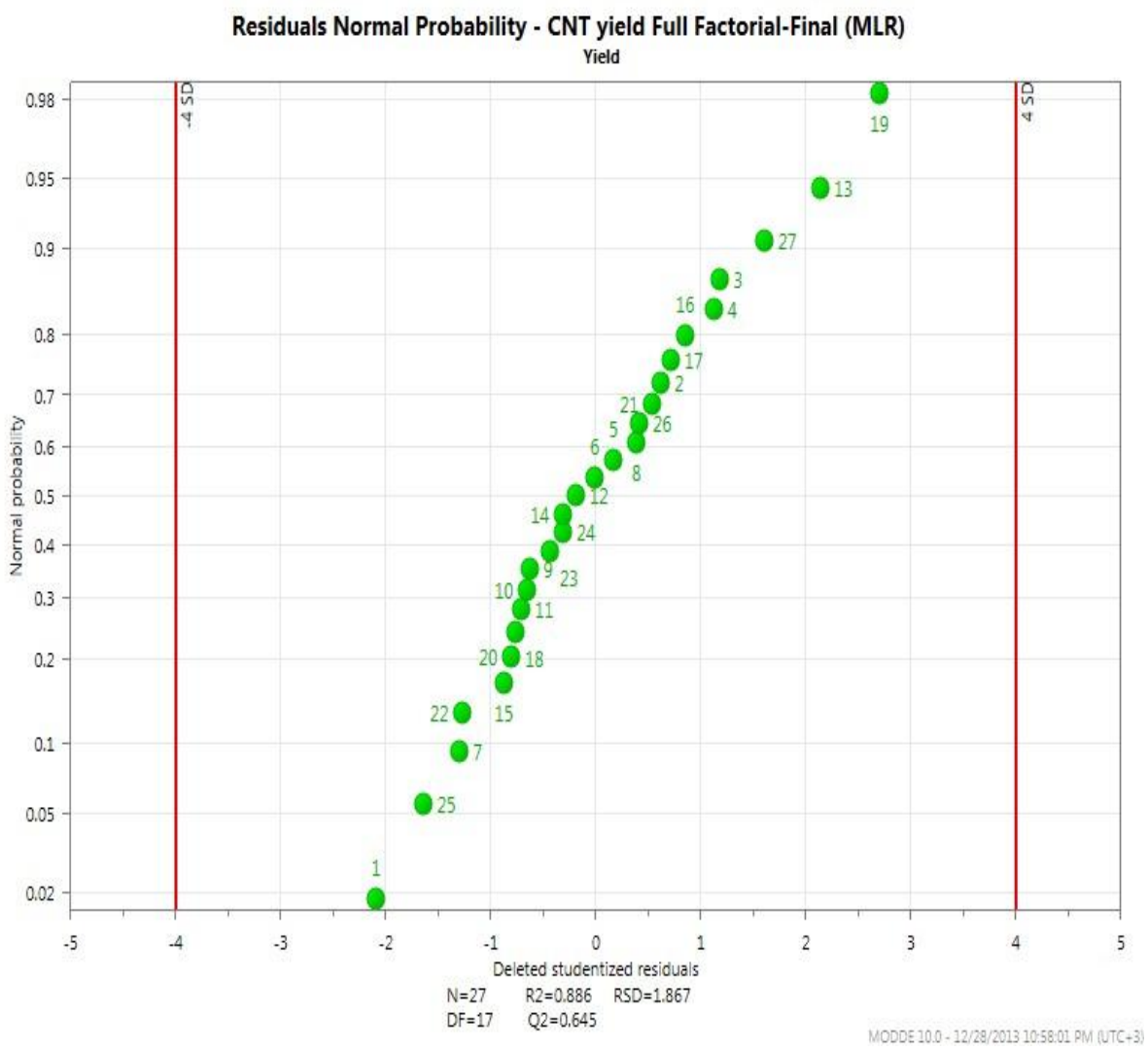

Appendix-C

OPTIMIZER SUMMARY

Setup

Factor	Role	Value	Low Limit	High Limit	Precision	Unit
Temp	Free		700	1000	7.5	C
H2 Flow	Free		100	3000	72.5	Ml/Mint
P-xylene Inj	Free		5	40	0.875	Ml/hr

Response	Criterion	Min	Target	Max	Pred. min	Pred. max	Unit
Yield	Maximize	4.89598	25		-1.14127	15.1898	wt%

Selected solution

Factor	Role	Value	Robust low edge	Robust high edge	Unit	Factor contribution	Robust resolution distance
Temp	Free	891.658			C	4.77243	
H2 Flow	Free	1496.78			Ml/Mint	2.47447	
P-xylene Inj	Free	5.00542			Ml/hr	92.7531	

Response	Criterion	Value	Unit	log(D)	DPMO	Cpk
Yield	Maximize	15.1871	wt%	-0.622972	0	3.33764

Appendix-C

OPTIMIZER SUMMARY

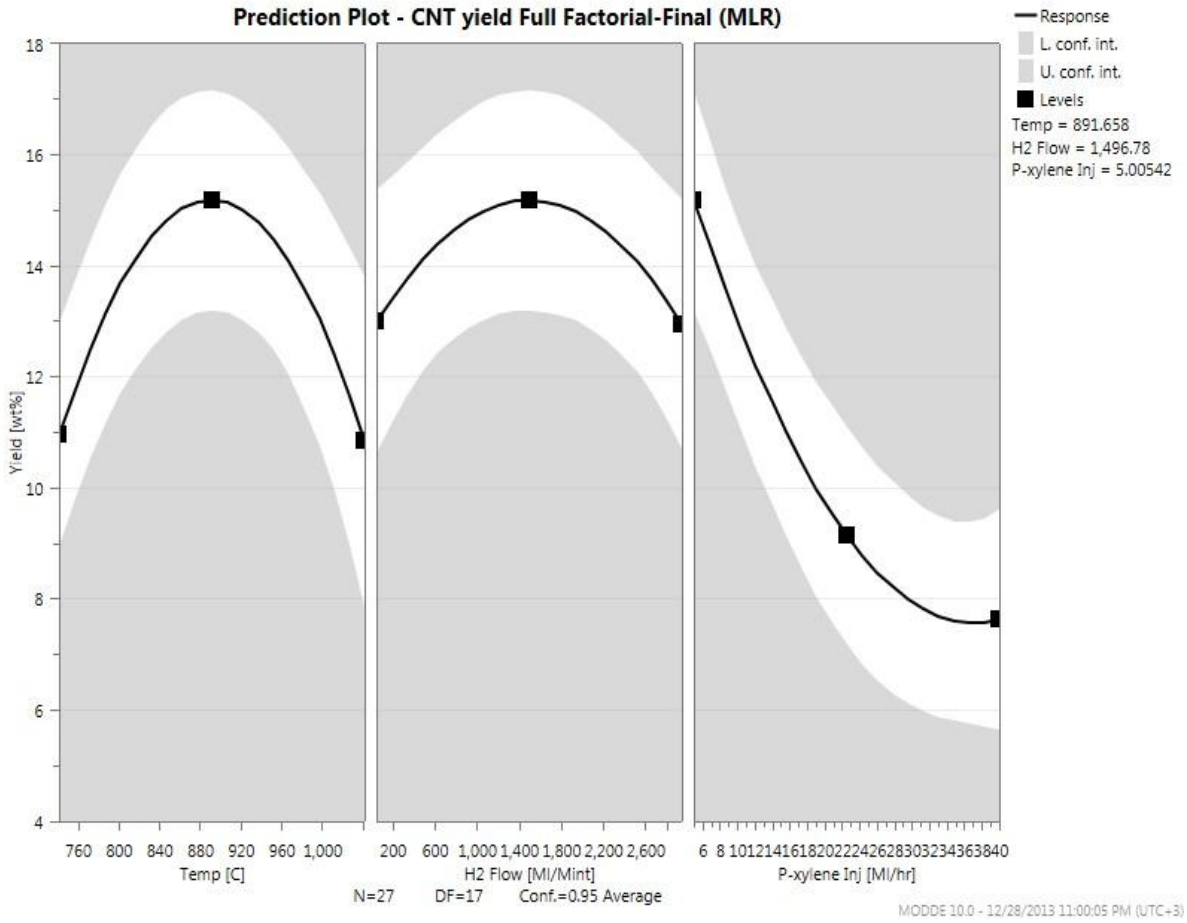

References

A., R. P. Lee, et al, Crystalline ropes of metallic carbon nanotubes, Science 273 (52), 483-487. Smalley, 1996.

Á. Kukovecz, D. Méhn, E. Nemes-Nagy, R. Szabó, I. Kiricsi, Optimization of CCVD synthesis conditions for single-wall carbon nanotubes by statistical design of experiments (DoE), Department of Applied and Environmental Chemistry, University of Szeged, H-6720 Szeged, Carbon; OI:10.1016/j.carbon.2005.06.001, 01/2005.

Bethune, D. S., C. H. Kiang, M. S. de Vries, G. Gorman, R. Savoy, J. Vazquez and R. Beyers, Cobalt-catalysed growth of carbon nanotubes with single-atomic-layer walls, Nature, 363, 605-607, 1993.

Baddour, C. and Briens C, Carbon Nanotube Synthesis: a review, International Journal of Chemical Reactor Engineering, Volume 3, Issue 1, Pages –, ISSN (Online) 1542-6580, DOI: 10.2202/1542-6580.1279, August 2005.

C.N. He, N.Q. Zhao *, C.S. Shi, S.Z. Song, Optimization of the chemical vapor deposition process for fabrication of carbon nanotube/Al composite powders, Materials Research Bulletin 45, 1182–1188, Tianjin University, Tianjin 300072, China, 2010.

Dresselhaus, M. G., and S. Riichiro, Physical Properties of Carbon Nano Tubes, London, Imperial College Press, 1998.

Dresselhaus, M. S., Dresselhaus G., and Phaedon A., Carbon nanotubes: synthesis, structure, properties, and applications, Berlin: Springer Publishers, 2001.

Dai H., Carbon nanotubes: opportunities and challenges, Surface Science, 500: 218-241, 2002.

Dresselhaus, M., Dresselhaus G., and S. Riichiro. Physical Properties of Carbon Nanotubes, London: Imperial College Press, 1998.

Dupuis, A.C. Prog. Mater. Sci. 2005; 50: 92961.

Ebbesen, T. W. and Ajayan P.M., Large-Scale Synthesis of Carbon Nano Tubes, Nature, 358 (6383), 220-222, 1992.

Edgar, Thomas F et al , Optimization Of chemical processes, 2nd ed. p. cm., (McGraw-Hill chemical engineering series.), ISBN 0-07-039359- 1, TP155.7 E34 2001.

Guldi D.M., Martin, N., Carbon Nanotubes and Related Structures Synthesis, Characterization, Functionalization, and Applications, Wiley VCH, Weinheim, 2010; 4-5 pp.

Haddon R.C., Carbon Nano Tubes, Acc. Chem. Res. 35, pp., 977–1113, 2002.

Harris P. Carbon Nanotube Science, Cambridge, Cambridge University Press, 43-72, 2009.

H.E. Unalan, M. Chhowalla, Investigation of single-walled carbon nanotube catalytic chemical vapor deposition, Nanotechnology 16 (2005) 2153–2163.

Iijima, S. and Ichihashi T., Single-shell carbon nanotubes of 1 nm diameter, Nature 363:603-605, 1993.

Iijima, S., Helical Microtubules of Graphitic Carbon, Nature, 354: 56-58, (1991).

James O. Westgard, The Replication Experiment, Tools, Technologies and Training for Healthcare Laboratories Westgard QC., 2013.

K.Safarova et al, Usage of AFM, SEM and TEM for the research of carbon nanotubes, Modern Research and Educational Topics in Microscopy.(Eds.) ©FORMATEX 2007.

Muataz A. Atieh, et al, Radiation Vulcanization of Natural Ruber Latex Loaded

With Caron Nanotubes, King Fahad University of Petroleum and Minerals, Taylor Francis Group, LLC, Fullerenes, Nanotubes and Carbon Nanostructures, 18: 1–15, 2010.

Mukul Kumar and Yoshinori Ando, Chemical Vapor Deposition of Carbon Nanotubes: A Review on Growth Mechanism and Mass Production, Journal of Nano science and Nanotechnology Vol. 10, 3739–3758, 2010.

M. Aksak, S. Kir, Y. Selamet, Effect of the growth temperature on carbon nanotubes grown by thermal chemical vapor deposition method, Department of

Physics, Izmir Institute of Technology, Urla, 35430, Izmir, Turkey, Journal of Optoelectronics and Advanced Materials – Symposia, p. 281 – 284, Vol. 1, No. 3, 2009.

Newbury, D. E.; Williams, D. B. Acta **Materialia**, 48, 323-46, 2000.

N.M. Mubarak, Faridah Yusof, and M.F. Alkhatib, The production of carbon nanotubes using two-stage chemical vapor deposition and their potential use in protein purification, Chemical Engineering Journal, 168 461–469, 2011.

O'Connell M. J., Carbon nanotubes properties and applications, Taylor & Francis, New York, 2006.

Oscar M. Dunens ⇑, Kieran J. MacKenzie, Andrew T. Harris, Screening and optimisation of the single- and double-walled carbon nanotube parameter space using a high-throughput methodology, Chemical Engineering Journal 209 407–419, University of Sydney, NSW 2006, Australia, 2012.

Paradise M and Goswami T. Carbon nanotubes Production and Industrial Applications, Materials & Design, 28:1477-89, 2007.

Sivaram Arepalli et al, Characterization of Single-Wall Carbon Nanotubes, Engineering, http://research.jsc.nasa.gov, Engineering.

See C. H. and Harris A. T., A review of carbon nanotube synthesis via fluidized-Bed chemical vapor deposition, Ind. Eng. Chem. Res, 46:997-1012, 2009.

Valentin N. Popov, Carbon nanotubes: properties and application, Materials Science and Engineering, R 43 61–102, 2004.

Wang, Z. L. Characterization of Nanophase Materials Wiley-VCH, Weinheim, 2000.

Xiefei Zhang et al, Carbon-Nanotube Fibers Spun from Long Carbon-Nanotube Arrays, General Nanotechnology, DOI: 10.1002/ smll.200600368, 2007.

Yacamán-José, M., M. Miki-Yoshida, L. Rendón and J. G. Santiesteban, Catalytic growth of carbon microtubules with fullerene structure, Applied Physics Letters, 62 (6), 657-659, 1993.

Vitae

1964: Born in Khobar, Saudi Arabia

1982: High School with science major

1982-1987: BS Chemical Engineering, King Fahad University of Petroleum and Minerals.

1987-2010: Saudi Aramco, Sr. Planning Consultant.

2010-2013: MS Chemical Engineering, King Fahad University of Petroleum and Minerals. Thesis Advisor Dr. Eid Al Mutairi